Molecular interactions of binary mixtures of deep eutectic solvents with organic solutes

By

Reitumetse Precious Molefi

22290159

Submitted in the fulfilment of the academic requirements for the degree of Master of Applied Science in Chemistry, Faculty of Applied Sciences, Department of Chemistry, Durban University of Technology

March 2024

PREFACE

I, Reitumetse Precious Molefi, declare that:

(i) The research work reported in this thesis, besides where indicated, is my original work.

(ii) This work has not been submitted for examination or degree at any other university.

(iii) This work does not contain other person's data, or information, unless otherwise stated.

Signed:

Reitumetse Precious Molefi Date: 15/03/2024

Signed:

Dr. B. Kabane (Supervisor) Date: 21/03/2024

Signed:

Prof. N. Deenadayalu (Co-supervisor) Date: 20/03/2024

DEDICATION

I would like to express my heartfelt appreciation to my cherished grandmother, Sediapelo Molefi, my dear brother, Monnaotsile Molefi, and my sister, Keikantseone Molefi. Their unwavering love, support, and constant words of encouragement have been instrumental in my journey. I am especially grateful to Dr. Kabo Matshetshe, my significant other, whose love has been a source of inspiration. Lastly, a special dedication goes to my son, Osego Molefi, whose presence brings immense joy and meaning to my life.

ACKNOWLEDGEMENTS

I greatly appreciate the following people for their valued contribution towards the success of this work.

- I extend my deepest gratitude and admiration to my dedicated supervisor, Dr. B. Kabane, whose unwavering support and guidance have been the cornerstone of my academic journey. His expertise, patience, and belief in my capabilities have been instrumental in shaping the success of this work. I am truly fortunate to have had such a supportive mentor by my side, and this dedication is a testament to the profound impact he had on my academic and personal growth.
- Prof. N. Deenadayalu for her valuable help, guidance, and financial support.
- My heartfelt gratitude to my wonderful mother-in-law, Mrs Kelebile Matshetshe for her unwavering support, love, and wisdom that have enriched my life in countless ways.
- A special Thanks to Dr. K. Matshetshe for his continual support.
- A special thanks to my friends, Itumeleng Nhlapo and Duduzile Silinda whose unwavering love, support and prayer has been a constant source of strength and inspiration.
- My gratitude to all my family for the support throughout the studies.
- Grateful to the DUT Scholarship scheme for funding.
- My deepest gratitude to God, for He gave me the strength to live.
  ‘Give thanks to the Lord, for he is good; his love endures forever.’
  1 Chronicles 16:40

PUBLICATIONS

1. **Molefi, R.**, Kabane, B. and Deenadayalu, N., 2023. Measurement of Activity Coefficients at Infinite Dilution for Various Organic Solutes in Deep Eutectic Solvent (1-Butyl-2, 3-dimethylimidazolium Chloride+ Ethylene Glycol) at Different Temperatures. *Journal of Chemical & Engineering Data*. https://doi.org/10.1021/acs.jced.3c00055
2. **Reitumetse Molefi**, Bakusele Kabane, Kabo Matshetshe, Nirmala Deenadayalu and Indra Bahadur. Pre-screening of an eco-friendly deep eutectic solvent for separating industrial mixtures: A useful tool for solvent selection. (Under Review)
3. **Reitumetse Molefi**, Bakusele Kabane, and Nirmala Deenadayalu, Densities, speed of sound, and refractive index of binary mixtures of pyrrolidinium based DES with acetic acid at (293.15 - 313.15) K. (In preparation for submission to a suitable journal)

ABSTRACT

Deep eutectic solvents are the new emerging solvents formed by the combination of hydrogen bond acceptor and hydrogen bond donor. This type of solvent is still under development for possible industrial application including in chemistry, biotechnology, and pharmaceutical processes. The deep eutectic solvents have attracted much attention because they are characterized as greener solvents when compared to the currently used volatile organic solvents. Deep eutectic solvents are to replace the ionic liquids, which are posed as green solvents, however, their toxic nature has turned to be its drawbacks. The deep eutectic solvents attracted great interest due to their unique properties such as biodegradability, thermal stability, less toxicity, easy and cheap to prepare.

This work explores the activity coefficients at infinite dilution of deep eutectic solvents. The deep eutectic solvents under investigation were carefully synthesized using hydrogen bond donors (HBD) and hydrogen acceptors (HBA) at a specific ratio. The analysis of these prepared deep eutectic solvents were analysed using spectroscopic techniques (FTIR and NMR) to confirm the formation of deep eutectic solvents and the type of interaction occurring between the HBD and the HBA. Additionally, thermal stability of the prepared deep eutectic solvents was investigated. The DESs were then used to measure the activity coefficients at infinite dilution for volatile organic compounds (alkanes, alkene, alkynes, aromatic hydrocarbons, ketones, acetonitrile, tetrahydrofuran, alcohols and thiophene) using the chromatography technique. The activity coefficients at infinite dilutions were conducted over a range of temperature (313.15 - 353.15) K. The prepared deep eutectic solvents for this include.

- DES1 {1- butyl-2,3-dimethylimidazolium chloride + ethylene glycol (1:3)}
- DES2 {1-butyl-2,3-dimethylimidazolium chloride + diethylene glycol (1:2)}
- DES3 {1-butyl-2,3-dimethylimidazolium tetrafluoroborate + ethylene glycol (1:3)}
- DES4 {1 -butyl-2,3-dimethylImidazolium tetrafluoroborate + diethylene glycol (1:3))

The study also focuses on understanding the behaviour of these DES through a comprehensive analysis of their thermophysical characteristics and their ability to dissolve solutes at infinite dilution. The investigation revealed intriguing trends in the solvation behaviour of different classes of solutes within the DES. Alkanes exhibited higher activity coefficients, with a clear dependence on the alkyl chain length. Cyclic hydrocarbons showed distinct behaviour due to stronger interactions with the imidazolium ring. Alkynes demonstrated the lowest activity coefficients, attributed to the presence of triple bonds influencing solute-solvent interactions. Aromatic hydrocarbons exhibited unique solvation behaviour influenced by the delocalized pi-π- electrons on the benzene ring.

To use the deep eutectic solvents at an industrial level, it is highly imperative to understand the intermolecular interactions and properties of the pure deep eutectic solvents and their mixtures with volatile organic solutes. The prepared deep eutectic solvents for thermophysical properties include.

- DES5 (1-butyl-1-methylpyrrolidinium bromide + ethylene glycol)
- DES6 (1-butyl-3-methylimidazolium chloride + ethylene glycol)

Thermophysical properties, such as densities, speed of sound, and refractive indices were measured as a function of temperature. The study investigated the binary mixtures containing (DES5 + acetic acid or ethanol) and (DES 6 + acetic acid or ethanol). These were investigated at temperatures ranging between (293.15 and 313.15) K and at atmospheric pressure (0.1MPa) over a range of mole fraction (x_1= 0 to 1) as a function of DES. The measured property values were used to compute the excess properties such as excess molar volumes, isentropic compressibilities, deviation in refractive indices, deviation in isentropic compressibilities and intermolecular free length. The data obtained provides insights into the molecular interactions within the DESs, shedding light on their structural arrangements and overall stability.

This study contributes to the fundamental understanding of deep eutectic solvents, offering a detailed exploration of their thermophysical properties and their solvation behaviour at infinite dilution. The findings have implications for the design and optimization of DESs for various applications, including their use as green solvents in chemical processes and separations.

TABLE OF CONTENTS

Table of Contents

LIST OF TABLES

LIST OF FIGURES

LIST OF ABBREVIATIONS AND SYMBOLS

DESs- Deep Eutectic Solvents.

ILs- Ionic Liquids.

VOCs- Volatile Organic Compounds.

GLC- Gas Liquid Chromatography.

HBD- Hydrogen Bond Donor.

HBA- Hydrogen Bond Acceptor.

[MEAHCl][MEA]- [Monoethanolamine hydrochloride] [Methyldiethanolamine]

UNIQUAC- Universal Quasi-chemical.

NRTL- Non-Random Two-Liquid.

GC-TCD- Gas Chromatography coupled with Thermal Conductivity Detector.

BDMIMCl- 1-butyl-2,3-dimethylImidazolium chloride.

BDMIMTFB- 1-butyl-2,3-dimethylimidazolium tetrafluoroborate.

BMPyrBr- 1-butyl-1-methylpyrrolidinium bromide.

EG- Ethylene Glycol.

DEG- Diethylene Glycol.

NMR- Nuclear Magnetic Resonance Spectrometer.

FTIR- Fourier Transform Infrared Spectroscopy Analysis.

TGA- Thermogravimetric Analysis.

γ_{13}^{∞} - Activity coefficient at infinite dilution.

$\Delta H_1^{E,\infty}$- Enthalpy.

$\Delta G_1^{E,\infty}$- Gibbs free energy.

$T_{ref}\Delta S_1^{E,\infty}$- Entropy.

$S_{13}{}^{\infty}$- Selectivity.

$K_1{}^{\infty}$ - Capacity.

ρ – Density.

u – Speed of Sound.

nD - Refractive Index.

$V_m{}^{E}$ - Excess Molar Volume.

Δn - Change in refractive index.

K_s - Isentropic Compressibility.

Δk_s - Deviation in isentropic compressibility.

L_f - intermolecular free length.

CHAPTER 1: INTRODUCTION

1.1 Background

A large portion of chemistry is performed and conducted in a liquid solution (Ramsey *et al.* 2009). This is clear from the physiology of plants and other living things in nature, as well as from geochemical processes. Industries include biomass processing, textile, paper, food, hydrometallurgy, bulk chemicals, and pharmaceuticals, as well as synthesis, purification, and laboratory analysis are a few examples (Ortiz *et al.* 2008; Roy Choudhury 2013; Shuai and Luterbacher 2016). As a result, it is necessary to use solvents which possess the desired characteristics for the activities to be performed, while also avoiding any unfavourable characteristics (Sheldon 2005). Liquids have a few characteristics that enable them to be effective solvents. Generally, a solvent should be in a liquid form at a reasonable range of temperatures and pressures, meaning that it should be liquid at room temperature and pressure. Solvents should be readily purifiable for the use and reasonably priced and be available in commercial quantities at the purity required for the proposed method. It ought to be environmentally friendly when disposed of and generally recyclable (though not always by distilling it out of the process mixture after the product has been recovered) (Jessop 2011).

Naturally, water is the main solvent for many geological and physiological processes. However, at room temperatures, water has demonstrated ineffectiveness as a solvent for nonpolar compounds, such as many industrial polymers, permanent gases, and solid materials with greater crystal energies can't be dissolved due to their solvation energies and entropy shifts (Smith 2006). As a result, other solvents with better solvent characteristics have been widely used in industry and to dissolve possible solutes in the lab that water is unable to sufficiently dissolve (Mallakpour and Dinari 2012). Organic liquids including dipolar, hydrogen-bonded, and nonpolar solvents, have long been used for this purpose with various types of solutes. Even though organic solvents are typically easily accessible commercially, their costs must be considered for industrial applications in high purity (Brennecke and Maginn 2001). Furthermore, certain organic solvents might be toxic, highly flammable, volatile, or bad for the environment, necessitating extra attention when using them (Cvjetko Bubalo *et al.* 2015). The industry is currently moving away from the commonly used organic

solvents and replacing them with greener solvents that are non-flammable, low levels of toxicity, non-volatile, and ecologically friendly (Phan and Luscombe 2019).

The need for greener solvents to be used in separation processes in a sustainable way preferably with little to no secondary waste produced is a strong drive for the development of alternative solvents which can replace and/or improve the existing ones. The different industries where separations are mainly used and impacted are, mining industry, petrochemical industry, chemical industry, food industry, and pharmaceutical industry (Noble and Agrawal 2005). Traditional solvents, also known as petrochemical solvents, have been utilized in the chemical industry for an extended period. These traditional solvents in the chemical and biochemicals industries, give rise to high energy costs, due to their use in separations, and significant progress in addressing the energy crisis which can be made by improving these separations (Knez *et al.* 2014). These solvents are widely used due to their abundance and affordability. There are several problems that can be encountered when using these traditional solvents in separations, such as, high toxicity, flammability, environmental impact, low recovery, compatibility, cost, and selectivity (Pacheco-Fernández and Pino 2019).

Due to the environmental, sustainability, and health and safety concerns associated with traditional solvents, research has been conducted to develop more environmentally friendly solvent processes or systems as alternatives to using traditional organic solvents. Ionic liquids (ILs) and deep eutectic solvents (DESs) have been recently used as advancements in recent years and have the potential to make the industry more environmentally friendly and efficient. Ionic liquids (ILs) are a type of salt that are in a liquid state at temperatures below 100 ºC (Holbrey and Seddon 1999). The properties of these ILs can be customized by adjusting the structure of either the organic cation or the organic or inorganic anion. Ionic liquids (ILs) have gained attention in recent years as a potential alternative to traditional solvents in separation processes. ILs have several unique properties that make them attractive for use in separations, low volatility, wide liquid range, tunable properties, high thermal stability, solubility, selectivity, and recovery (Liu, Jiang and Jönsson 2005). Overall, the properties of ILs make them a promising alternative to traditional solvents in separation processes, and further research is being conducted to fully understand their potential in this area.

Certain applications, such as nuclear fuel reprocessing, metallurgical applications, and coolants and moderating agents for nuclear reactors, the commonly recommended solvent in the past have been ionic liquids. Due to their elevated temperature function, they are restricted for application to the solutes that withstand those temperatures involved which in turn excludes most organic solutes. Ionic liquids at room temperature are typically non-volatile, but if they are utilized below ambient temperatures, they have high viscosities. In industrial applications, it's essential to factor in their prices since they could still pose hazards, be combustible, and present difficulties in recycling processes.

Since the noticed drawbacks of ionic liquids at room temperature, researchers have continued to look for alternatives. (Abbott *et al.* 2003) suggested an alternate solvent in 2003 that is a choline chloride and urea combined in a eutectic state (Abbott *et al.* 2003). The deep eutectic solvents field, which is the focus of the study, was opened by these findings. DESs are made by mixing two or more components in specific proportions to form a new substance with unique properties. DESs exhibit a lower melting point compared to the individual components, hence the name "deep eutectic". They are gaining attention as a potentially greener alternative to traditional solvents because they can be made from renewable resources, have low toxicity, and can be easily produced. They have a wide range of applications, including in extraction processes, biorefineries, and electrochemistry, among others.

In separations, deep eutectic solvents (DESs) have gained attention as a novel and effective alternative to traditional solvents. They have been shown to possess several advantages in separation processes, such as high selectivity, good solubility, and low toxicity (Huang *et al.* 2019). They can be used as a medium in separations such as liquid-liquid extraction, solid-liquid extraction, and gas-liquid separation. Additionally, the low melting point of DESs enables easier separation of the desired components. Their unique properties make them particularly useful in the pharmaceutical and petrochemical industries, where separations are essential for purifying and isolating active compounds. Although deep eutectic solvents (DESs) have been recognized as a viable alternative to volatile organic compounds (VOCs) in many industrial separations, the practical implementation of DESs as a replacement requires the cost-effective and environmentally friendly large-scale production of these alternative solvents.

The study of thermodynamic equilibrium systems is a crucial and essential tool for understanding the factors that drive separation processes. The focus in recent studies is to address the significance of thermodynamic data to be applied in industry. Understanding activity coefficients at infinite dilution and ternary combinations of deep eutectic solvents and solutes (volatile organic solvents) has proven to be of much importance as it demonstrates the degree of interaction between the solute and the deep eutectic solvent molecules. Additionally, thermodynamic properties also help us to understand and know more about the interactions between the solutes and deep eutectic solvents which determine whether it is a weak or strong separating agent.

Thermodynamics plays a crucial role in separation processes as it governs the behaviour of chemical species when subjected to changes in temperature, pressure, and concentration (Hendriks *et al.* 2010). Separation processes involve the separation of a mixture of components into individual pure components or groups of components, which can be accomplished through various physical or chemical processes. The thermodynamic properties of solvents provide valuable information for the design and optimization of chemical processes (Zafarani-Moattar, Shekaari and Sadrmousavi-Dizaj 2022). By understanding the thermodynamics of solvents, researchers can select solvents that are more effective in dissolving specific solutes, or that are more efficient in energy consumption during the separation and purification of compounds. The thermodynamic properties of solvents can also provide insight into their environmental impact, as certain solvents can have high toxicity or low biodegradability (Martins, Pinho and Coutinho 2019). Understanding the thermodynamic properties of solvents can help to identify safer and more sustainable solvents for chemical processes. The thermodynamic properties of solvents are closely related to their physical properties, such as viscosity, density, and vapor pressure. Knowing these properties is important for predicting and controlling the behaviour of solvents in chemical processes, such as crystallization, extraction, and distillation. Some of the important thermodynamic properties of solvents include enthalpy, entropy, Gibbs free energy, heat capacity, and activity coefficient. By knowing these properties, researchers can predict the solubility, vapor pressure, and other properties of solutes in different solvents. This information can help in the selection of solvents for specific applications and in the optimization of chemical processes.

Activity coefficients at infinite dilution are a measure of the activity of a solute in a solvent at very low concentrations. In separations, activity coefficients are used to predict the behaviour of solutes in a solvent and help to determine the optimal conditions for a separation process. The activity coefficient at infinite dilution provides data on the relative strength of the interactions between the solute and solvent, which is important in selecting the appropriate solvent for a given separation (Duarte Ramos Matos, Calabro and Mobley 2019). High activity coefficients at infinite dilution indicate weak interactions between the solute and solvent, making it easier to separate the components. On the other hand, low activity coefficients indicate strong interactions, making separation more difficult (Kabane and Redhi 2020). Therefore, activity coefficients at infinite dilution are a useful tool for optimizing separations and choosing the best solvent for a particular application.

The Gas Liquid Chromatography (GLC) method is one of the methods that can be used to determine activity coefficients at infinite dilution by using the retention time of the solutes in the chromatography process, which are important in separation processes. GLC involves the separation of a mixture of gases or volatile liquids into its individual components based on their relative distribution between the mobile gas phase and the stationary liquid phase. The activity coefficients at infinite dilution can be calculated from the retention times of the solutes acquired by the GLC process, and the information obtained can be used to optimize the separation conditions and select the appropriate solvent for a given separation. By calculating the activity coefficients, one can determine the relative strengths of the interactions between the solute and solvent, and thus, estimate the selectivity and capacity factors. Selectivity is a measure of how well a particular solvent separates a mixture of solutes, while capacity is a measure of how much of a solute can dissolve in a solvent. These factors are important in determining the suitability of a solvent for a particular separation.

1.2 Problem statement

Industrial separation operations such as distillation are energy-intensive processes and consume a significant amount of energy. The energy consumption in these processes can be attributed to several factors, including the energy required to heat the feed and to provide the necessary work for separation (Li *et al.* 2022). Distillation is a widely used separation process in the chemical industry, and it is responsible for a significant portion of the energy consumption in the industry. Separations based on distillation account for about 3% of the total U.S. energy consumption (Soave and Feliu 2002). The distillation of crude oil into its fractions is also a very energy-intensive process, requiring about 40% of the total energy used in crude-oil refining (Soave and Feliu 2002). The problem with energy-intensive processes occurring during separation processes is that they consume a significant amount of energy, which can be a major cost factor in industrial processes. This not only affects the overall profitability of the operation but also has a significant impact on the environment due to the associated greenhouse gas emissions and other environmental impacts.

The use of large quantities of organic solvents in separation processes can have a significant environmental impact due to their high volatility and toxicity. Traditional organic solvents and ionic liquids have several environmental limitations that make their usage problematic for industrial separation processes. These limitations include:

1. Volatility: Organic solvents are highly volatile and can evaporate into the atmosphere, leading to air pollution and loss of the solvent. This can also result in occupational health hazards for workers. Ionic liquids, although less volatile than volatile organic solvents, can still have high vapor pressures and pose similar environmental and occupational hazards.

2. Toxicity: Organic solvents can be toxic and harmful to the environment and human health. Excessive to these solvents can lead to acute or chronic health effects, including respiratory problems, skin irritation, and even cancer. Ionic liquids are generally considered to be less toxic than traditional organic solvents, but they can still have negative effects on the environment and human health.

3. Non-biodegradability: Organic solvents and ionic liquids are often non-biodegradable and can persist in the environment for a long period of time,

leading to long-term environmental damage. This can also result in contamination of soil, groundwater, and surface water.

4. High Energy Consumption: Traditional organic solvents and ionic liquids used in separation processes can be energy-intensive and require significant amounts of energy to be used, leading to high carbon emissions and a significant environmental impact.

The high energy consumption in separation processes is a major challenge that must be addressed to ensure the sustainability of the chemical industry and reduce its environmental impact (Gupta *et al.* 2017). Therefore, there is a need to develop more efficient and sustainable separation processes that can reduce energy consumption and associated environmental impacts while maintaining and improving the product quality. Hence, the development of deep eutectic solvents offers a potential solution to the environmental limitations posed by the traditional organic solvents and ionic liquids, as DESs are more environmentally friendly and have the potential to be produced from renewable sources. Their use in separation processes can minimize energy demand, reduce environmental impact, and increase the efficiency of existing processes.

1.3 Justification

Many researchers are investigating the use of DESs in separation of azeotropes (Wazeer *et al.* 2018; Brouwer and Schuur 2021; Castro-Muñoz *et al.* 2022). The studies on DESs as greener solvents to replace the volatile organic solvents and some ionic liquids have attracted much interest owing to their unique properties such as less volatile and toxicity, more biodegradable, and can be produced from renewable sources. Imidazolium-based deep eutectic solvents (DESs) have gained significant attention in recent years as a promising alternative to traditional solvents. Some of their thermodynamic properties that make them suitable for application in separation processes: Tuneable properties, imidazolium-based DESs can be easily synthesized with different cations and anions, allowing for the tuning of their thermodynamic properties to suit specific separation processes; Low vapor pressure, Imidazolium-based DES have very low vapor pressure, making them ideal for use in separation processes where volatile solvents can be problematic; Low toxicity, imidazolium-based

DESs are generally considered to be less toxic solvents, making them safer for the use in separation processes.

The study by Bhagour et al. 2013 investigated the thermodynamic properties of binary mixtures of imidazolium-based ionic liquids with acetonitrile and water (Bhagour *et al.* 2013). The authors used experimental and computational methods to determine activity coefficients and other thermodynamic properties as a function of temperature and composition. They found that the activity coefficients of the ionic liquid-acetonitrile mixtures were higher than those of the ionic liquid-water mixtures, indicating stronger interactions between the ionic liquid and acetonitrile. Both mixtures showed an increase in activity coefficients with temperature, suggesting weaker interactions at higher temperatures. The computational simulations provided insights into the molecular-level interactions between the components. This study provides important information on the thermodynamic properties of these binary mixtures that could be useful for designing and optimizing these solvents for various applications.

In this research work, two different types of quaternary salt were used as hydrogen bond donor (1-butyl-2,3-dimethylimidazolium chloride and 1-butyl-2,3-dimethylimidazolium tetrafluoroborate) and hydrogen bond acceptor (ethylene glycol and diethylene glycol) to prepare deep eutectic solvents at different molar ratios. The selected deep eutectic solvents were used to calculate the activity coefficients at infinite dilution in 29 solutes (alkanes, alkenes, alkynes, alcohols, tetrahydrofuran, ketones, aromatic hydrocarbons, thiophene, acetonitrile) at a temperature range of (313.15 – 343.15) K and at atmospheric pressure of 101 kPa. The column loading was composed of 30 mass percentage of DES and 70% solid support material (chromosorb). To gain a better understanding of the types of interactions between solutes and the DESs being studied, various thermodynamic functions at infinite dilution, including Gibbs free energies, entropies, and partial molar enthalpies, were calculated. The capacity and selectivity values were used to evaluate the separation potential of the DESs in different industrial mixtures.

Furthermore, binary systems comprising of {DES5(1-butyl-1-methylpyrrolidinium bromide + ethylene glycol) with alcohol or acetic acid and DES6(1-butyl-3-methylimidazolium chloride + ethylene glycol) with alcohol or acetic acid}. The physical properties such as densities, speed of sound and refractive indices of the prepared

binary mixtures were measured at temperatures *T*= (293.15 – 313.15) K and at atmospheric pressure. The interactions between the systems were interpreted by the computed excess properties such as excess molar volumes, isentropic compressibilities, deviation in isentropic compressibilities, deviation in refractive index, and intermolecular free lengths.

1.4 Aims and objectives

Aim

The aim of this work is to determine the intermolecular interactions in the synthesized deep eutectic solvents (DESs) and evaluate the effectiveness of the latter in separating azeotropic industrial mixtures at different temperatures.

Objectives

- To prepare DESs using imidazolium or pyrolidinium cation
- To calculate activity coefficients at infinite dilution for different solutes in deep eutectic solvents using retention data acquired by GLC.
- To assess the separation performance of the deep eutectic solvents by calculating the selectivity and capacity data.
- To determine the influence of temperature on the binary mixtures.
- To measure the physical properties (density, speed of sound, viscosity, and refractive index) of the DESs and alcohol mixtures at different temperatures.
- To determine the intermolecular interactions by computing thermodynamic parameters such as excess molar volume, Gibbs free energies, enthalpies, entropies, intermolecular free length, isentropic compressibility, and deviation in isentropic compressibility.
- To correlate the experimental data with the Lorentz-Lorenz equation.

1.5 Outline of thesis

Chapter 1: Introduction describes the background, problem statement, justifications and aims and objectives.

Chapter 2: Literature review will provide review of relevant literature, forming the basis and motivation of this study.

Chapter 3: Theoretical framework will discuss the thermodynamic framework and calculations in relation to this work.

Chapter 4: Experimental procedures, materials, and equipment

Chapter 5: Results and discussions of the activity coefficient at infinite dilution for the test system.

Chapter 6: Results and discussions of the thermophysical properties investigated for binary systems.

Chapter 7: Conclusions

CHAPTER 2: LITERATURE REVIEW

2.1 Historical Background of Deep Eutectic Solvents (DESs)

Ionic liquids became popular in the 20th century due to their unique properties which led to an increase in the interest of different industries applications. However, the ionic liquids 'green' characteristics came into question due to their unfavourable properties which include high toxicity, poor biodegradability, and lack of biocompatibility (Li and Row 2016). The concept of deep eutectic solvents was then introduced by Abbott et al in 2003 (Abbott *et al.* 2003). Deep eutectic solvents (DESs) are solvents formed from mixing two or more components, often a hydrogen bond donor (HBD) and a hydrogen bond acceptor (HBA), which when combined their melting point is much lower than those of the individual constituent components which create a eutectic mixture (Abbott *et al.* 2011). The deep eutectic solvents have gained recognition as 'greener' alternatives to conventional solvents due to their low toxicity and biodegradability. For better understanding of the different types of deep eutectic solvents Abbot et al 2007 divided the DESs in two four categories namely, type i (quaternary salt and metal halide), type ii (quaternary salt and hydrated metal halide, type iii (quaternary salt and hydrogen bond donor), and type iv (metal halide and hydrogen bond donor)(Abbott *et al.* 2007). There is a recently proposed type v of the deep eutectic solvents which are solely prepared from non-ionic precursors(Abranches *et al.* 2019; Abranches and Coutinho 2022).

The development of the deep eutectic solvents has led to exploration of the DESs as alternative solvents to traditionally used organic solvents in a wide range of applications(Tang and Row 2013). The deep eutectic solvents have gained recognition as 'greener' alternatives to conventional solvents due to their low toxicity and biodegradability. The discovery of deep eutectic solvents sparked much interest in different research fields including material science and chemistry. Deep eutectic solvents have been investigated and exhibited tuneable properties including viscosity, polarity and solubility, which makes them adaptable for a wide range of applications. More research is being conducted to understand the solvation behaviour of DESs in different applications such extraction, and catalysis. The field of deep eutectic solvents continue to evolve, with ongoing research focusing on understanding their properties,

developing new formulations, and exploring the different applications. The number of scientific manuscripts related to DESs has grown over the past years as illustrated on Figure 2. 1.

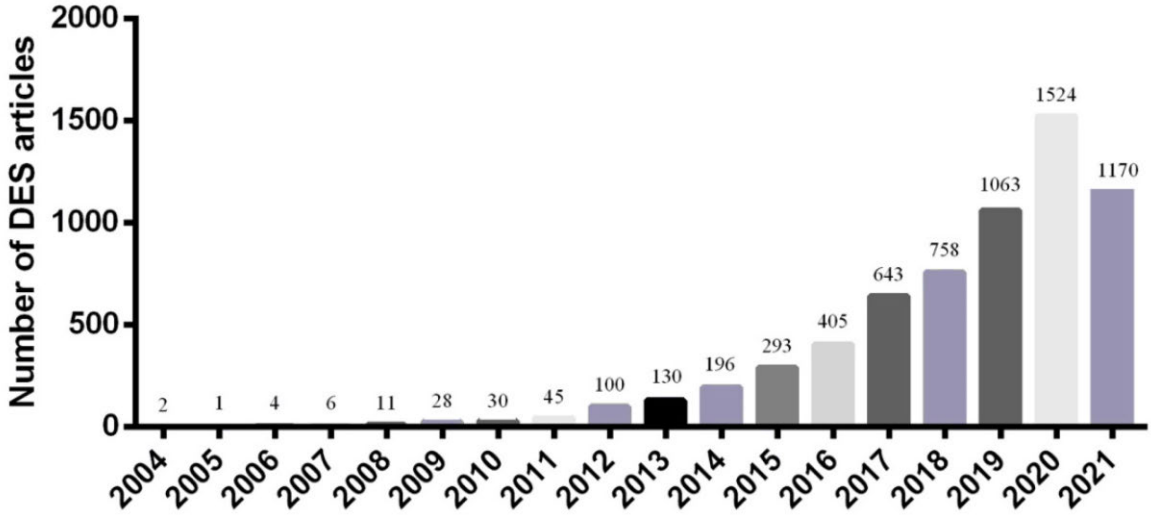

Figure 2. 1: The number of manuscripts between 2004 and 2021 about DESs (Lomba et al. 2021).

2.2 Structures of commonly used compounds in preparing DESs

As already mentioned, deep eutectic solvents are solvents prepared from mixture of hydrogen bond acceptors and hydrogen bond donors. The term eutectic refers to the melting point of the combined components which is much lower than those of the individual components. Figure 2. 2 shows the commonly used hydrogen bond acceptors and hydrogen bond donors.

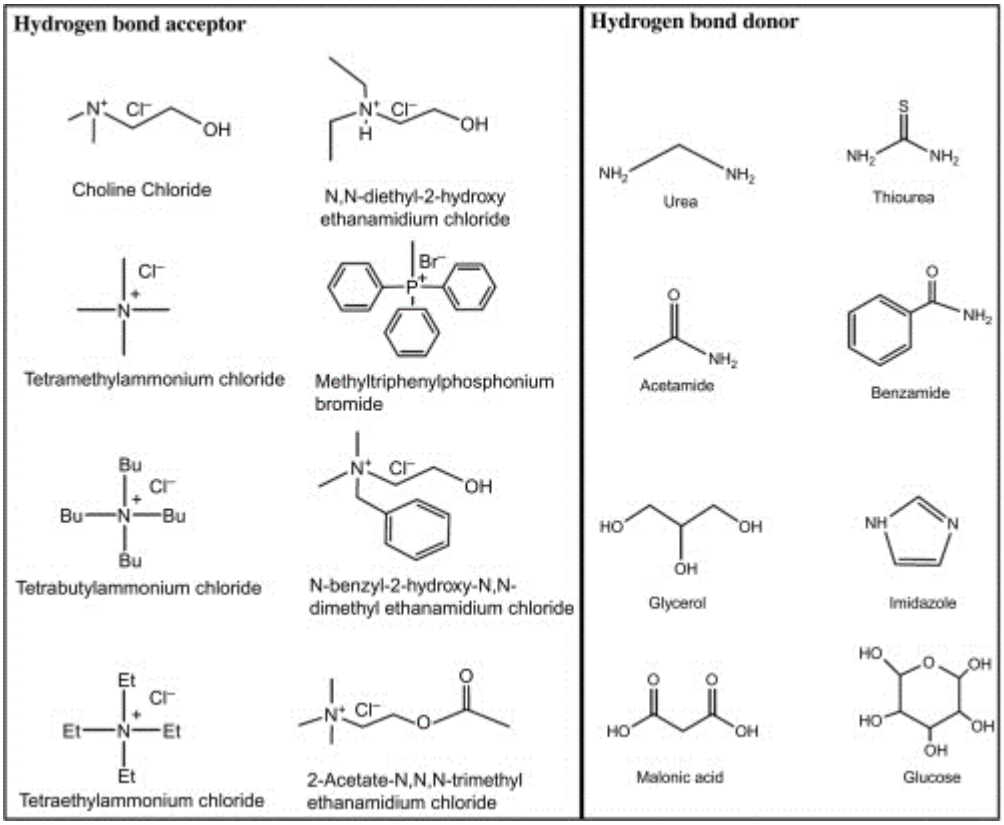

Figure 2. 2: Commonly used HBA and HBD in DESs (Arriaga and Aizpuru 2019).

2.3 Significance of deep eutectic solvents

DESs have gained significant attention and importance in various fields due to their unique properties and versatile applications. DESs are often considered more environmentally friendly than traditional solvents as they can be derived from renewable resources, making them a sustainable alternative to conventional solvents (Schuur *et al.* 2019). Wen et al. 2015 assessed the toxicity and biodegradability of cholinium-based deep eutectic solvent (DES) on diverse organisms including garlic (a plant), E. coli (a bacterium), and hydra (an invertebrate) (Wen *et al.* 2015). The two DESs were regarded as easily degradable through natural processes which proves that the DESs are biodegradable with low toxicity. The synthesis of DES typically involves low energy consumption and mild conditions, contributing to the principles of green chemistry. Bi et al. 2020 synthesized [MEAHCl] [MEA] using one-pot method by mixing NH_4Cl and MEA at a temperature of 303.15 K for 30 min, the results showed that on-site preparation is viable for industrial implementation and provides an efficient, cost-effective, and secure system for capturing CO_2 using the DES prepared (Bi *et al.* 2020).

DES exhibit excellent performance in extraction and separation processes. They have a potential to replace traditional organic solvents in processes such as liquid-liquid extraction, making these processes more environmentally friendly. Liu et al. 2022synthesized choline-based DESs using glycerol, ethylene glycol (EG), and urea for the use in azeotropic separation of methanol (MeOH)-*n*-hexane (NHA) azeotropes (Liu *et al.* 2022). The findings indicated that the deep eutectic solvents (DESs) were effective in separating MeOH-NHA azeotropes. Pekel et al. 2020 synthesized menthol-based deep eutectic liquid for the extraction of the carbamazepine from its aqueous solution (Pekel *et al.* 2020). The most effective extractant has been suggested to be a eutectic mixture of menthol and acetic acid (in a 1:1 molar ratio). This combination significantly improved the extraction yield compared to conventional diethyl succinate, resulting in an efficiency increase ranging from 11% to 36%. The DESs tuneable nature allows for customization to optimize selectivity in extraction processes.

2.4 Significance of studying activity coefficients at infinite dilutions in DESs

The behaviour of solutes in DESs at extremely low concentrations can be investigated using activity coefficients at infinite dilutions. This information is crucial for optimizing separation processes, especially in scenarios where trace amounts of a particular component need to be separated efficiently. Nkosi, Tumba and Ramsuroop 2019 used DES consisting of tetramethylammonium chloride and 1,6 hexanediol and measured activity coefficients at infinite dilution for 22 organic solutes (Nkosi, Tumba and Ramsuroop 2019). The most effective separation performance for the investigated DES was observed in mixtures containing n-alkanes and either thiophene or pyridine. Consequently, resulting conclusion was that the investigated DES stands as a viable entrainer for the denitrogenating and desulfurization of transportation fuels.

Understanding activity coefficients helps in predicting the selectivity of DES as a solvent. It provides information on the preference of the solvent for specific solutes, guiding the selection of the most suitable DES for a particular separation task. Hizaddin et al. 2015 investigated the use of DES (tetrabutylammonium bromide and ethylene glycol), the results showed elevated selectivity values (Hizaddin *et al.* 2015). Making the prepared DES suitable for separating aromatics from aliphatic hydrocarbons.

Studying activity coefficients allows for a comparative analysis of DES with traditional solvents. Domańska and Paduszyński 2010 utilized gas-liquid chromatography (GLC) to measure γ_{13}^{∞} of 33 diverse organic solutes, including cycloalkanes, alkynes, alkanes, benzene, alkylbenzene, alkenes, water, tetrahydrofuran, methyl tert-butyl ether, alcohols, and thiophene, in tri-iso-butylmethylphosphonium tosylate ionic liquid over a temperature range of 298.15 K to 368.15 K (Domańska and Paduszyński 2010). Their findings revealed that the examined ionic liquid exhibited superior capacity and selectivity at infinite dilution compared to commonly used solvents such as sulfolane or NMP for the separation of aliphatic hydrocarbons from aromatic hydrocarbons. This comparison aids in assessing the advantages and limitations of using DES in separation processes and helps position DES as potential alternatives or improvements over conventional solvents.

Activity coefficients reflect the molecular interactions between solute molecules and the components of the DESs. This understanding is crucial for designing DES with specific properties tailored to the requirements of different separation processes. (Kabane and Redhi 2020) calculated the activity coefficients at infinite dilution for 33 solutes in deep eutectic solvent, specifically (1-butyl-3-methylimidazolium chloride + glycerol). The measurements of activity coefficients allowed for the determination of separation capacity and molecular interactions of solutes within the deep eutectic solvent. Moreover, the activity coefficient data were utilized to calculate separation parameters, including selectivity and capacity, for specific industrial extraction scenarios involving hexane/benzene, cyclohexane/benzene, acetone/ethanol, and cyclohexane/ethanol. Excess thermodynamic functions were computed to provide additional insights into the interactions between the investigated DES and solutes. These thermodynamic parameters revealed the hydrophobic nature of the prepared DES. The separation parameters indicated a suboptimal capacity (<1), signifying the DES's limited performance as a separation solvent.

2.5 Thermophysical properties of deep eutectic solvents

The thermophysical properties of deep eutectic solvents (DES) are of significant importance due to their implications in various industrial processes and applications. Understanding properties of DESs provides insights into their behaviour and performance, influencing their design, optimization, and utilization. Thermophysical properties, including density, viscosity, speed of sound, and refractive index, are

crucial for designing and optimizing processes involving DESs. Shekaari et al 2017 investigated the thermophysical properties of deep eutectic solvent (choline chloride/urea) at a temperature range of (293.15 to 323.15) K (Shekaari, Zafarani-Moattar and Mohammadi 2017). Measurements of densities, speed of sound, and refractive indices were conducted for both the pure DES and its aqueous solutions. The obtained data were utilized to calculate various thermodynamic and transport properties. The excess molar volumes were consistently negative throughout the concentration range and temperatures studied, suggesting the breaking of hydrogen bonds in water molecules and the incorporation of DES molecules into the water network. Additionally, the isentropic compressibilities of the DES solutions decreased with increasing DES concentration at all temperatures, indicating the disruption of the hydrogen-bond network in water due to mixing with the DES.

Thermophysical properties provides information about molecular interactions within the DES. (Sánchez *et al.* 2019) reported densities, refractive indices and speed of sound for deep eutectic solvents (betaine + dl-lactic acid + water at (1:1:1), betaine + citric acid + water at (2:1:6), betaine + dl-lactic acid at (1:2), betaine + dl-lactic acid at (1:5), betaine + levulinic acid at (1:2), l-proline + levulinic acid at (1:2) and l-proline + dl-lactic acid at (1:1) at temperatures T= 293.15 K - 343.15 K. From the data obtained in the experiments, the thermal expansion coefficients, isentropic compressibility, and molar refraction coefficients were computed to determine interactions occurring as all these DESs, show a decrease in viscosity when temperature increases. The viscosity of DES affects the flow characteristics and ease of handling, influencing aspects of sustainability and safety.

Understanding the thermophysical properties of DES in binary or ternary mixtures with other solvents is crucial for predicting their behaviour in co-solvent systems. Thermophysical properties were identified to gain insights into the interactions between solutes and deep eutectic solvents in aromatic mixtures reported by (Shekaari, Zafarani-Moattar and Mohammadi 2020). The outcomes reveal that the deep eutectic solvent (ChCl:DGA) at a molar ratio of 1:5 exhibits a higher B-coefficient and lower V^0_ϕ or κ_ϕ values. These findings suggest more pronounced solute-solvent interactions between benzene or thiophene and DES (ChCl:DGA)(1:5) compared to other solvents. This knowledge is essential in applications where multiple solvents are used for enhanced performance and specific functionalities.

The newly introduced deep eutectic solvents (DESs), consisting of tetrabutylammonium chloride paired with 3-amino-1-propanol, tetrabutylammonium bromide paired with 3-amino-1-propanol, or 2-(methylamino) ethanol, or 2-(butylamino) ethanol, exhibit promising properties (Nowosielski *et al.* 2022). These properties make them appealing for further assessment and optimization in the development of cost-effective eco-solvents and other valuable materials. The comprehensive investigation covered key physicochemical properties, including densities, speed of sound, refractive indices, and viscosities, measured in their aqueous solutions across the entire composition range at atmospheric pressure and temperatures ranging from 293.15 K to 313.15 K. The application of the Jouyban–Acree model successfully correlated the experimental physical properties with concentration, demonstrating the accuracy of this mathematical equation for predicting the properties of aqueous DES.

Considering all the information provided above and the knowledge derived from the existing literature, the systems examined in this study have not been explored previously.

CHAPTER 3: THEORETICAL FRAMEWORK

3.1 Introduction to thermodynamics

Thermodynamics is the study focused on the relationship between energy, heat and work. The concept of thermodynamics was first introduced to understand how the engine works. The concept was used to explain how the engine convert heat into motion (Bejan 2016). This then formed a branch of physics that dealt with the properties of matter and their mechanical work, until Gibbs realized that there is a chemical reaction involved in energy change, and hence started studying the relationship between the chemical reaction and energy transformation. This involved the monitoring of chemical reactions occurring due to a change in temperature, pressure, and volume.

3.1.1 Significance of thermodynamics

Thermodynamics is a fundamental area of science that is used in different fields such as chemistry, physics, engineering, and biological sciences. The main significance of this concept is that it is used to study the behaviour of materials at different conditions, from high pressure and temperature to low pressure and temperature environments (O'Connell and Haile 2005). Thermodynamics has proven to be a fundamental key component in understanding and designing engines (Astumian 2010). These engines are then used to optimize the energy use such as power plant and car engines. Thermodynamics has also proven its importance when it comes to the environmental studies, as it is used in research areas which deals with climate, that helps in understanding the energy transfer in oceans, land and the atmosphere (Dincer 2000).

In chemical reactions, the principle has proven to be essential in understanding the chemical reactions and interactions occurring between molecules for better design of chemical processes. This knowledge is now used in industries such as pharmaceuticals, food processing and petrochemicals. Thermodynamics is also crucial in material science as it helps to explain different properties and behaviours of materials as the condition around that material change such as temperature and pressure changes.

3.2 Fundamentals of activity coefficient at infinite dilution

Thermodynamic properties of solute in a solution can be described using the activity coefficients at infinite dilution and this is done when the solute is infinitely diluted in the solution. Activity coefficients at infinite dilution is the ratio of activity of the solute in the solution to the activity of the solute in its pure form. Activity coefficients at infinite dilution is a crucial parameter in different chemical processes such as separation processes, solvent extraction and the separation design processes (Gautreaux Jr and Coates 1955). Activity coefficient at infinite dilution is based on thermodynamics to understand the deviation of the solute from the ideal behaviour as it interacts with a solvent as its concentration approaches zero.

There are different factors affecting the activity coefficient at infinite dilution which include temperature, pressure, as well as the nature of the solute and solvent (Sandler 1996). Generally, the activity coefficient decreases with increasing temperature and pressure. There are various experimented methods used to determine the activity coefficients, these include extrapolation of the solubility data to infinite dilution (Sandler 1996), measuring the osmotic coefficient (Lindenbaum and Boyd 1964), and use of retention data and pressure from the gas liquid chromatography and the use of activity coefficient equations (Kabane and Redhi 2019).

3.2.1 Importance of activity coefficients

The activity coefficient measurements are imperative in understanding how the solute behaves and interacts with the solvent in mixtures. The activity coefficient at infinite dilution is important as it is used to predict the behaviour of mixtures for different industrial applications, such as in the design and operation of separation processes like crystallization, distillation, and extraction (Królikowski *et al.* 2022). Accurate activity coefficient measurements at different concentrations and temperatures helps with the optimization of the conditions' processes, improve efficiency, and reduce the operation costs associated with the process. Activity coefficients provides insight into the thermodynamic properties of the system and interactions occurring between the solute and solvent, which in turn determine the stability of the solvent in separation processes. Thus, determination of activity coefficients serves as a crucial element in designing and optimization of industrial processes and for developing a fundamental understanding of the behaviour of the solvent investigated for further application in different industries.

3.2.2 Different methods used to determine the activity coefficients at infinite dilution.

There are various methods used to determine the activity coefficients at infinite dilutions, this includes the theoretical and experimental techniques. The theoretical methods are commonly used as they estimate the behaviour of solutes at infinite amount in a mixture.

The activity coefficient models are UNIQUAC (universal quasichemical) and NRTL (Non-Random Two-Liquid), these can be used to estimate the activity coefficient at infinite dilution based on parameters obtained from experimental data at finite concentrations. Molecular dynamics simulations can also be used to theoretically predict the activity coefficients at infinite dilution, where a computer simulation is used to model the behaviour of solutes at molecular level. Then the simulated system at infinite dilution will be used to analyse the solute-solvent interactions and finally estimate the activity coefficients at infinite dilution. Theoretical models commonly used are briefly explained.

3.2.2.1 UNIFAC (UNIQUAC Functional-group Activity Coefficients)

The Universal Quasi chemical Functional Group Activity Coefficients (UNIFAC) is a collective contribution method used to predict the activity coefficients of liquid mixtures. The model was first designed for mixtures (Fredenslund, Jones and Prausnitz 1975).The concept is based on the fact that the interaction of different molecules with different functional groups in a mixture can determine the thermodynamic property of the mixture. The model has since been improved by (Wang *et al.* 2008) to accommodate new developed liquids such as ionic liquids where the model uses a novel group segmentation group, which recommend all strong electronegative atoms (N and F) and the surrounding atoms are treated as one combined group in order to comply with the group neutrality assumption. UNIFAC is widely used in different areas such as process design for modelling, chemical engineering and simulations of different industrial processes including liquid-liquid extraction, distillation and extraction. The method has proven to be effective and provide efficient computational computed thermodynamic properties of complex mixtures using limited data obtained experimentally.

3.2.2.2 Conductor-like Screening Model (COSMO)

The Conductor-like Screening Model for Real Solvents (COSMO-RS) and Conductor-like Screening Model for Segment Activity Coefficient (COSMO-SAC), the extension of COSMO-RS explicitly designed for solvent mixtures where SAC represent the Segment Activity Coefficient model (Klamt *et al.* 1998). COSMO-RS is a model which determines the solute-solvent interaction through the use of statistical thermodynamics concept of the reference system. There are different properties which can be predicted using the COSMO-RS model which include solubility, activity coefficients, partition coefficients (Gerber and Soares 2010; Klamt, Eckert and Arlt 2010). These predictions are done by simulating a solvation process of molecules in different solvents and put to consideration both the electrostatic interactions and dispersion forces between the solute and solvent molecules. There are different areas which uses the COSMO-RS such as in drug designing, solvent selection and optimization processes in chemical engineering. Unlike COSMO-RS, in COSMO-SAC the molecules are divided into different segments based on their structural differences and they are assigned activity coefficients based on their segments. Through the consideration of each segment contribution, the COSMO-SAC predicts the activity coefficients in complex solvents.

3.3 Determining Activity coefficient by Gas liquid chromatography.

Gas liquid chromatography method was used to determine the activity coefficient at infinite dilution for all the prepared deep eutectic solvents in this work. Martin and Synge (1941) were the first to explore the method of using chromatography to determine the activity coefficients through a research paper (Martin and Synge 1941) based on the use of gas as a mobile phase and a liquid solvent as a stationary phase. The coefficient partitioned at equilibrium was related to the retention property through plate theory. The gas-liquid chromatography with constant pressure across the column, established a connection between the solute's retention volume (VR), the gas hold-up volume (VG), and the net retention volume of the solute (KV3), leading to the general formula;

$$V_R = V_G + KV_3 \qquad (3.1)$$

The equation created by Everett (Everett 1965) and Cruickshank et al. (Cruickshank *et al.* 1969) was utilized in this study to determine the γ_{13}^{∞} values of solutes partitioning between the carrier gas (helium) and the deep eutectic solvent. In this work the solute

will be referred to as component 1, the carrier gas as component 2 and the solvent as component 3.

$$ln\,\gamma_{13}^{\infty} = ln\left(\frac{n_3 RT}{V_N P_1^*}\right) - \frac{(B_{11} - V_1^*)}{RT} + \frac{J_2^3 P_0\,(2B_{12} - V_1^{\infty})}{RT} \tag{3.2}$$

where n_3 is the number of moles of the stationary phase, T is the temperature of column in the GC oven, V_N is the net retention volume, P_0 is the outlet pressure which is the same as the atmospheric pressure, P_1^* represents the saturated vapour pressure of the solute at temperature T, B_{11} is the second virial coefficient of pure solute, V_1^* denotes the molar volume of the solute, V_1^{∞} is the partial molar volume of the solute at infinite dilution (taken to be equal to V_1^*), B_{12} represents the cross second virial coefficient of the solute (1) and the carrier gas (2), and $J_2^3 P_0$ is the mean column pressure. B_{11} and B_{12} were determined using the McGlashan and Potter (McGlashan and Potter 1962) equation:

$$\frac{B}{V_C} = 0.43 - 0.886\left(\frac{T_C}{T}\right) - 0.694\left(\frac{T_C}{T}\right)^2 - 0.0375(n-1)\left(\frac{T_C}{T}\right)^{4.5} \tag{3.3}$$

where n refers to the number of carbon atoms of the solute. The combining rules of Hudson and McCoubrey (Hudson and McCoubrey 1960) were used to calculate the values of pseudo-critical volume and temperature (V_{12}^C and T_{12}^C) of the mixture from the critical properties of the pure components. The net retention volumes of the solutes, V_N, is given by:

$$V_N = J_2^3 (t_R - t_G) q_o \tag{3.4}$$

where t_R is the retention time for the solutes and t_G, the unretained gas (air) retention time. U_0 denotes the inert gas flow rate at the column outlet.

$$q_{ov} = q_o \left(\frac{T}{T_f}\right)\left[1 - \frac{P_w^*}{P_o}\right] \tag{3.5}$$

Where q_o is the measured flow rate, T_f the flow-meter temperature and P_w^* the saturated vapour pressure of water at T_f.

The pressure correction term J_2^3 detailed by Everett (Everett 1965) is given by:

$$J_2^3 = \frac{2}{3}\frac{\left(\frac{P_i}{P_0}\right)^3 - 1}{\left(\frac{P_i}{P_0}\right) - 1} \quad (3.6)$$

Saturated vapour pressures were calculated using the Antoine, or modified Antoine equations in compliance with the applicability range of each correlation. (Poling, Prausnitz and O'connell (2001) constants for the vapour pressure correlations were found in the literature, (Poling, Prausnitz and O'connell 2001; Lide 2004).The data for critical properties of solutes were obtained from the literature were used to calculate B_{11} and $B_{12}$and ionization energies used in the calculation of T_{12}^C,(Klincewicz and Reid 1984).

The cross second virial coefficient of the pure solute, B_{11}, was given by the correlation of (Tsonopoulos 1974):

$$\frac{B_{11}}{V_c} = 0{,}430 - 0{,}866\left(\frac{T_c}{T}\right) - 0{,}694\left(\frac{T_c}{T}\right)^2 - 0{,}0375(n-1)\left(\frac{T_c}{T}\right)^{4{,}5} \quad (3.7)$$

$$\frac{BP_c}{RT_c} = \frac{B}{V^*} = f^{(0)} + \omega f^{(1)} + af^{(2)} + bf^{(3)} \quad (3.8)$$

$$f^{(0)} = 0{,}1445 - \frac{0{,}330}{T_r} - \frac{0{,}1385}{T_r^2} - \frac{0{,}0121}{T_r^3} - \frac{0{,}000607}{T_r^8} \quad (3.9)$$

$$f^{(1)} = 0{,}0637 + \frac{0{,}331}{T_r^2} - \frac{0{,}423}{T_r^3} - \frac{0{,}008}{T_r^8} \quad (3.10)$$

$$f^{(2)} = \frac{1}{T_r^6} \quad (3.11)$$

$$f^{(3)} = -\frac{1}{T_r^8} \quad (3.12)$$

B_{11} is the virial coefficient, P_c, the critical pressure, T_c, the critical temperature, V^* , the characteristic volume, ω, the accentric factor, and T_r the reduced temperature. For values of a and b, correlations were used from the work of (Tsonopoulos and Heidman 1990), and (Tsonopoulos and Dymond 1997).

The second virial coefficient, B_{12}, is calculated by using equation (*3.6*), with mixing rules of (Tsonopoulos 1974):

$$T_{cij} = \left(T_{cii}T_{cjj}\right)^{1/2}(1 - k_{ij}) \quad (3.13)$$

$$V_{ij}^{*} = \frac{(V_{cii}^{1/3} + V_{cij}^{1/3})^3}{4(Z_{cii} + Z_{cjj})} \quad (3.14)$$

$$\omega_{ij} = (\omega_{ii} + \omega_{jj})/2 \quad (3.15)$$

$$a_{ij} = (a_{ii} + a_{jj})/2 \quad (3.16)$$

$$b_{ij} = (b_{ii} + b_{jj})/2 \quad (3.17)$$

where k_{ij} is the binary interaction parameter and V_c, the critical volume. An estimation of the binary interaction parameter is given by the relationship of Chueh and Prausnitz (1967) for the reduction of dipole moment (μr) close to zero (Chueh and Prausnitz 1967).

3.3.1 Excess thermodynamic properties

The excess thermodynamic properties including enthalpies, entropies, and Gibbs free energies at infinite dilution were also calculated for all the chosen volatile organic solutes. The values of entropies and enthalpies at infinite dilution were calculated using the Van't Hoff relation show below.

$$\ln(\gamma_{13}^{\infty}) = \frac{\Delta H_1^{E,\infty}}{RT} - \frac{\Delta S_1^{E,\infty}}{R} \quad (3.17)$$

The thermodynamic excess properties were obtained by fitting of the natural logarithm of the experimental activity coefficients at infinite dilution.

$$\ln(\gamma_{13}^{\infty}) = \frac{a}{T} + b \quad (3.18)$$

b represents intercepts, while a represents the slope in such that $\Delta H_i^{E,\infty}$ = aR and $\Delta S_i^{E,\infty} = -bR$. The Gibbs free energies were obtained using equation (*3.19*) below.

$$\Delta G_i^{E,\infty} = RT \ln(\gamma_i^{\infty}) = \Delta H_i^{E,\infty} - \Delta S_i^{E,\infty} \quad (3.19)$$

3.3.2 Selectivity and capacity

In the current study, the selectivity and capacity values were calculated using equations (3.20 and 3.21).

$$S_{ij}^{\infty} = \frac{\gamma_i^{\infty}}{\gamma_j^{\infty}} \quad (3.20)$$

$$K_j^{\infty} = \frac{1}{\gamma_j^{\infty}} \quad (3.21)$$

Where *i* and *j* are the solutes being represented by the subscripts.

3.4 Thermophysical properties

3.4.1 Density

Density is described the mass of one compound per unit volume. The general formula for calculating density of a compound is as follows.

$$\rho = \frac{m}{v} \tag{3.22}$$

Where m and v represent the mass and volume of the compound, respectively.

3.4.2 Speed of sound

Speed of sound also referred to as sound velocity is determined by the distance and time of the sound wave transmitted between the receiver and transmitter. Speed of sound can be calculated by using the equation (*3.23*) below.

$$u = \frac{l \times \left(\frac{1}{1 \times 10^{-5} \times \Delta T}\right)}{\left(\frac{P_s}{512}\right) - A \times f_3} \tag{3.23}$$

l, ΔT, P_s, A and f_3 represent the path length, the deviation in temperature, the oscillation interval of the sound waves received, A denotes constant speed of sound apparatus, and the correction term for temperature, respectively. The density and speed of sound are temperature dependent.

3.4.3 Viscosity

Viscosity is defined as a function of temperature and pressure. It is an important property of liquids. Viscosity is measured by the ratio of shearing stress to the velocity gradient in a fluid. If a ball is dropped into a fluid, the viscosity can be determined using the following formula:

$$\eta = \frac{2ga^2(\Delta\rho)}{9v} \tag{3.24}$$

Where $\Delta\rho$, a, g, and v represent the density difference between fluid and the ball tested, radius of the ball, the acceleration due to gravity, and velocity of the ball.

3.4.4 Refractive index

Refractive index is the ratio of the velocity of light in a vacuum to the velocity of light in a specified medium. Refractive index is defined by the formula.

$$n = \frac{c}{v} \tag{3.25}$$

Where n, c, and v represent the refractive index, speed of light and phase velocity light, respectively.

3.4.5 Excess molar volumes

Excess molar volume is the fundamental property in thermodynamic properties of liquid mixtures. The excess molar volume is defined from the molar volume equation (refs; Walas 1985, McGlashan 1979, Letcher 1975).

$$V_m^E = \frac{X_1M_1 + X_2M_2}{\rho} - \left(\frac{X_1M_1}{\rho_1} + \frac{X_2M_2}{\rho_2}\right) \tag{3.26}$$

Where X_1 and M_1 represent the molar fraction and molar mass of the component 1, and X_2 and M_2 represent the molar fraction of component 2. In this, ρ, ρ_1 and ρ_2 represent the densities of the binary mixture, pure component 1 and pure com ponent 2. The excess molar volume for the binary or ternary liquid mixtures are derived from the density results obtained experimentally which are valuable in explaining the intermolecular interactions between the two components interacting. The excess molar volume of liquid mixtures play a significant role in providing information about specific interactions such hydrogen donor or acceptor, specifically in liquid mixtures, dipole-dipole and Van der Waal interactions.

3.4.6 Isentropic compressibility

Isentropic compressibility is a thermodynamic property that impacts the interactions between the molecules in the binary or ternary liquid mixtures. The isentropic compressibility can be calculated using the indirect method derived by the Newton-Laplace equation given by equation (*3.27*).

$$k_s = \frac{1}{u^2 \rho} \tag{3.27}$$

Where ρ, and u represent he density and speed of sound of the mixture.

3.4.6.1 Deviation in isentropic compressibility

The deviation in isentropic compressibilities ($\Delta\kappa_S$) are used to study the variation of a real mixtures from ideal and understand the strength and nature of interactions between molecules in a liquid mixture.

$$\Delta k_s = k_s - k_s^{id} \tag{3.28}$$

Where Δk_s, k_s, and k_s^{id} are the deviation in isentropic compressibilities, isentropic compressibilities for the real and ideal mixtures, respectively.

Where the ideal isentropic compressibility is calculated using;

$$k_s^{id} = \sum_{i=1}^{n} \phi_i k_{si} \tag{3.29}$$

Where ϕ_i and k_{si} are volume fraction and isentropic compressibility of pure component i, respectively.

3.4.7 Intermolecular free length

The concept of intermolecular free length which defines the distance between surfaces of two molecules, is used to explain the sound velocity in pure liquids and liquid mixtures as introduced by (Jacobson 1951; 1952a; 1952b). According to Jacobson:

$$u_{lib} = \frac{K}{L_f \rho^{1/2}} \quad (3.30)$$

where K is a temperature dependent constant, ρ is the density and L_f is the free length in the liquid. Free length theory (FLT) of Jacobson was used to evaluate the sound velocities in the liquid mixtures. Free length (L_f) of pure liquids is calculated using the equation.

$$L_f = \frac{K}{u_{exp} \rho_{exp}^{1/2}} \quad (3.31)$$

Where K represent the Jacobson's constant dependent on temperature and u_{exp} and ρ_{exp} represent the sound velocity and density determined experimentally.

3.4.8 Correlation

3.4.8.1 Correlation of excess molar volumes by the Lorentz-Lorenz approximation

Correlation of the excess molar volume of liquid mixtures can be obtained using the refractive index obtained for the binary mixtures by the Lorentz-Lorenz approximation. Within the framework of the Lorentz-Lorenz approximation, V_m^E can be correlated via the change in reduced free volume, namely:

$$\Delta\left(\frac{V_{m,f}}{R}\right) = \frac{V_{m,f}}{R} - \left(\frac{V_{m,f}}{R}\right)^2 \quad (3.32)$$

Application of the Lorentz-Lorenz equation allows this expression to be reduced to:

$$\Delta\left(\frac{V_{m,f}}{R}\right) = \frac{3}{n^2 - 1} - \frac{3}{(n^2)^{id} - 1} \quad (3.33)$$

The assumption R = Rid, is most often a highly accurate approximation. The following expression can then be obtained from equation (3.8):

$$\Delta\left(\frac{V_{m,f}}{R}\right) = \frac{V_m^E}{R} \tag{3.34}$$

Therefore,

$$V_m^E = (-\Delta n)\frac{3R(n^{id}+n)}{(n^2-1)(n^{id})^2-1)} \tag{3.35}$$

3.4.8.2 Prediction of densities by the Lorentz-Lorenz approximation

The equation below is used to correlate the densities of the binary system.

$$\rho = \frac{\left(\frac{n^2-1}{n^2+2}\right)(x_1M_1 + x_2M_2)}{\left(\frac{n_1^2-1}{n_1^2+2}\right)x_1\frac{M_1}{\rho_1} + \left(\frac{n_2^2-1}{n_2^2+2}\right)x_2\frac{M_2}{\rho_2}} \tag{3.36}$$

Where n, n_1, n_2, x_1, x_2, M_1, M_2, ρ , ρ_1, ρ_2 represent the refractive index for mixture ,component 1, component 2, molar ratio of component 1, molar ratio of component 2, molar mass of component 1, molar mass of component 2, density of mixture, density of component 1, and density of component 2.

3.4.8.3 Prediction of refractive index by the Lorentz-Lorenz approximation

The equation below utilized for the correlation of refractive index

$$n = \left(\frac{2\left(\left(\frac{n_1^2-1}{n_2^2+2}\right)x_1\rho\frac{M_1}{M_1} + \left(\frac{n_1^2-1}{n_2^2+2}\right)x_2\rho\frac{M_2}{M_2}\right) + (x_1M_1 + x_2M_2)}{[x_1M_1 + x_2M_2] - \left(\frac{n_1^2-1}{n_2^2+2}\right)x_1\rho\frac{M_1}{\rho_1} + \left(\frac{n_1^2-1}{n_2^2+2}\right)x_2\rho\frac{M_2}{\rho_2}}\right)^{1/2} \tag{3.37}$$

3.4.8.4 Root mean square deviation.

The root mean square deviation of excess molar volumes, densities and refractive indices obtained by using the Lorentz-Lorenz equations are calculated using equation (*3.38*).

$$\sigma = \sqrt{\frac{1}{n}\sum_{i=1}^{n}(x_i - \bar{x}_i)^2} \qquad (3.38)$$

where x_i is the set of n random variables, and $\bar{x}_i$ the corresponding set of accepted values.

CHAPTER 4: EXPERIMENTAL PROCEDURES

4.1 Preparation of deep eutectic solvents

4.1.1 Materials

The investigated deep eutectic solvents were prepared using the imidazolium based ionic salts (1-butyl-2,3-dimethylimidazolium chloride and 1-buty-2,3-dimethylimidazolium tetrafluoroborate), as the hydrogen bond acceptor and hydrogen bond donors (ethylene Glycol and diethylene Glycol) purchased from Sigma-Aldrich (South Africa), depicted in Figure 4. 1 (a-d). The analytical balance was used to accurately weigh components needed. The ultrasonic bath was used to mix the components together at a specified temperature. The water content of the prepared DESs were determined by Karl-Fischer auto titrator before beginning of the analysis.

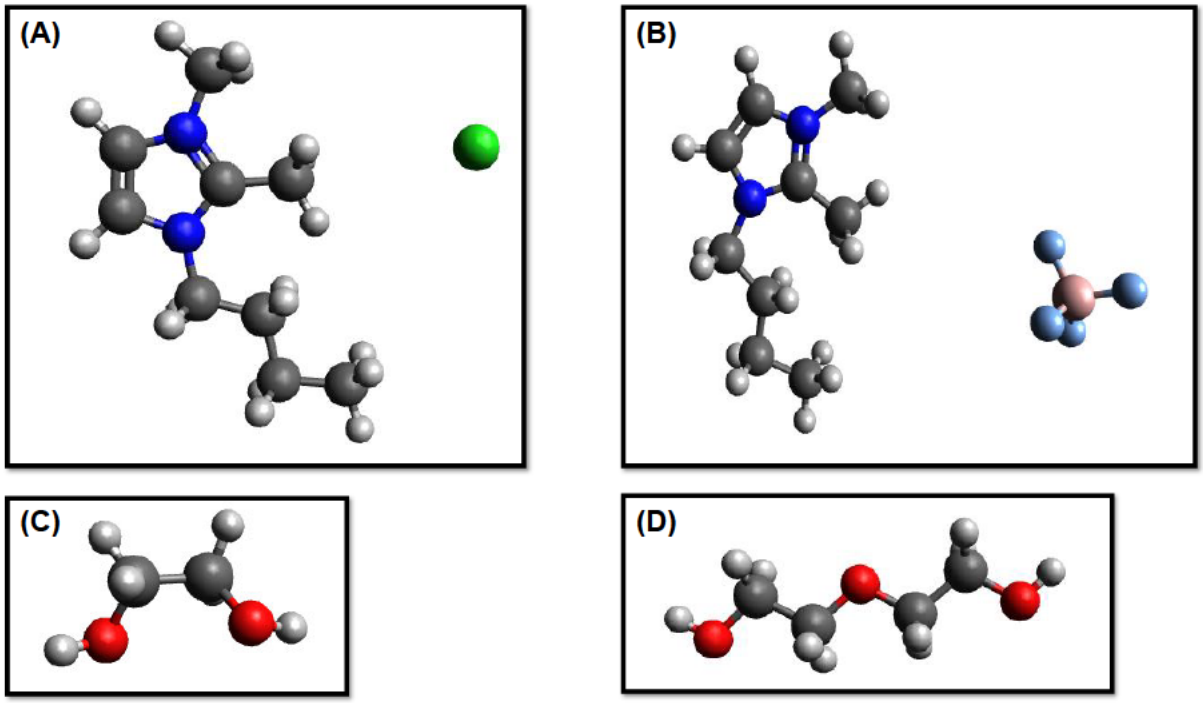

Figure 4. 1: Structure of (A) 1-butyl-2,3-dimethylimidazolium chloride, (B) 1-buty-2,3-dimethylimidazolium tetrafluoroborate, (C) ethylene Glycol, and (D) diethylene Glycol.

4.1.2 Methods

The method for the preparation of the deep eutectic solvents was adopted from a reported procedure (Fan *et al.* 2021; Manyoni and Redhi 2022b; Zafarani-Moattar, Shekaari and Sadrmousavi-Dizaj 2022). The two-imidazolium based ionic salts and hydrogen bond donors were used to prepare four different Deep eutectic solvents namely; DES1 (1-butyl-2,3-dimethylimidazolium chloride + ethylene Glycol), DES2 (1-

butyl-2,3-dimethylimidazolium chloride + diethylene Glycol), DES3 (1-buty-2,3-dimethylimidazolium tetrafluoroborate + ethylene Glycol), and DES4 (1-buty-2,3-dimethylimidazolium tetrafluoroborate + diethylene Glycol).

The DESs were all prepared by accurately weighing imidazolium ionic salt and hydrogen bond donor at a molar ratio of 1:3. The reason for choosing the 1:3 molar ratio is that the 1:3 ratio has a larger difference in availability of HBA and HBD compared to 1:2. The ratio 1:3 of HBA to HBD have lower melting point compared to DES formed with a 1:2 molar ratio, making it more suitable for low temperature applications. The two compounds were weighed using an analytical balance. The prepared weighed components were mixed for a period of 2-3 hours through stirring using the Ultrasonic water bath at a temperature, T = 333.15 K, until a clear homogeneous solvent was obtained. The obtained solvent was purified using a rotary evaporator for a period of 4-5 hours. Before starting the experimental work, the amount of water in the deep eutectic solvent was evaluated using a Karl-Fischer auto titrator. To prevent any undesirable species from contaminating the solvents, the homogeneous solvent was cooled, stored in an airtight vial and placed in a desiccator.

4.1.3 Instrumentation

4.1.3.1 Analytical Balance

Analytical balance instruments designed for precise weighing was used to weigh the compounds with a maximum capacity weight of 120g. Several advantages for weighing compounds and provide high levels of accuracy includes, high precision capabilities, often measuring weights up to four decimals (0,0001g). This level of precision allowed for an accurate weighing of small quantities of compounds, ensuring precise measurements for analytical purposes, regular calibration to maintain their accuracy, and designed to deliver consistent and reproducible results.

4.1.3.2 Karl-Fischer titrator

The Karl Fischer titration method is a widely used technique for determining the water content in a sample. It relies on a chemical reaction between water and a reagent known as the Karl Fischer reagent. The Karl Fischer titration method offers high accuracy and sensitivity, allowing for precise measurement of water content in a wide range of samples, including solids, liquids, and gases. It detects water in the parts per

million (ppm)-(ppb) range, depending on the specific setup and detection method. It is specific to water, meaning it selectively measures the water content without interference from other substances present in the sample. Its advantages make it a preferred choice as precise determination of water content is crucial for research, and process optimization. Figure 4. 2 shows the picture of the Karl-Fisher auto titrator 870 KF Titrino plus provided by Metrohn.

Figure 4. 2: Karl-Fisher auto titrator 870 KF Titrino plus (DUT Seve biko campus)

4.2 Preparation of stationary phase

4.2.1 Materials

The prepared DESs were used as the stationary phase. In order to make the stationary phase the DESs were mixed with the chromosorb which acts as a solid support for the DESs. Chromosorb (WHP 80/100) mesh which was provided by Supelco. The rotary evaporator was used to spread the DES evenly on the solid support. A 1-meter-long stainless-steel column was used to pack the stationary phase using the vacuum pump.

4.2.2 Methods

The prepared DESs were mixed at a specified amount of deep eutectic solvent with Chromosorb, which served as the support material, and then adding methanol to

ensure even distribution of the DES. The mass of solid support and stationary phase were weighed in a precision of about 0.0001 g. Methanol was then removed using a rotary evaporator, and the column was cleaned with hot soapy water, rinsed with distilled water, and dried with acetone. The resulting stationary phase contained (30-32) % of DES by mass and was packed into a 1-meter-long stainless-steel column with a 4mm internal diameter. The DES mass percentage was sufficient to prevent any adsorption onto the column packing.

4.2.3 Instrumentation

4.2.3.1 Rotary evaporator

Rotary evaporator is the commonly used technique in separating low boiling points solvents. The technique approach also enables the extraction of a solvent from a sample that contains a liquid compound, if there is minimal simultaneous evaporation (known as azeotropic behaviour) and a significant disparity in boiling points under the selected temperature and reduced pressure conditions (Craig, Gregory and Hausmann 1950). Figure 4.3 shows the photograph of a rotary evaporator. Advantages of the rotary evaporator is that the rotating flask of the rotary evaporator aids in spreading the liquid mixture (DES) evenly on the solid surface (supporting material). As the flask rotates, the DES is distributed over a larger surface area, promoting better contact and distribution of the liquid on the solid supporting material. The gentle heating provided by the rotary evaporator helps in evaporating the assisting solvent without overheating or damaging the liquid or the solid. This controlled heating ensures that the solvent evaporates evenly, preventing any concentration gradients or uneven spreading on the solid.

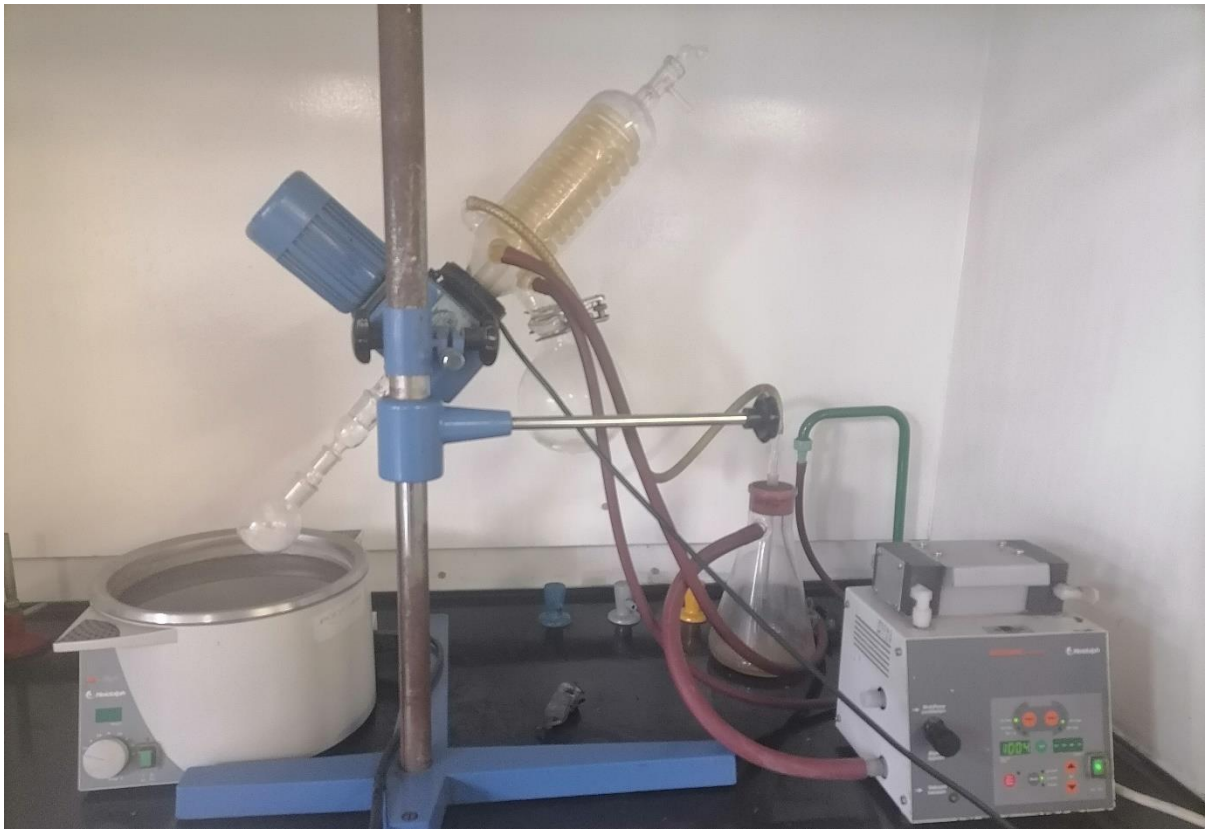

Figure 4. 3: Photograph of rotary evaporator (DUT ML Saltun campus)

4.3 Gas liquid chromatography

The gas liquid chromatography method was first proposed for investigating the physical properties at infinite dilution in the 1950s (Kojima, Zhang and Hiaki 1997). The method has become more common for the measurements of activity coefficient at infinite dilution for volatile organic solutes in non-volatile solvents as the measurements are rapid and proven to be reliable. The solvents used in investigating the activity coefficients at infinite dilution are coated on the inside of the column with the supporting material. The reported uncertainty for using this method lies between 3 to 5% (Domańska and Paduszyński 2010; Singh *et al.* 2016; Nkosi, Tumba and Ramsuroop 2018).

4.3.1 Materials

To obtain retention data for solutes in the DES, a GC-2014 Shimadzu Gas Chromatography coupled with Thermal Conductivity Detector (GC-TCD) was used. Helium which is an inert gas with purity of more than 0.99999, was used as a carrier gas and was provided by Afrox. A digital barometer was used to measure an atmospheric pressure which has an uncertainty of about 0.1 hPa. A soap bubble flow

meter which was located at the outlet of the detector was used to examine the carrier gas flow rate. A micro syringe was used to inject the solutes manually. The different solutes analysed are listed below on Table 4.1.

Table 4. 1: Solute specifications: supplier, mass fraction purity and CAS number

Solutes	Supplier	Mass fraction purity	CAS No.
2,2-Dimethylbutane	Merck	≥0.99	75-83-2
n-Pentane	Sigma-Aldrich	≥0.99	109-66-0
n-Hexane	Sigma-Aldrich	≥0.99	110-54-3
n-Heptane	Sigma-Aldrich	≥0.99	142-82-5
n-Octane	Sigma-Aldrich	≥0.99	111-65-9
n-Nonane	Merck	≥0.99	111-84-2
n-Decane	Merck	≥0.99	124-18-5
1-Pentene	Sigma-Aldrich	≥0.99	109-67-1
1-Hexene	Sigma-Aldrich	≥0.99	592-41-6
1-Heptene	Sigma-Aldrich	≥0.99	592-76-7
1-Nonene	Fluka	≥0.99	124-11-8
1-Decene	Fluka	≥0.99	872-05-9
Cyclohexene	Merck	≥0.99	110-83-8
Cyclohexane	Merck	≥0.99	110-82-7
Cyclooctane	Merck	≥0.99	292-64-8
1-Pentyne	Sigma-Aldrich	≥0.99	627-19-0
Hex-1-yne	Sigma-Aldrich	≥0.97	693-02-7
Hept-1-yne	Sigma-Aldrich	≥0.98	628-71-7
Benzene	Sigma-Aldrich	≥0.99	71-43-2
Toluene	Sigma-Aldrich	≥0.99	108-88-3
Ethylbenzene	Sigma-Aldrich	≥0.99	100-41-4
o-Xylene	Sigma-Aldrich	≥0.99	95-47-6
m-Xylene	Sigma-Aldrich	≥0.99	108-38-3
p-Xylene	Sigma-Aldrich	≥0.99	106-42-3
Methanol	Sigma-Aldrich	≥0.99	67-56-1
Ethanol	Sigma-Aldrich	≥0.99	64-17-5
Propan-1-ol	Sigma-Aldrich	≥0.99	71-23-8
Butan-1-ol	Sigma-Aldrich	≥0.99	71-36-3
THF	Sigma-Aldrich	≥0.99	109-99-9
Thiophene	Sigma-Aldrich	≥0.99	110-02-1
Acetonitrile	Sigma-Aldrich	≥0.99	75-05-8
Acetone	Sigma-Aldrich	≥0.99	67-64-1
2-Butanone	Sigma-Aldrich	≥0.99	78-93-3

4.3.2 Methods

The column was installed and conditioned in the gas-liquid chromatography oven by passing a carrier gas (helium) through it for 8 hours at T=360 K. The carrier gas flow rate was measured using an automated soap bubble flow meter linked to the GC detector outlet. The flow rate was at 30 mL/min. A pressure transducer application was used to measure the pressure drop with uncertainty of about 0.1 hPa. To obtain retention data for solutes in the DES, a GC-2014 Shimadzu Gas Chromatography coupled with Thermal Conductivity Detector (GC-TCD) was employed. The measurements were facilitated using the GC-Solution software program. The solutes were injected manually using a micro syringe, and the analysis was performed within a column temperature range of (313.15-353.15) K. Injection volumes ranging from 0.1 µL to 0.3 µL were used for the solutes to ensure that the solvents were in an infinite dilution state. The column temperature was kept constant at about 0.02 K. The reproducibility was checked by repeating the experiments 2-3 times at all given temperatures. The predicted measurement error for the infinite dilution activity coefficients was estimated to be 5%, considering the errors in solvent preparation, column packing, vapor pressure, and solute retention data measurements.

4.3.3 Instrumentation

4.3.3.1 Gas chromatography

Gas chromatography is a commonly used analytical technique in separation and analysis of volatile compounds in mixtures. One common application of GC is to determine the activity coefficient at infinite dilution using the retention data obtained. The determination of the activity coefficient at infinite dilution involves the use of a packed stainless-steel column. Where the column is filled with the stationary phase. Figure 4.4. shows the representation of the GLC setup. A Shimadzu GC-2014 gas chromatograph equipped with thermal conductivity detectors (TCD) was utilised for experimental measurements.

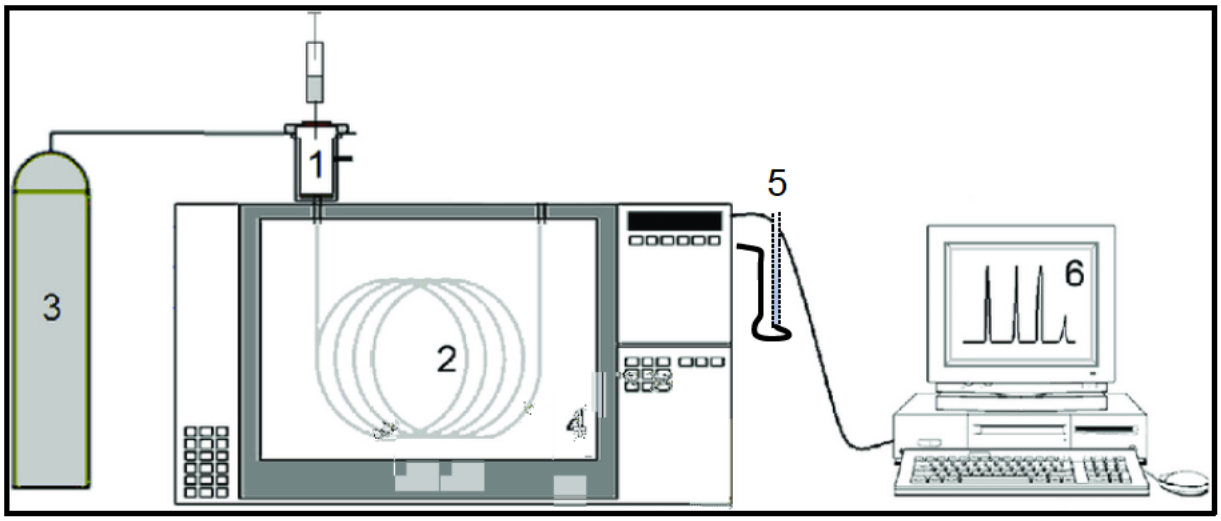

Figure 4. 4: shows the setup for the GLC technique for the determination of activity coefficients at infinite dilution. This experimental setup is similar to those used by other researchers (Letcher, 1978; Tumba, 2010). (1) Sample injection port. (2) packed column. (3) Helium gas carrier. (4) GC oven. (5) soap bubble flow meter. (6) results Display.

4.4 Thermophysical property measurements

4.4.1 Materials

The prepared deep eutectic solvents include DES5 (1-butyl-1-methylpyrilidinium bromide + Ethylene glycol) and DES6 (1-butyl-3-methylimidazolium chloride + ethylene glycol). Sigma-Aldrich (South Africa), depicted in Figure 4.5 (a-c). The used organic solvents, ethanol and acetic acid were also provided by Sigma Aldrich (South Africa). The chemicals water content was determined by the Karl-Fischer auto titrator before commencement of the experimental work.

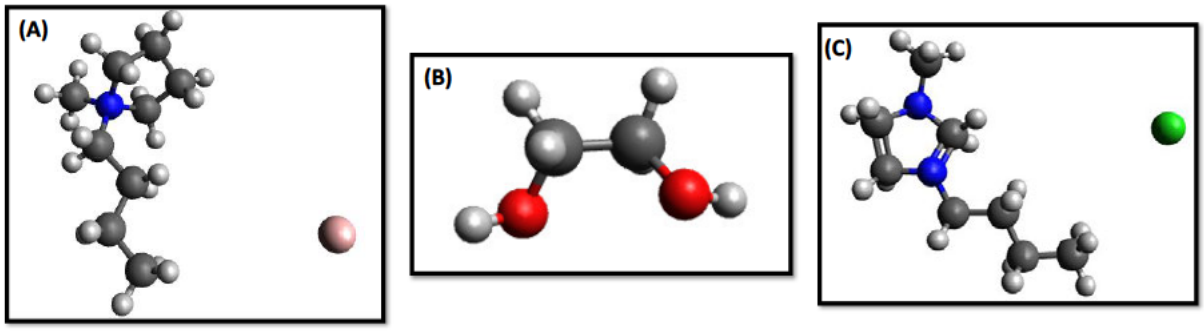

Figure 4. 5: Structure of (A) 1-butyl-1-methylPyrolidinium bromide, (B) ethylene Glycol, and (C) 1-butyl-3-methylimidazolium chloride.

Table 4. 2: The Table below shows the list of materials, supplier, purity and CAS numbers.

Solvents	Supplier	Mass fraction purity	CAS No.
1-butyl-1-methylpyrrolidinium Bromide	Sigma-Aldrich	≥0.99	93457-69-3
1-butyl-3-methylimidazolium Chloride	Sigma-Aldrich	≥0.98	79917-90-1
Ethylene glycol	Sigma-Aldrich	≥0.99	107-21-1
Acetic acid	Sigma-Aldrich	≥0.99	64-19-7
Ethanol	Sigma-Aldrich	≥0.99	64-17-5

Table 4. 3: Density and speed of sound experimental values and among literature of DES1 and ethanol.

Solutes	T/K	ρ/g·cm^{-3}			u/(m·s^{-1})		
		Exp	Lit.	Ref.	Exp	Lit.	Ref.
DES1(BMPYRBr + EG)	293.15	1.1699			1729.48		
	298.15	1.1666			1718.04		
	303.15	1.1632			1706.33		
	308.15	1.1598			1694.24		
	313.15	1.1565			1682.44		
Ethanol	293.15	0.7928	0.7910 0.7897	(Khattab *et al.* 2012) (Álvarez *et al.* 2006)	1169.31	- 1160.00	(Pereiro and Rodriguez 2007)
	298.15	0.7885	0.7913 0.7853	(Khattab *et al.* 2012) (Álvarez *et al.* 2006)	1152.78	1145.00 1143.00	(Hasan *et al.* 2011) (Pereiro and Rodriguez 2007)
	303.15	0.7842	0.7761 0.7809	(Khattab *et al.* 2012) (Álvarez *et al.* 2006)	1135.60	1125.00 1127.00	(Hasan *et al.* 2011) (Pereiro and Rodriguez 2007)

	308.15 313.15	0.7798 0.7754	0.7718 0.7765 0.7651 0.7722	(Khattab *et al.* 2012) (Álvarez *et al.* 2006) (Khattab *et al.* 2012) (Álvarez *et al.* 2006)	1118.72 1101.94	1104.00 - 1093.00 -	(Hasan *et al.* 2011) (Hasan *et al.* 2011)
DES2(BMIMCl + EG)	293.15 298.15 303.15 308.15 313.15	1.0895 1.0863 1.0831 1.0799 1.0767			1759.11 1747.39 1735.47 1723.50 1711.52		
Acetic acid	293.15 298.15 303.15 308.15	1.0512 1.0456 1.0400 1.0343	1.0497 1.0493 1.0441 1.0436 1.0384 1.0380 1.0328 1.0325	(Singh *et al.* 2014) (González, Domínguez and Tojo 2004) (Singh *et al.* 2014) (González, Domínguez and Tojo 2004) (Singh *et al.* 2014) (González, Domínguez and Tojo 2004) (Singh *et al.* 2014) (González, Domínguez and	1164.18 1146.94 1129.73 1112.61	1152.70 1149.00 1135.70 1132.00 1118.40 1115.00 1101.20 -	(Singh *et al.* 2014) (González, Domínguez and Tojo 2004) (Singh *et al.* 2014) (González, Domínguez and Tojo 2004) (Singh *et al.* 2014) (González, Domínguez and Tojo 2004) (Singh *et al.* 2014) (González, Domínguez and

	313.15	1.0287	1.0271 -	Tojo 2004) (Singh *et al.* 2014) (González, Domínguez and Tojo 2004)	1095.59	1084.00 -	Tojo 2004) (Singh *et al.* 2014) (González, Domínguez and Tojo 2004)

4.4.2 Methods

4.4.2.1 Preparation of the binary systems

The binary mixtures of the deep eutectic solvent and ethanol or acetic acid were prepared by mixing the two solvents at a specific molar ratios into an airtight glass vials. Each solvent was weighed accurately using OHAUS analytical mass balance with high accuracy of 0.0001 g. The mixtures were then mixed vigorously to ensure ansolute homogeneity. The components with their purification percentage, CAS number and suppliers used in prepraration of the DESs and the binary mixtures are presented in Table 4. 2. Table 4. 3 shows the comparison of the experimental values to the previously reported values of the speed of sound and density for ethanol and acetic acid. However, it is noted that the DESs prepared in this work had not been used previously and therefore, there is no previosly reported densities and speed of sound to compare with.

4.4.3 Instrumentation

4.4.3.1 Sound velocity and density

The sound velocity and density of the binary mixture and the pure components were conducted using an Anton Paar DSA 5000 M equiped with the digital vibrating tube density meter and sound velocity analyser. The velocity and sound velocity meter Anton Paar DSA 5000M has an accuracy in density, sound velocity and temperature of ±5×10^{-6} g·cm^3, ±0.5 m·s^{-1}, and ±0.01 K, respectively. The instrument cells were first cleaned with toluene and dried with acetone through automatic X sampler 452 module. The cleaning routine was carried out after each measurement to avoid cross contamination. The instrument is also equiped with a built-in thermostat controller which has ability to maintain the temperature exactly to ±0.01 K whilst measuring density.

Figure 4.6 shows the DSA 5000 M coupled with microviscometer Lovis 2000 ME used to measure the density, sound velocity and viscosity. The velocity and sound velocity meter is capable of measuring the sensity over a range of (0-3×10^3) kg·m^{-3} and speed of sound between (1000 – 2000) m·s^{-1}, at various temeprature ranges of (273.15 -343.15) K, with a pressure difference of (0-0.3) MPa. Table 4.4 gives information about the instrument.

Figure 4. 6: Density and sound velocity meter DSA 5000 M coupled with microviscometer LOVIS 2000 ME and X sampler 452.

Table 4. 4: Density and sound velocity meter DSA 5000 M instrument specifications

Property	Range
Measurement range for density	0 to 3 g·cm^{-3}
Measurement range for speed of sound	1000 to 2000 m·s^{-1}
Range of pressure	0 to 3 MPa
Repeatability density	0.000001 g·cm^{-3}
Measurement range of temperature	298.15 to 343.15 K
Repeatability speed of sound	0.1 m·s^{-1}
Measurement time per sample	1 to 4 min
Repeatability temperature	298.15 K
Sample volume	Approximately 3 ml
Automatic bubble detection	Yes
Reference oscillator	Yes
Visual check of the density measuring cell	Camera
Ambient air pressure sensor	Yes

CHAPTER 5: RESULTS

Activity coefficients at infinite dilution

5.1. DES1: 1-butyl-2,3-dimethylimidazolium chloride + ethylene glycol

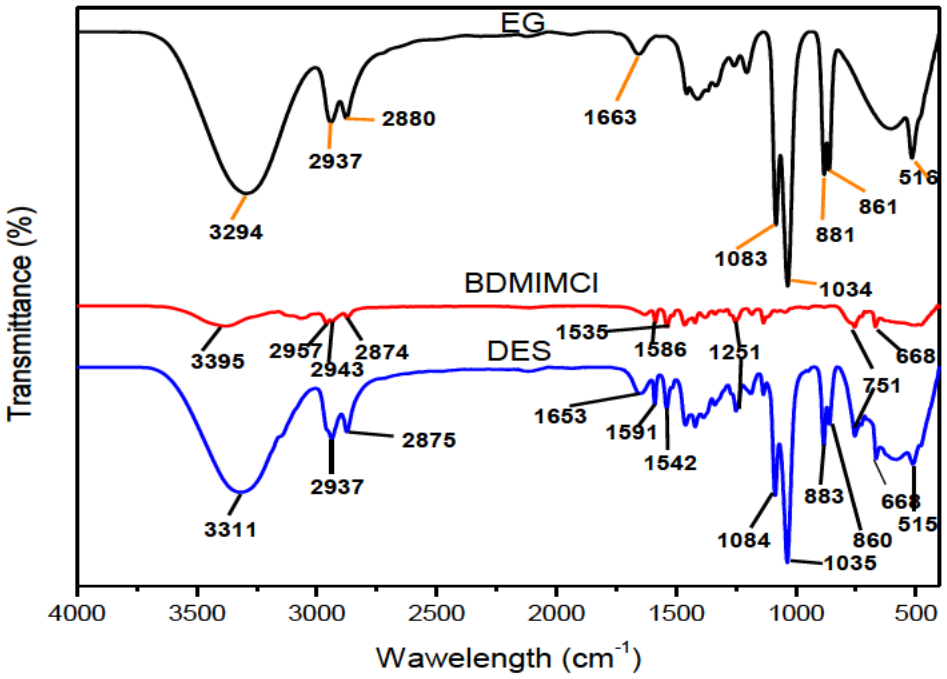

Figure 5.1. 1: FT-IR spectra of ethylene glycol (EG), 1-butyl-2,3-dimethylimidazolium chloride (BDMIMCl), and DES (BDMIMCl +EG).

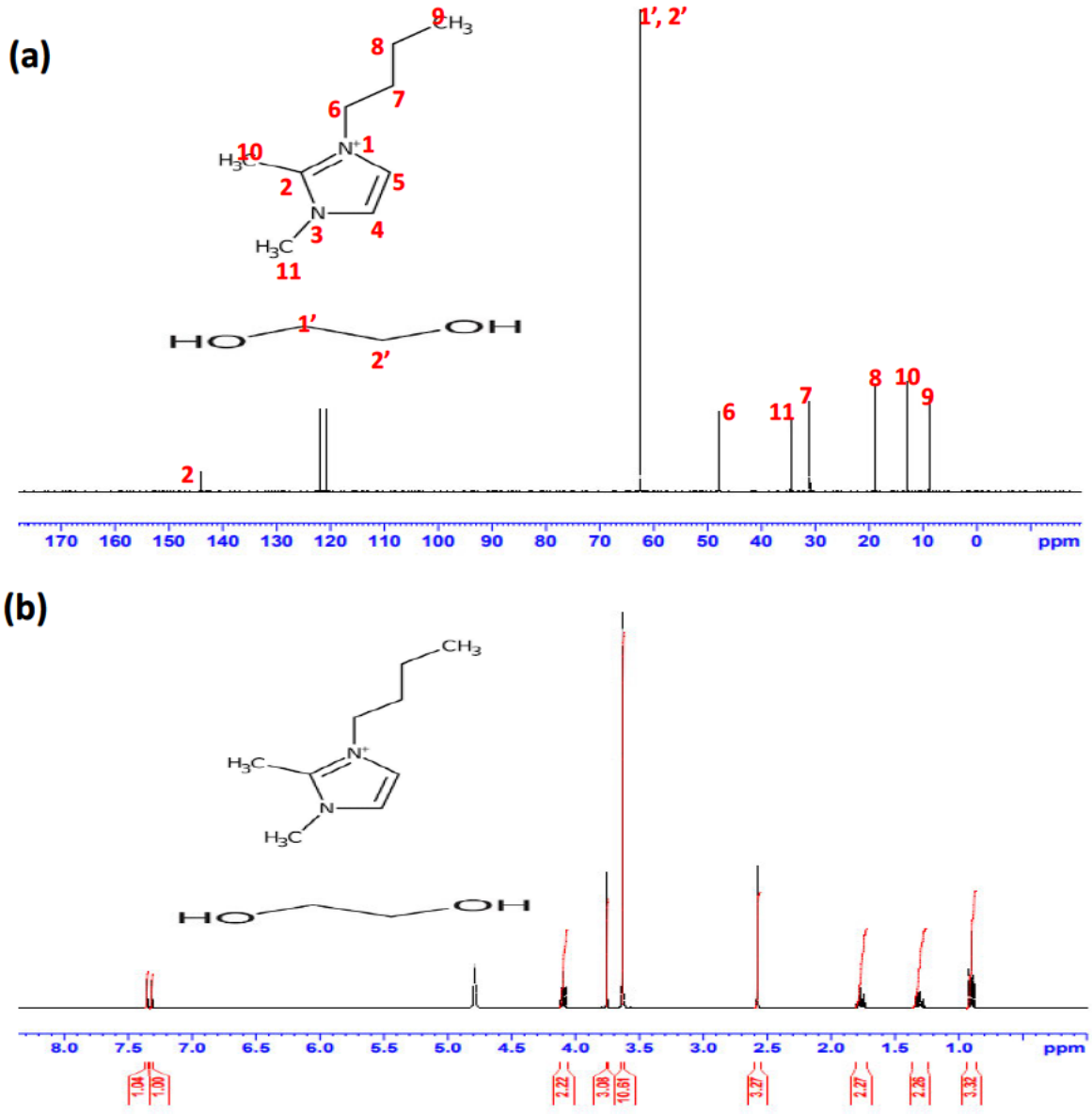

Figure 5.1. 2: (a) ^{13}C-NMR spectra, (b) ^{1}H-NMR spectra of DES (BDMIMCl +EG).

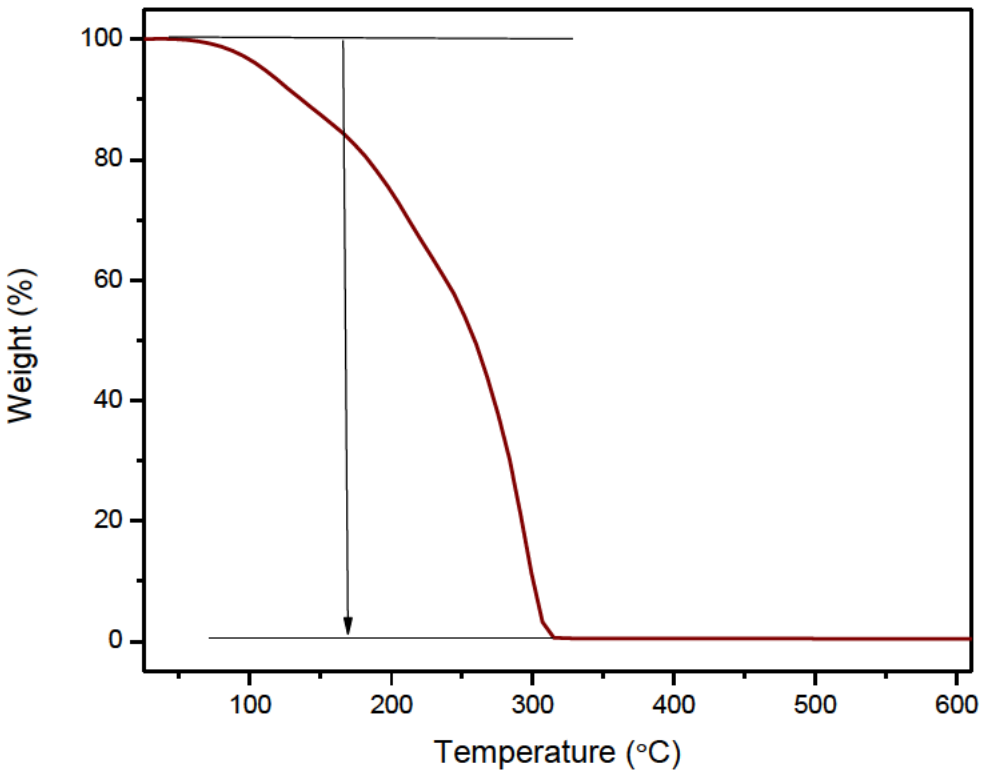

Figure 5.1. 3: Thermogravimetric analysis (TGA) curve of DES (BDMIMCl +EG) showing the thermal stability.

Table 5.1. 1: Activity coefficients at infinite dilution for the solutes in deep eutectic solvent [1-butyl-2,3-dimethylimidazolium chloride + ethylene glycol] at temperatures *T* = (313.15 - 353.15) K.

Average γ_{13}^{∞} values					
Solutes	*T* = 313.15 K	*T* = 323.15 K	*T* = 333.15 K	*T* = 343.15 K	*T* = 353.15 K
2,2-dimethylbutane	57.65	34.94	22.1	14.43	9.58
Pentane	36.81	21.75	14.3	9.07	5.98
Hexane	75.04	44.66	29.9	19.90	12.58
Heptane	160.92	98.71	67.4	43.80	30.84
Octane	257.64	150.57	98.0	64.98	44.02
n-Nonane	350.48	197.54	130.1	89.64	59.87
n-Decane	437.08	275.74	185.4	121.98	76.76
1-Pentene	23.75	16.95	11.6	8.28	5.99
1-Hexene	50.69	31.59	22.4	16.24	11.70
1-Heptene	134.50	82.42	55.2	39.49	26.86
1-Nonene	295.49	180.03	117.9	71.75	51.23
1-Decene	417.13	264.64	177.4	110.99	71.84
Cyclohexene	10.90	8.01	5.5	4.12	3.13
Cyclohexane	18.53	11.09	7.3	4.88	3.54
Cyclooctane	112.69	67.15	43.9	29.13	20.14
1-Pentyne	2.15	1.96	1.8	1.63	1.49
1-Hexyne	2.57	2.32	2.1	1.93	1.76
1-Heptyne	3.18	2.85	2.6	2.41	2.23
Benzene	6.83	5.38	4.3	3.68	2.97
Toluene	12.00	9.63	7.8	6.19	5.06
Ethylbenzene	33.87	30.24	25.4	22.29	19.42
m-Xylene	40.03	35.46	30.4	26.93	23.43
p-Xylene	37.28	32.98	27.3	24.24	21.78
o-Xylene	26.58	24.08	20.7	17.70	15.70
Methanol	0.16	0.16	0.17	0.18	0.18
Ethanol	0.20	0.21	0.21	0.23	0.24
1-Propanol	0.26	0.29	0.30	0.30	0.32
1-Butanol	---	0.35	0.36	0.37	0.37
THF	0.19	0.23	0.28	0.35	0.42
Acetonitrile	0.30	0.36	0.44	0.53	0.62
Thiophene	0.47	0.55	0.64	0.75	0.89
Acetone	0.10	0.12	0.14	0.17	0.21
Butanone	0.24	0.29	0.37	0.46	0.56

[a] Standard uncertainties u are u(γ_{13}^{∞}) = 5 %, u(*T*) = 0.02 K, u(*x*) = 0.006.

Table 5.1. 2: Partial molar excess properties, enthalpies ($\Delta H_1^{E,\infty}$), Gibbs free energies ($\Delta G_1^{E,\infty}$), and entropies ($T_{ref}\Delta S_1^{E,\infty}$) for the various organic solutes in DES1 [BDMIMCl + EG], at the temperature, *T* = 323.15 K.

Molecular solutes	$\Delta H_1^{E,\infty}$/kJ .mol^{-1}	$\Delta G_1^{E,\infty}$/kJ.mol^{-1}	$T_{ref}\Delta S_1^{E,\infty}$/kJ.mol^{-1}
2,2-dimethylbutan	41.20	9.55	31.65
Pentane	41.51	8.27	33.23
Hexane	40.32	10.21	30.11
Heptane	37.92	12.34	25.58
octane	40.31	13.47	26.84
n-Nonane	39.87	14.20	25.67
n-Decane	39.30	15.10	24.20
1-Pentene	31.94	7.60	24.34
1-Hexene	33.17	9.28	23.89
1-Heptene	36.47	11.85	24.61
1-Nonene	40.76	13.95	26.81
1-Decene	40.34	14.99	25.35
Cyclohexene	29.09	5.59	23.49
Cyclohexane	38.12	6.47	31.66
Cyclooctane	39.44	11.30	28.13
1-Pentyne	8.46	1.81	6.65
1-Hexyne	8.68	2.26	6.42
1-Heptyne	8.10	2.81	5.29
Benzene	18.84	4.52	14.32
Toluene	19.95	6.09	13.86
Ethylbenzene	13.03	9.16	3.87
m-Xylene	12.38	9.59	2.80
p-Xylene	12.74	9.39	3.35
o-Xylene	12.50	8.55	3.95
Methanol	-3.67	-5.23	1.56
Ethanol	-4.71	-4.52	-0.19
1-Propanol	-3.95	-3.58	-0.37
1-Butanol	-1.78	-3.01	1.24
THF	-18.15	-3.93	-14.22
Acetonitrile	-16.68	-2.71	-13.96
Thiophene	-14.39	-1.61	-12.78
Acetone	-16.66	-5.69	-10.97
Butanone	-19.92	-3.34	-16.58

[a] Standard uncertainties u are u(γ_{13}^{∞}) = 5 %, u(*T*) = 0.02 K, u(*x*) = 0.006.

Table 5.1. 3: Selectivity and Capacity at Infinite Dilution of Various Solvents for Common Industrial Separation Problems at T = 323.15 K.

Solvent abbreviation	S_{ij}^{∞}			K_j^{∞}			ref
	Cyclohexane/benzene	**hexane/thiophene**	**Cyclohexane/ethanol**	**Benzene**	**Thiophene**	**Ethanol**	
([BDMIM]Cl + EG)[1:3]	2.713	159.659	92.65	0.146	2.126	5.0	This work
([EMPYR]Br + EG)1:4	1.434	-	1.629	1.086	-	1.23	(Manyoni and Redhi 2022b)
([C4H12N]Cl:EG)[1:2]	276	1695.22	140.024	0.050	0.937	0.443	(Nkosi, Tumba and Ramsuroop 2018)
[BMIM][Cl] + [Gly] 2:1	8.23	31.261	3.206	0.34	1.883	0.189	(Kabane and Redhi 2020)
[EMIM][SCN]	26.95	-	98.83	0.288	-	1.057	(Domańska and Marciniak 2008)
Sulfolane	9.03	-	8.504	0.426	-	0.345	(Möllmann and Gmehling 1997)
NMP	7.11	-	-	0.99	-	-	(Krummen and Gmehling 2004)

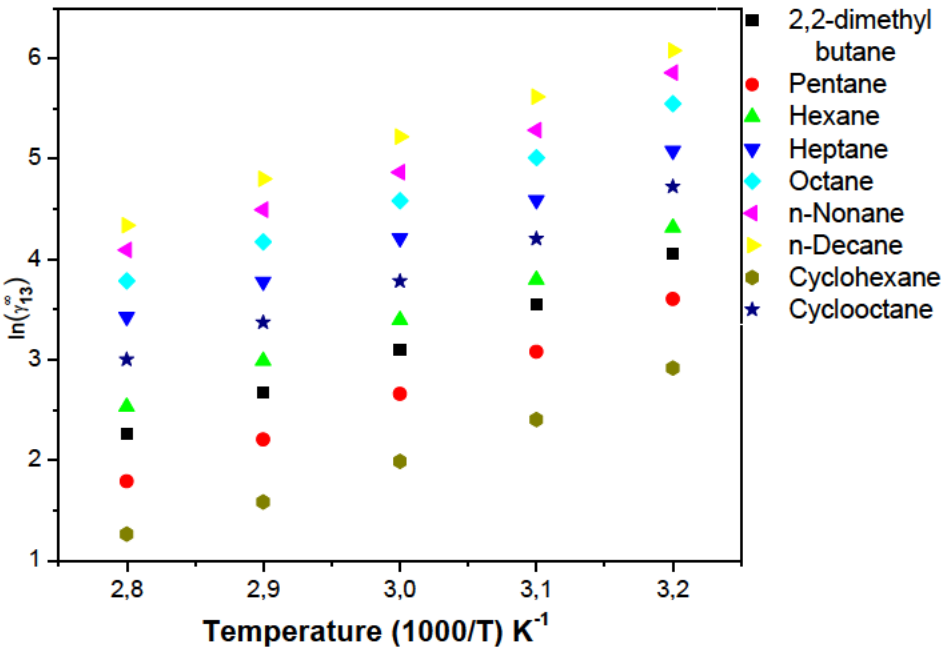

Figure 5.1. 4: Plot of $ln\,\gamma_{13}^{\infty}$ against 1000/T(K^{-1}) for the selected alkanes in DES1 [BDMIMCl + EG], at different temperatures, *T*= (313.15 – 343.15) K.

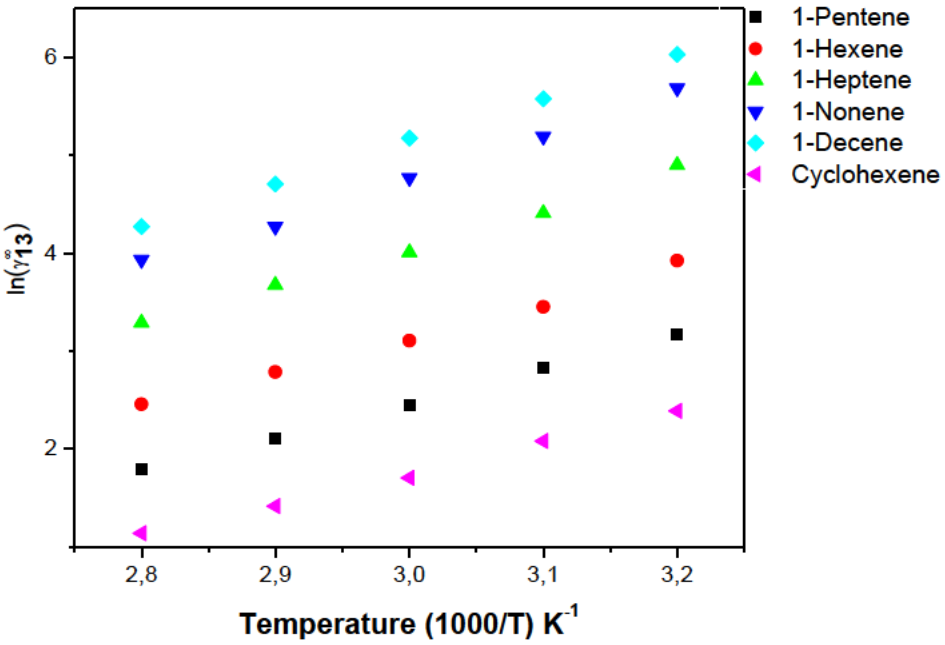

Figure 5.1. 5: Plot of $\ln\gamma_{13}^{\infty}$ against 1000/T(K^{-1}) for the selected alkenes in DES1 [BDMIMCl + EG], at different temperatures, *T*= (313.15 – 343.15) K.

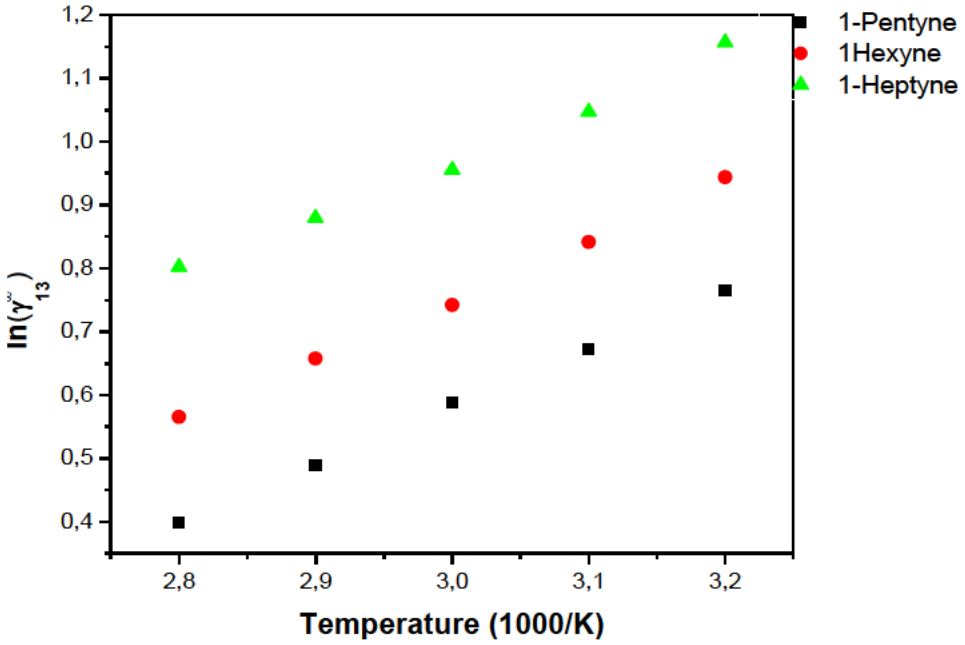

Figure 5.1. 6: Plot of $\ln \gamma_{13}^{\infty}$ against 1000/T(K^{-1}) for the selected alkynes in DES1 [BDMIMCl + EG], at different temperatures, *T*= (313.15 – 343.15) K.

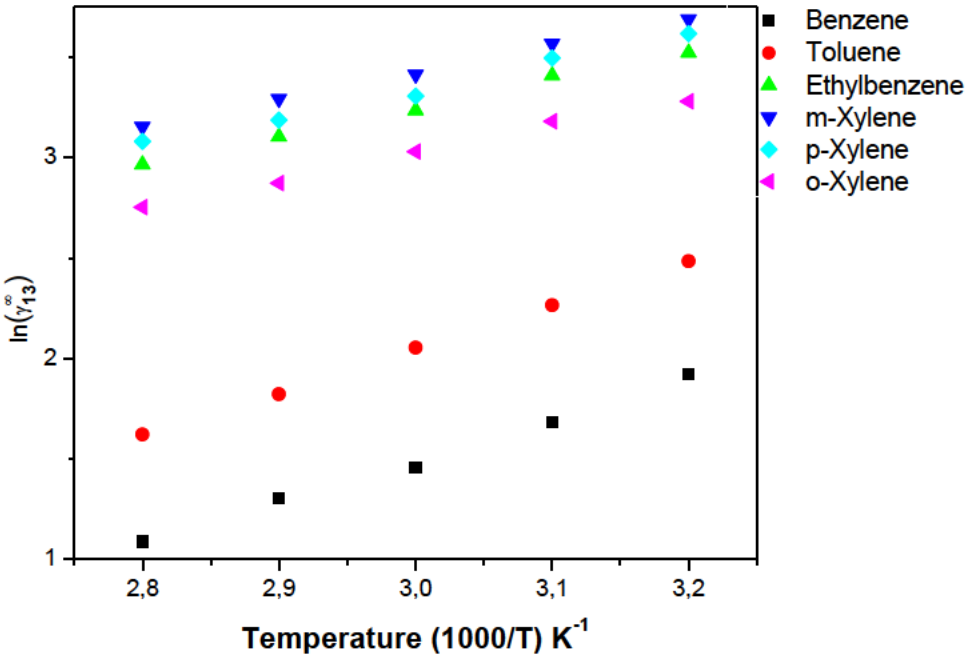

Figure 5.1. 7: Plot of $\ln \gamma_{13}^{\infty}$ against 1000/T(K^{-1}) for the selected aromatic hydrocarbons in DES1 [BDMIMCl + EG], at different temperatures, *T*= (313.15 – 343.15) K.

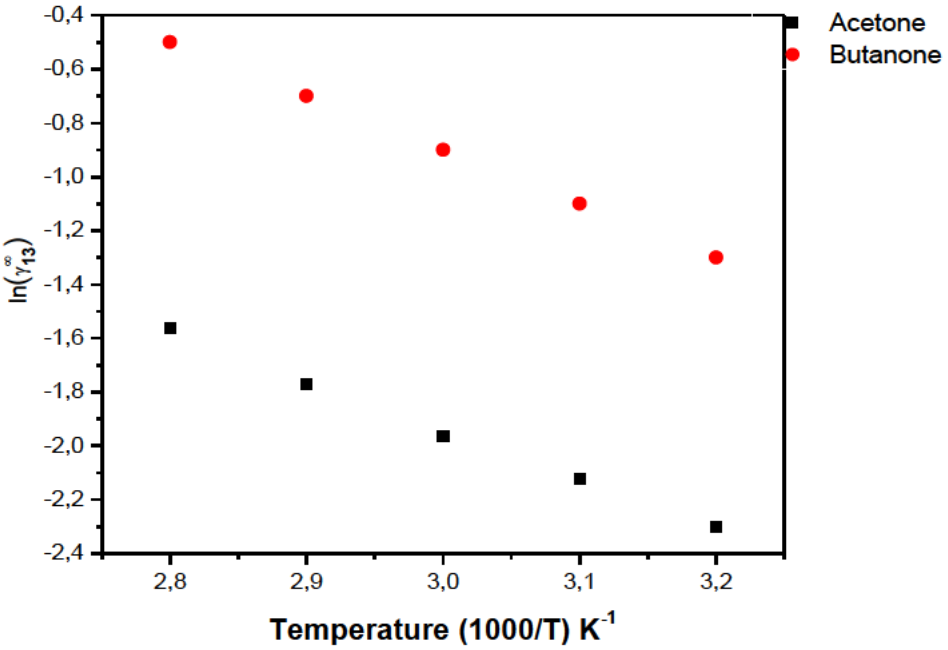

Figure 5.1. 8: Plot of $\ln \gamma_{13}^{\infty}$ against 1000/T(K^{-1}) for the selected ketones in DES1 [BDMIMCl + EG], at different temperatures, *T*= (313.15 – 343.15) K.

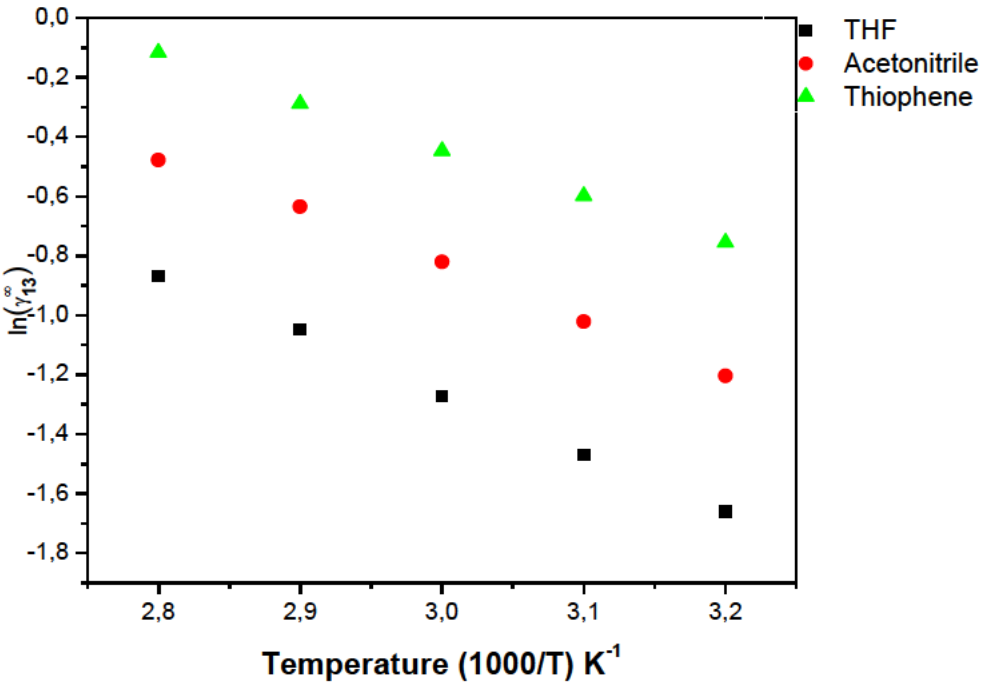

Figure 5.1. 9: Plot of $\ln \gamma_{13}^{\infty}$ against 1000/T(K^{-1}) for the THF, Acetonitrile and Thiophene in DES1 [BDMIMCl + EG], at different temperatures, *T*= (313.15 – 343.15) K.

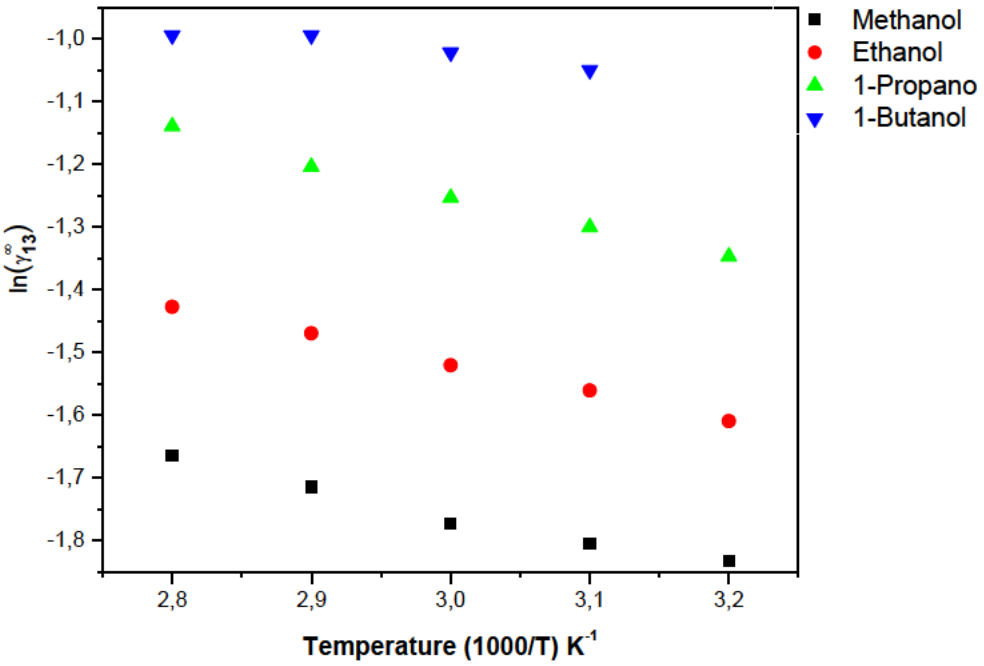

Figure 5.1. 10: Plot of $\ln \gamma_{13}^{\infty}$ against 1000/T(K^{-1}) for the selected alcohols in DES1 [BDMIMCl + EG], at different temperatures, *T*= (313.15 – 343.15) K.

5.2 DES2; 1-butyl-2,3-dimethylimidazolium chloride + diethylene glycol

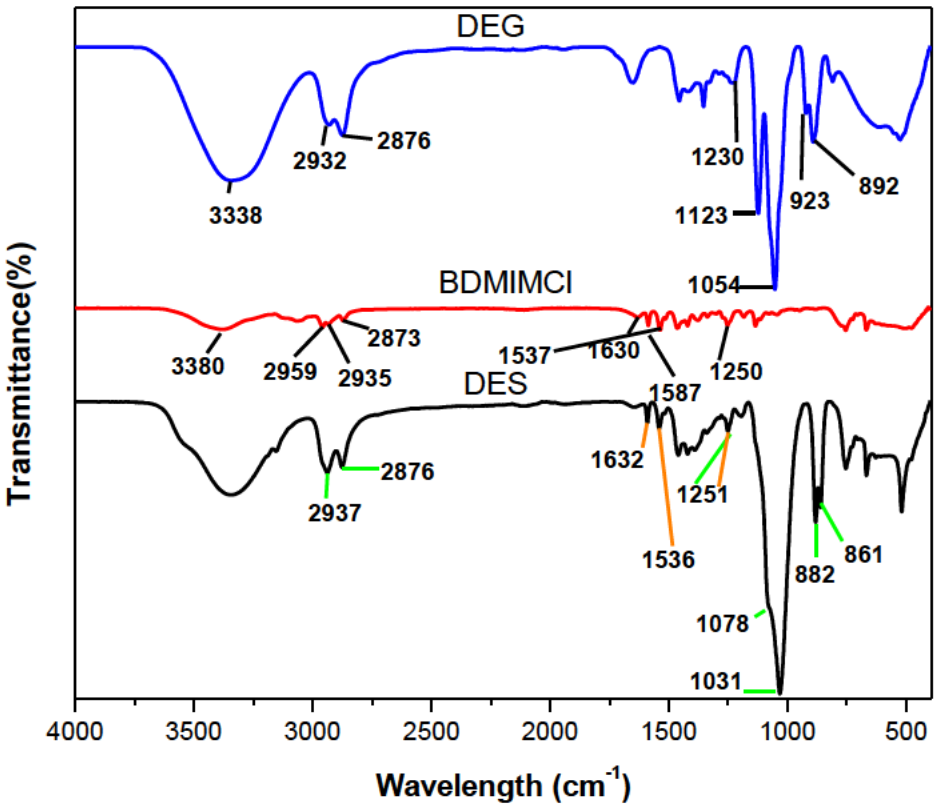

Figure 5.2. 1: FT-IR spectra of diethylene glycol (DEG), 1-butyl-2,3-dimethylimidazolium chloride (BDMIMCl), and DES (BDMIMCl + DEG).

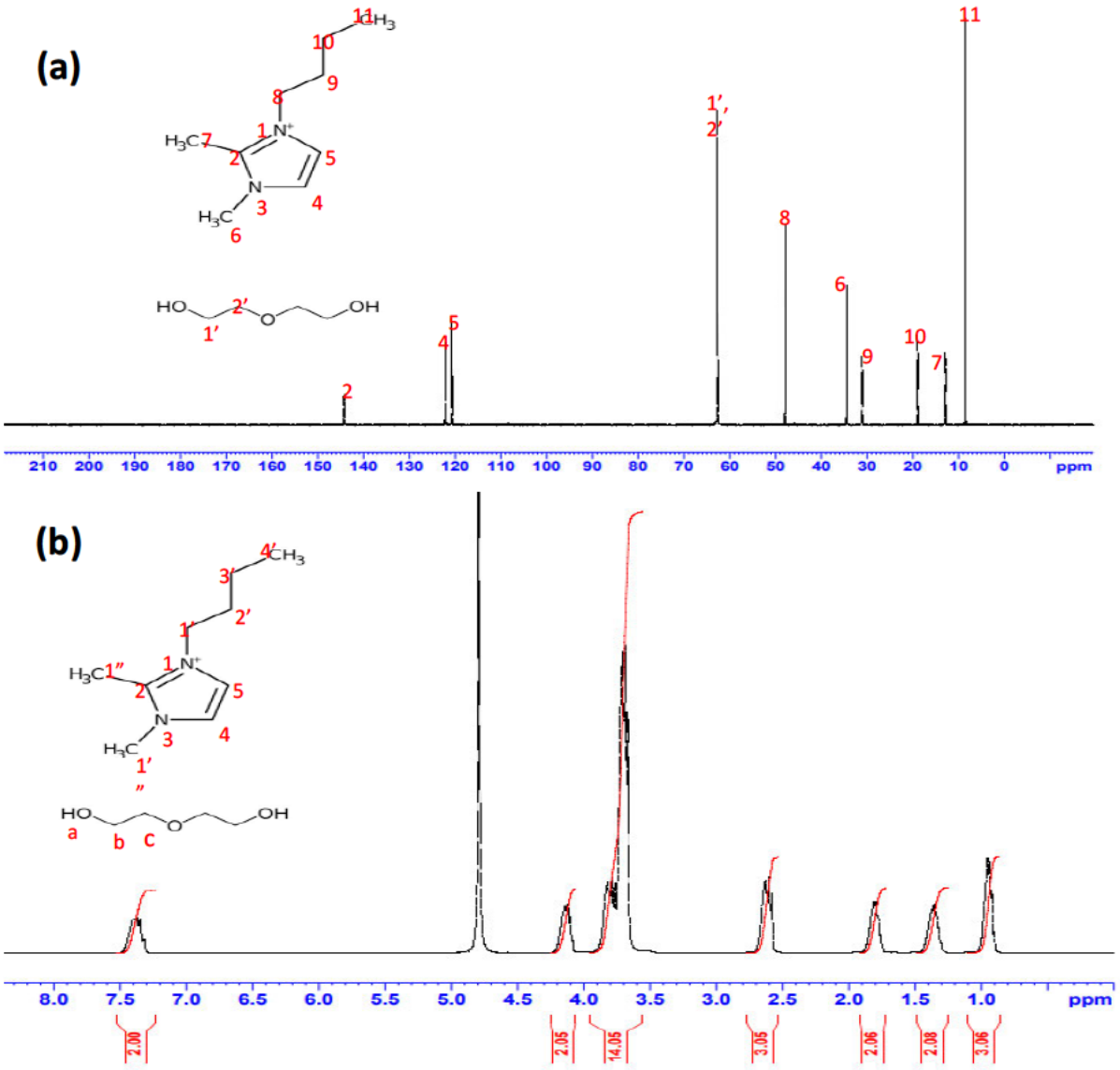

Figure 5.2. 2: (a) ^{13}C-NMR spectra, (b) ^{1}H-NMR spectra of DES (BDMIMCl + DEG).

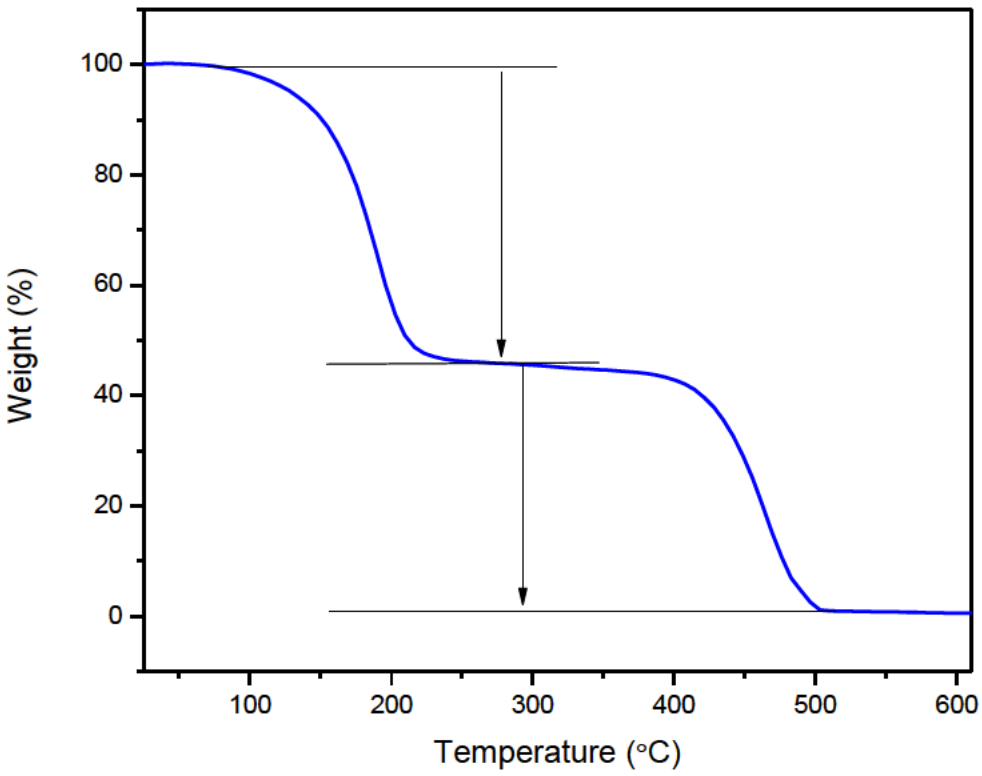

Figure 5.2. 3: Thermogravimetric analysis (TGA) curves of DES (BDMIMCl + DEG).

Table 5.2. 1: Activity coefficients at infinite dilution for the solutes in deep eutectic solvent [1-butyl-2,3-dimethylimidazolium chloride + diethylene glycol] at temperatures (313.15-353.15 K).

Average γ_{13}^{∞} values					
Solutes	T = 313.15 K	T = 323.15 K	T = 333.15 K	T = 343.15 K	T = 353.15 K
2,2-dimethylbutan	28.57	23.47	19.2	16.20	14.16
Pentane	20.29	16.86	13.7	11.53	10.07
Hexane	48.76	38.50	32.1	24.44	20.21
Heptane	108.49	81.61	67.8	55.36	43.09
Octane	183.12	148.79	124.7	103.24	88.24
n-Nonane	391.34	296.39	239.9	190.11	147.76
n-Decane	732.24	548.44	434.3	333.72	262.06
1-Pentene	14.11	11.89	10.3	9.13	8.36
1-Hexene	28.92	24.57	21.5	18.40	16.34
1-Heptene	69.79	57.77	51.3	46.64	41.17
1-Nonene	155.75	135.69	123.6	115.65	100.73
1-Decene	239.81	222.80	199.7	188.38	170.27
Cyclohexene	22.73	19.53	16.7	14.56	12.74
Cyclohexane	43.79	33.56	28.1	22.37	17.71
Cyclooctane	70.90	53.77	42.4	34.44	27.58
1-Pentyne	7.35	6.91	6.4	6.05	5.59
1-Hexyne	11.50	10.54	9.7	8.95	8.22
1-Heptyne	15.97	14.66	13.3	12.23	11.33
Benzene	6.24	5.60	5.0	4.45	4.00
Toluene	10.27	9.27	8.4	7.69	6.99
Ethylbenzene	16.66	15.28	13.9	12.66	11.72
m-Xylene	18.75	16.71	15.6	14.49	13.38
p-Xylene	17.66	15.47	14.7	13.49	12.34
o-Xylene	14.32	12.95	11.9	10.84	9.91
Methanol	1.66	1.53	1.45	1.35	1.27
Ethanol	2.73	2.49	2.32	2.18	2.04
1-Propanol	3.80	3.48	3.24	3.01	2.85
1-Butanol	4.63	4.39	4.09	3.79	3.57
THF	10.00	9.23	8.67	8.18	7.77
Acetonitrile	7.27	6.71	6.36	5.96	5.61
Thiophene	5.32	5.73	6.10	6.52	6.96
Acetone	5.91	5.90	5.87	5.86	5.81
Butanone	6.99	6.95	6.92	6.87	6.84

[a]Standard uncertainties u are u (γ_{13}^{∞}) = 0.05, u(T) = 0.02 K, u(BDMIMCl : DEG) = 0.007

Table 5.2. 2: Partial molar excess properties, enthalpies ($\Delta H_1^{E,\infty}$), Gibbs free energies ($\Delta G_1^{E,\infty}$), and entropies ($T_{ref}\Delta S_1^{E,\infty}$) for the various organic solutes in DES2 [BDMIMCl + DEG], at the temperature, T = 323.15 K.

Solutes	$\Delta H_1^{E,\infty}$/kJ .mol^{-1}	$\Delta G_1^{E,\infty}$/kJ.mol^{-1}	$T_{ref}\Delta S_1^{E,\infty}$/kJ.mol^{-1}
2,2-dimethylbutane	16.36	8.48	7.88
Pentane	16.41	7.59	8.82
Hexane	20.38	9.81	10.57
Heptane	20.56	11.83	8.74
octane	16.81	13.44	3.37
n-Nonane	22.01	15.29	6.71
n-Decane	23.49	16.95	6.54
1-Pentene	12.09	6.65	5.44
1-Hexene	13.18	8.60	4.57
1-Heptene	11.71	10.90	0.82
1-Nonene	9.49	13.19	-3.70
1-Decene	7.84	14.53	-6.69
Cyclohexene	13.37	7.98	5.38
Cyclohexane	20.38	9.44	10.94
Cyclooctane	21.50	10.71	10.80
1-Pentyne	6.24	5.19	1.05
1-Hexyne	7.67	6.33	1.35
1-Heptyne	7.99	7.21	0.78
Benzene	10.29	4.63	5.66
Toluene	8.80	5.98	2.81
Ethylbenzene	8.22	7.33	0.89
m-Xylene	7.53	7.57	-0.03
p-Xylene	7.86	7.36	0.50
o-Xylene	8.41	6.88	1.53
Methanol	6.04	1.09	4.95
Ethanol	6.57	2.47	4.09
2-Propanol	6.63	3.45	3.17
1-Butanol	6.11	4.14	1.97
THF	5.77	5.97	-0.20
Acetonitrile	5.86	5.11	0.74
Thiophene	-6.17	4.69	-10.86
Acetone	0.38	4.77	-4.39
Butanone	0.50	5.21	-4.71

[a]Standard uncertainties u are u (γ_{13}^{∞}) = 0.05, u(T) = 0.02 K, u(BDMIMCl : DEG) = 0.007

Table 5.2. 3: Selectivity and Capacity at Infinite Dilution of Various Solvents for Common Industrial Separation Problems at T = 323.15 K.

Solvent abbreviation	S_{ij}^{∞}			K_j^{∞}			ref
	heptane/toluene	pentane/ethylbenzene	heptane/ethanol	Toluene	Ethylbenzene	Ethanol	
([BDMIM]Cl + DEG) 1:3	10.56	1.218	39.739	0.097	0.0600	0.366	This work
([EMPYR]Br + EG)1:4	1.845	1.282	1.629	1.031	1.909	1.23	(Manyoni and Redhi
[BMIM][Cl] + [Gly] 2:1	9.851	0.728	3.206	0.34	1.883	0.189	(Kabane and Redhi 2020)
[THTDPh][C10H19O] +EG	5.217	2.034	7.824	0.570	0.455	5.882	(Ghaedi *et al.* 2022)
[PEG] + CC	6.640	---	5.541	0.901	---	0.752	(Królikowski *et al.* 2022)
[TMAM][Cl] + EG	36.404	---	694.76	0.023	---	0.444	(Nkosi, Tumba and Ramsuroop
[EMIMCl4Al][DEG] 1:4	17.34	3.11	217	0.296	0.179	3.704	(Kabane *et al.* 2023)
Sulfolane	15.492	6.172	18.666	0.286	0.203	0.345	(Möllmann and
NMP	10.301	-	-	0.752	-	-	(Krummen and

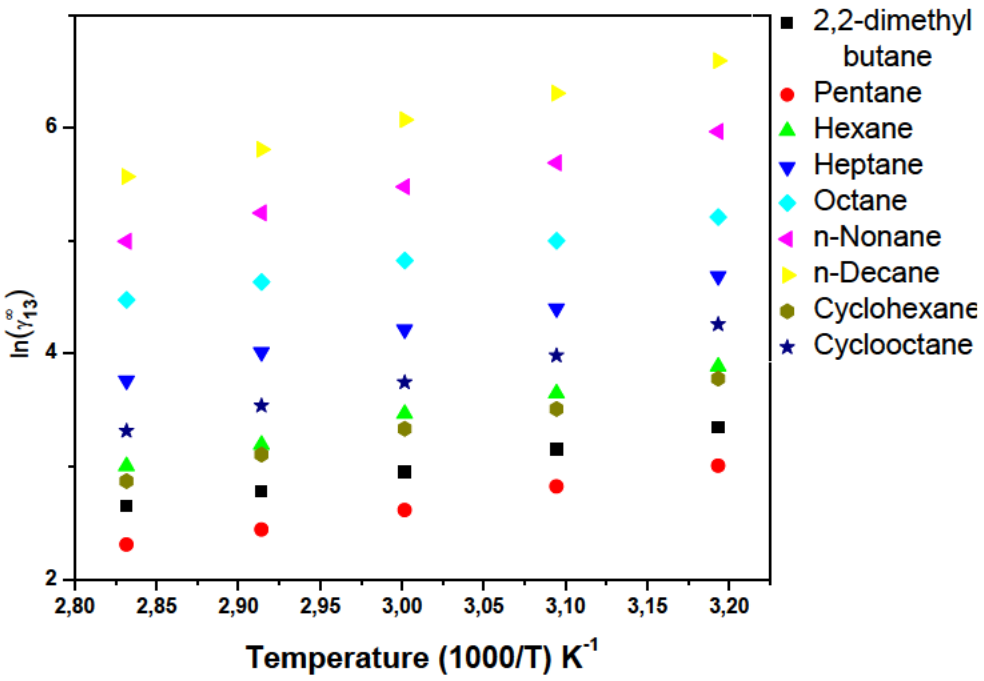

Figure 5.2. 4: Plot of $ln\,\gamma_{13}^{\infty}$ against 1000/T(K^{-1}) for the selected alkanes in DES2 [BDMIMCl + DEG], at different temperatures, *T*= (313.15 – 343.15) K.

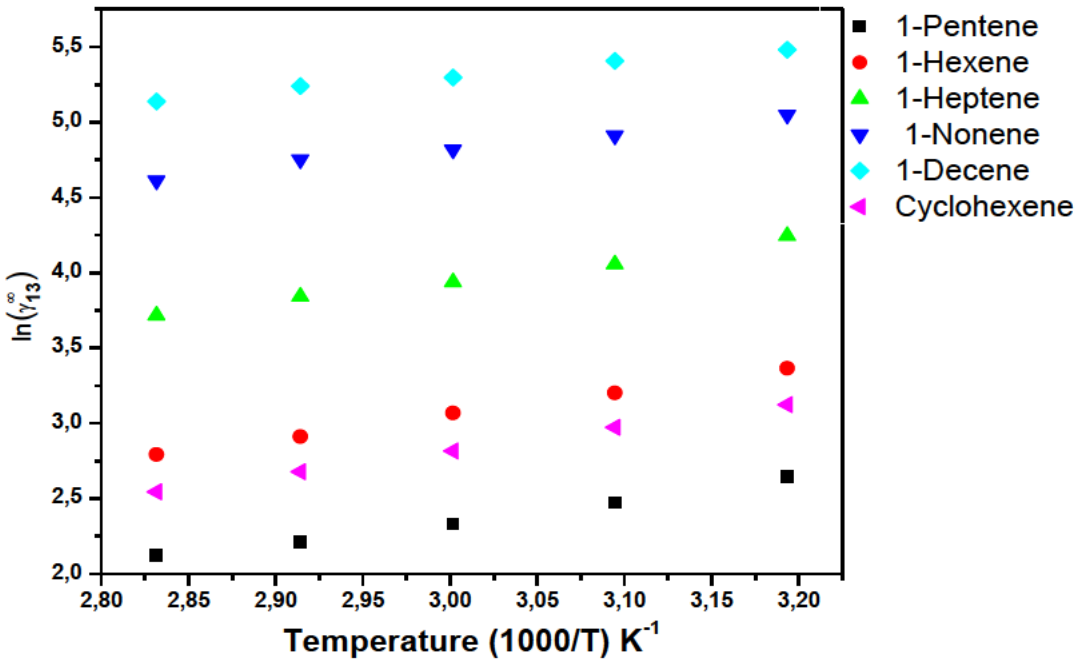

Figure 5.2. 5: Plot of $\ln\gamma_{13}^{\infty}$ against 1000/T(K^{-1}) for the selected alkenes in DES2 [BDMIMCl + DEG], at different temperatures, *T*= (313.15 – 343.15) K.

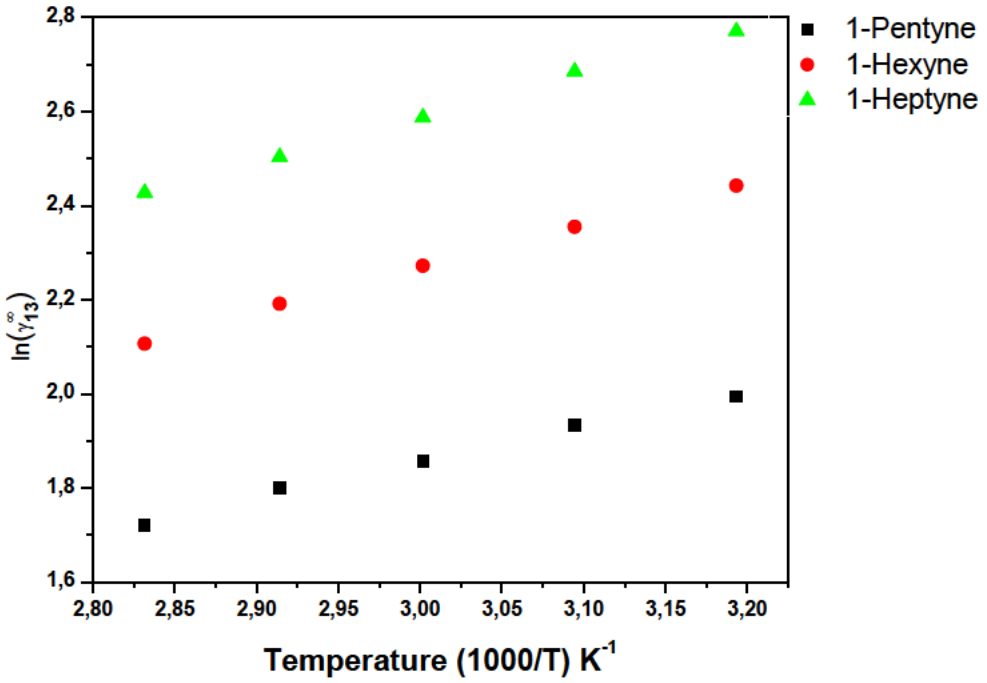

Figure 5.2. 6: Plot of $\ln \gamma_{13}^{\infty}$ against 1000/T(K^{-1}) for the selected alkynes in DES2 [BDMIMCl + DEG], at different temperatures, *T*= (313.15 – 343.15) K.

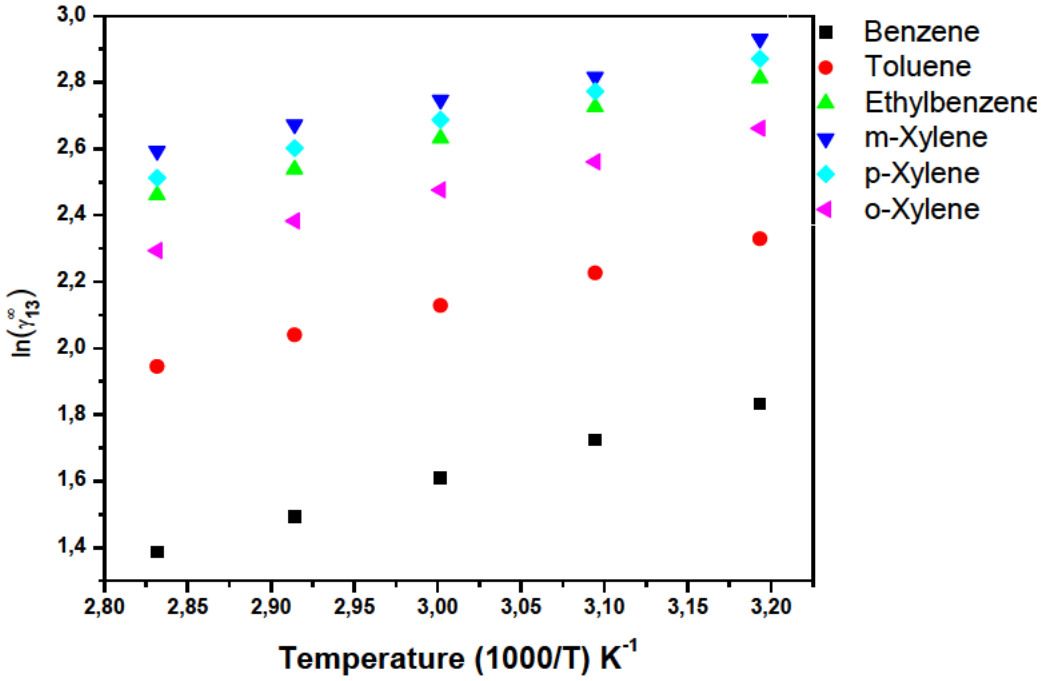

Figure 5.2. 7: Plot of $\ln \gamma_{13}^{\infty}$ against 1000/T(K^{-1}) for the selected cyclic aromatics in DES2 [BDMIMCl + DEG], at different temperatures, *T*= (313.15 – 343.15) K.

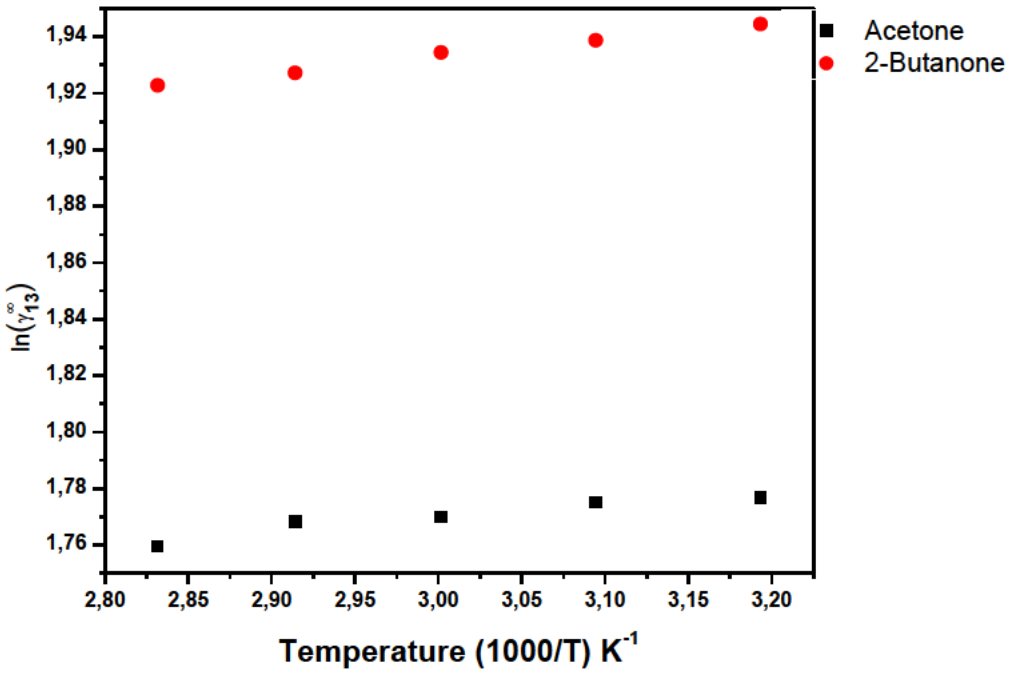

Figure 5.2. 8: Plot of $\ln \gamma_{13}^{\infty}$ against 1000/T(K^{-1}) for the selected ketones in DES2 [BDMIMCl + DEG], at different temperatures, *T*= (313.15 – 343.15) K.

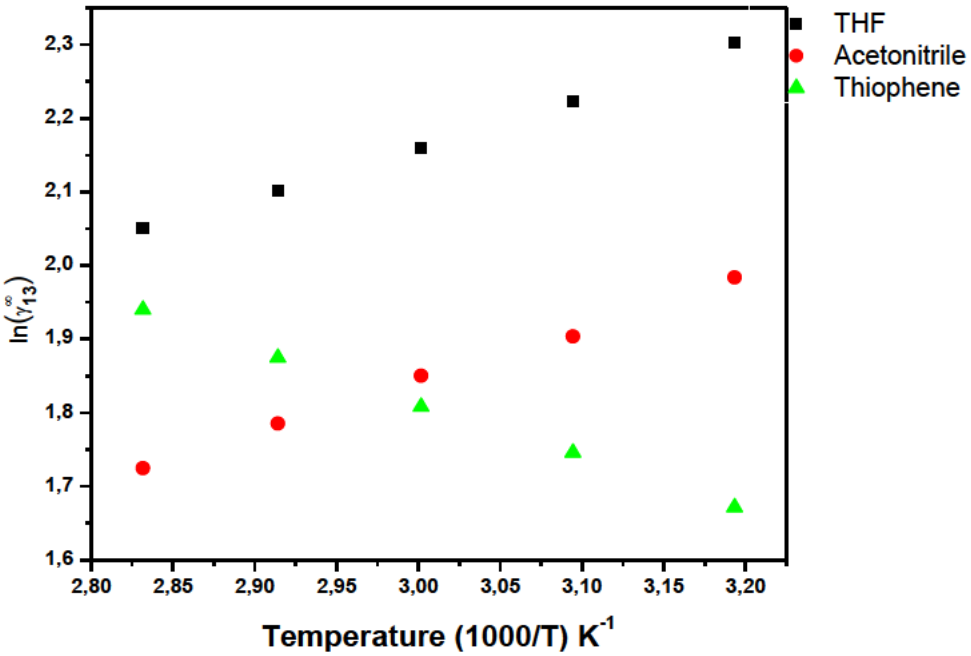

Figure 5.2. 9: Plot of $\ln \gamma_{13}^{\infty}$ against 1000/T(K^{-1}) for the THF, acetonitrile and thiophene in DES2 [BDMIMCl + DEG], at different temperatures, *T*= (313.15 – 343.15) K.

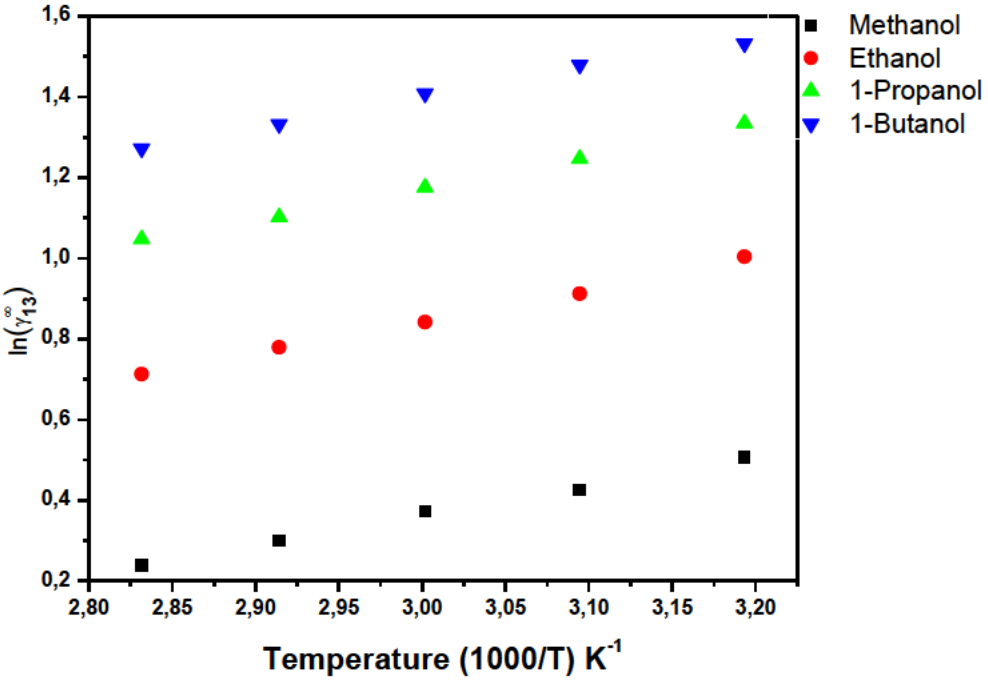

Figure 5.2. 10: Plot of $\ln \gamma_{13}^{\infty}$ against 1000/T(K^{-1}) for the selected alcohols in DES2 [BDMIMCl + DEG], at different temperatures, *T*= (313.15 – 343.15) K.

5. 3 DES3: 1-butyl-2,3-dimethylimidazolium tetrafluoroborate + ethylene glycol

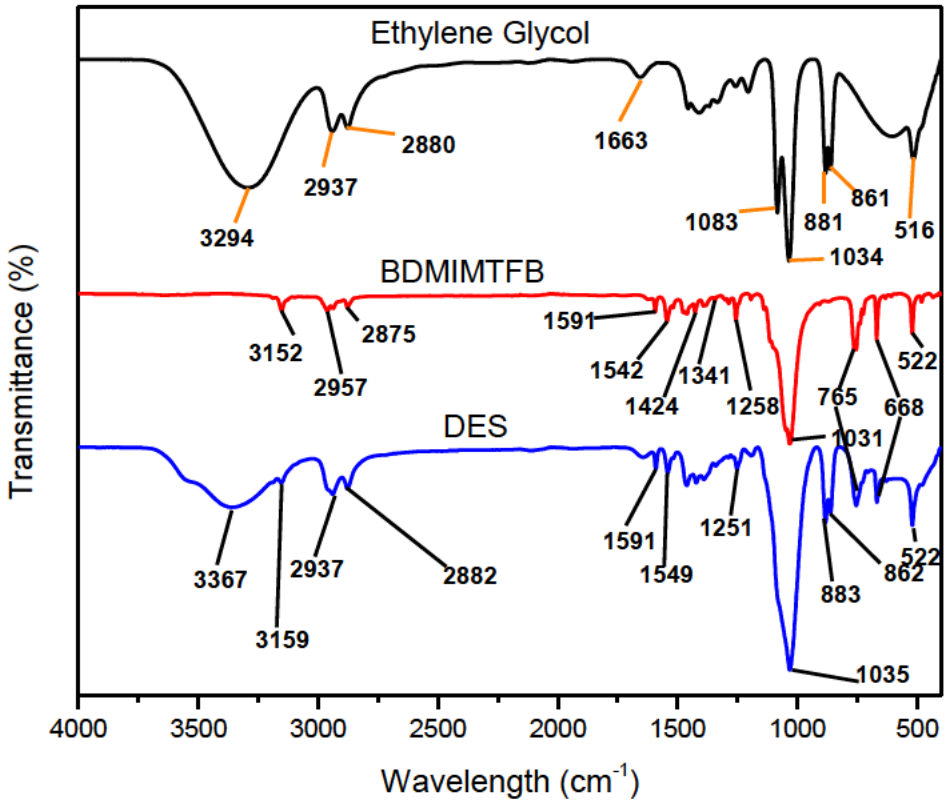

Figure 5.3. 1: FT-IR spectra of ethylene glycol (EG), 1-butyl-2,3-dimethylimidazolium tetrafluoroborate (BDMIMTFB), and DES (BDMIMTFB+ EG).

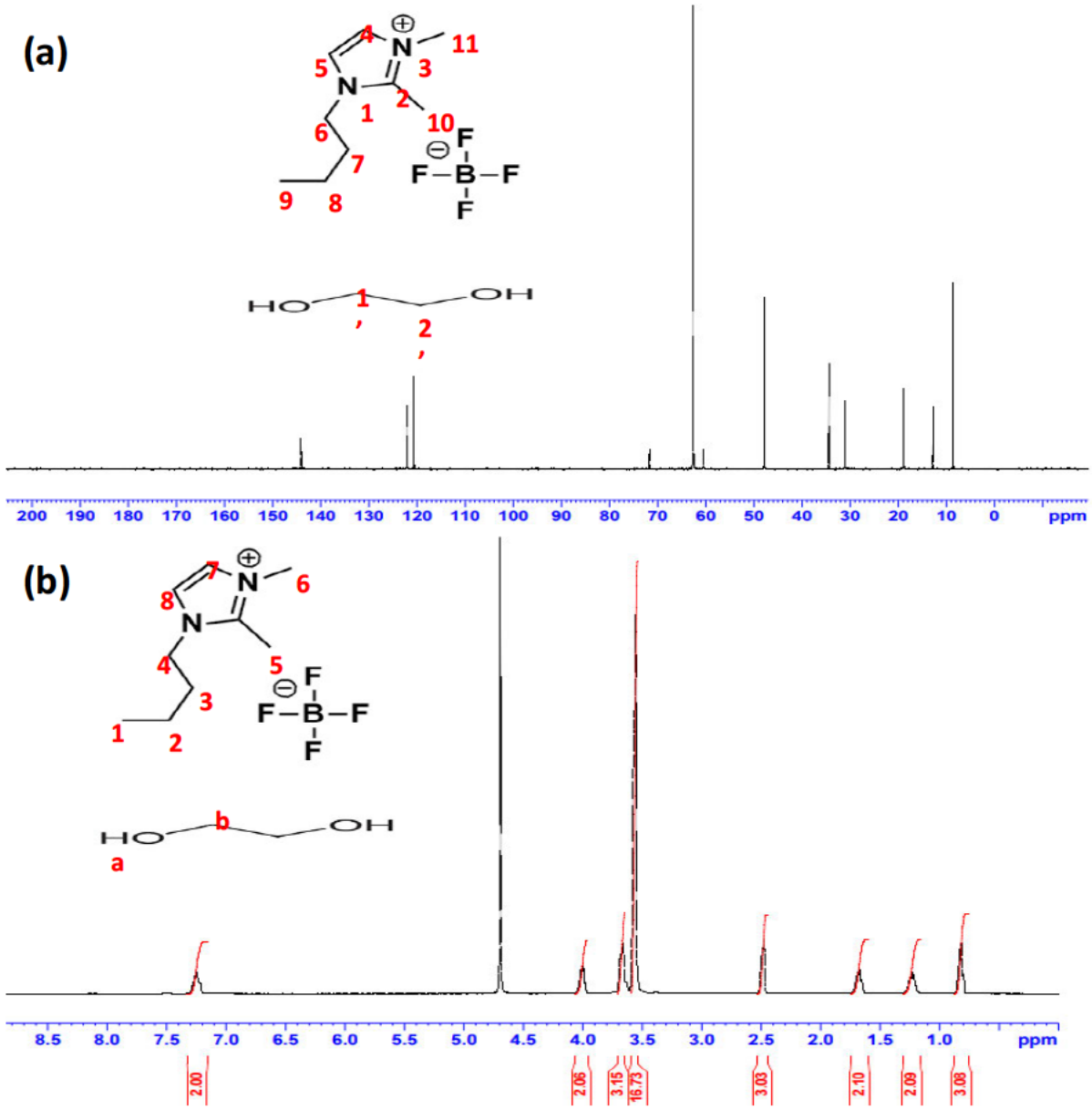

Figure 5.3. 2: (a) ^{13}C-NMR spectra, (b) ^{1}H-NMR spectra of DES (BDMIMTFB+ EG).

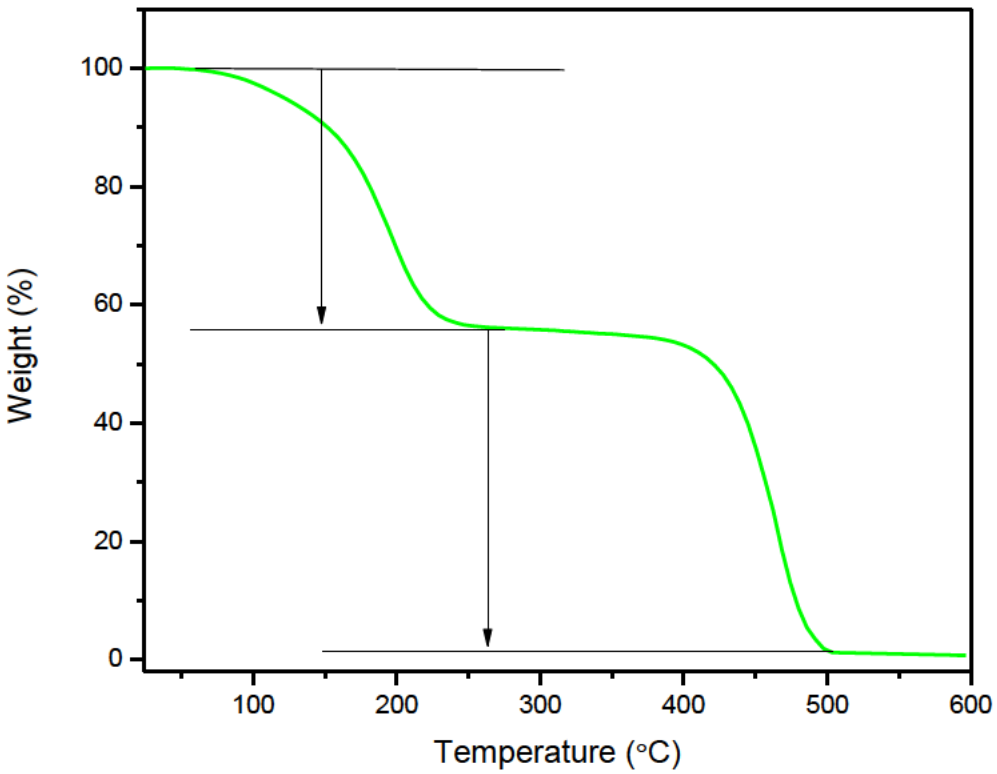

Figure 5.3. 3: Thermogravimetric analysis (TGA) curves of DES (BDMIMTFB + EG).

Table 5.3. 1: Activity coefficients at infinite dilution for the solutes in deep eutectic solvent [1-butyl-2,3-dimethylimidazolium tetrafluoroborate + Ethylene Glycol] at temperatures T = (313.15 - 353.15) K.

Average γ_{13}^{∞} values					
Solutes	T = 313.15 K	T = 323.15 K	T = 333.15 K	T=343.15 K	T=353.15 K
2,2-dimethylbutane	46.71	37.22	31.7	27.24	23.21
Pentane	30.69	24.60	21.6	18.13	15.78
Hexane	85.11	69.53	56.2	43.74	35.56
Heptane	217.28	158.64	127.7	102.69	84.79
Octane	400.00	313.71	254.3	208.75	164.14
n-Nonane	709.36	565.88	459.1	365.72	293.64
n-Decane	1231.79	975.84	784.5	613.39	491.81
1-Pentene	20.98	18.79	16.5	14.87	13.03
1-Hexene	67.49	53.06	42.7	34.61	28.96
1-Heptene	155.19	125.62	103.8	85.85	69.77
1-Nonene	432.67	357.93	317.1	274.41	241.80
1-Decene	634.03	550.42	490.4	433.14	378.76
Cyclohexene	60.23	47.58	40.0	31.94	26.15
Cyclohexane	78.71	60.88	48.2	38.54	32.33
Cyclooctane	344.10	285.31	226.6	184.43	149.81
1-Pentyne	14.62	13.17	12.2	11.12	10.26
1-Hexyne	28.33	25.86	23.7	21.79	19.24
1-Heptyne	57.67	52.53	46.8	41.94	37.17
Benzene	10.53	10.22	10.0	9.66	9.46
Toluene	19.67	18.82	18.3	17.91	17.38
Ethylbenzene	35.87	34.08	32.7	30.91	29.30
m-Xylene	39.11	36.10	34.2	32.66	31.18
p-Xylene	37.38	34.53	33.0	31.35	30.09
o-Xylene	29.87	28.65	27.6	26.57	25.61
Methanol	4.37	3.68	3.37	2.99	2.68
Ethanol	8.83	7.21	6.07	5.43	4.78
2-Propanol	19.69	16.61	14.47	12.54	10.55
1-Butanol	25.66	21.23	18.08	15.92	13.63
THF	6.42	6.28	6.13	5.98	5.88
Acetonitrile	5.15	4.93	4.72	4.50	4.31
Thiophene	6.97	7.05	7.08	7.15	7.24
Acetone	3.91	3.74	3.59	3.44	3.30
2-butanone	4.69	4.47	4.27	4.08	3.92

[a]Standard uncertainties u are u(γ_{13}^{∞}) = 0.05, u(T) = 0.02 K, u(BDMIMBF$_4$: EG) = 0.005

Table 5.3. 2: Partial molar excess properties, enthalpies ($\Delta H_1^{E,\infty}$), Gibbs free energies ($\Delta G_1^{E,\infty}$), and entropies ($T_{ref}\Delta S_1^{E,\infty}$) for the various organic solutes in DES3 [BDMIMBF4 + EG], at the temperature, T = 323.15 K.

Solutes	$\Delta H_1^{E,\infty}$/kJ .mol^{-1}	$\Delta G_1^{E,\infty}$/kJ.mol^{-1}	$T_{ref}\Delta S_1^{E,\infty}$/kJ.mol^{-1}
2,2-dimethylbutan	15.78	9.72	6.06
Pentane	15.07	8.61	6.47
Hexane	20.30	11.40	8.90
Heptane	21.37	13.61	7.76
Octane	20.13	15.45	4.69
n-Nonane	20.24	17.03	3.21
n-Decane	21.16	18.49	2.66
1-Pentene	10.90	7.88	3.02
1-Hexene	19.52	10.67	8.85
1-Heptene	18.21	12.99	5.22
1-Nonene	13.17	15.80	-2.63
1-Decene	11.68	16.96	-5.27
Cyclohexene	19.02	10.38	8.64
Cyclohexane	20.61	11.04	9.58
Cyclooctane	19.30	15.19	4.11
1-Pentyne	8.07	6.93	1.15
1-Hexyne	8.68	8.74	-0.06
1-Heptyne	10.14	10.64	-0.51
Benzene	2.48	6.25	-3.76
Toluene	2.74	7.89	-5.14
Ethylbenzene	4.61	9.48	-4.87
m-Xylene	5.11	9.64	-4.53
p-Xylene	4.90	9.52	-4.62
o-Xylene	3.53	9.01	-5.49
Methanol	10.91	3.57	7.34
Ethanol	13.95	5.30	8.65
2-Propanol	14.06	7.85	6.22
1-Butanol	14.31	8.50	5.81
THF	2.09	4.94	-2.85
Acetonitrile	4.09	4.29	-0.20
Thiophene	-0.83	5.25	-6.08
Acetone	3.86	3.55	0.31
2-butanone	4.12	4.02	0.10

[a]Standard uncertainties u are u(γ_{13}^{∞}) = 0.05, u(T) = 0.02 K, u(BDMIMBF$_4$: EG) = 0.005

Table 5.3. 3: Selectivity and Capacity at Infinite Dilution of Various Solvents for Common Industrial Separation Problems at T = 313.15 K.

Solvent abbreviation	S_{ij}^{∞}			K_j^{∞}			ref
	hexene/toluene	Hexane/acetone	heptane/ethanol	Toluene	Acetone	Ethanol	
([BDMIM]BF4 + EG) 1:3	7.115	21.76	24.607	0.050	0.2557	0.1132	This work
[N-C3OHPY][DCA]	14.21	158.29	370	0.118	0.535	0.769	(Domańska *et al.* 2017)
(C4H12NCl):(EG)	25.42	337.2	694.7	0.02	0.189	0.444	(Nkosi, Tumba and Ramsuroop 2018)
NMP	5.025	14.73	---	0.51	0.763	---	(Krummen and Gmehling 2004)

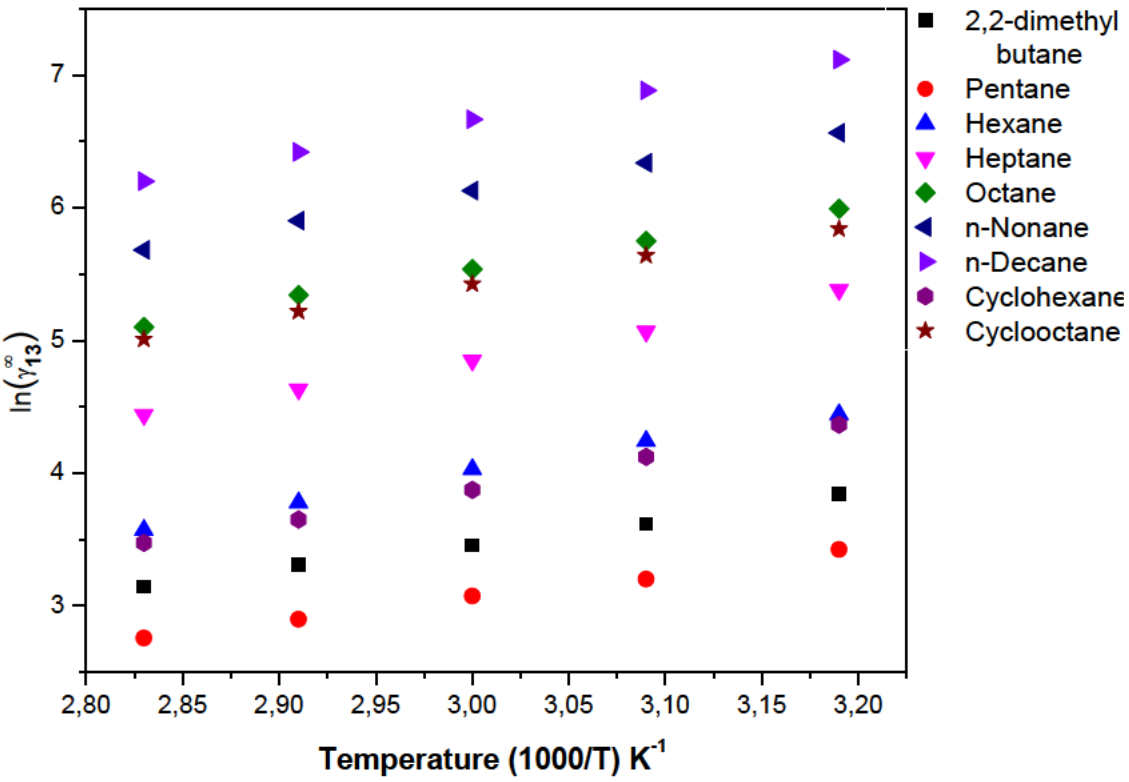

Figure 5.3. 4: Plot of $ln\,\gamma_{13}^{\infty}$ against 1000/T(K^{-1}) for the selected alkanes in DES3 [BDMIMBF$_4$ + EG], at different temperatures, *T*= (313.15 – 343.15) K.

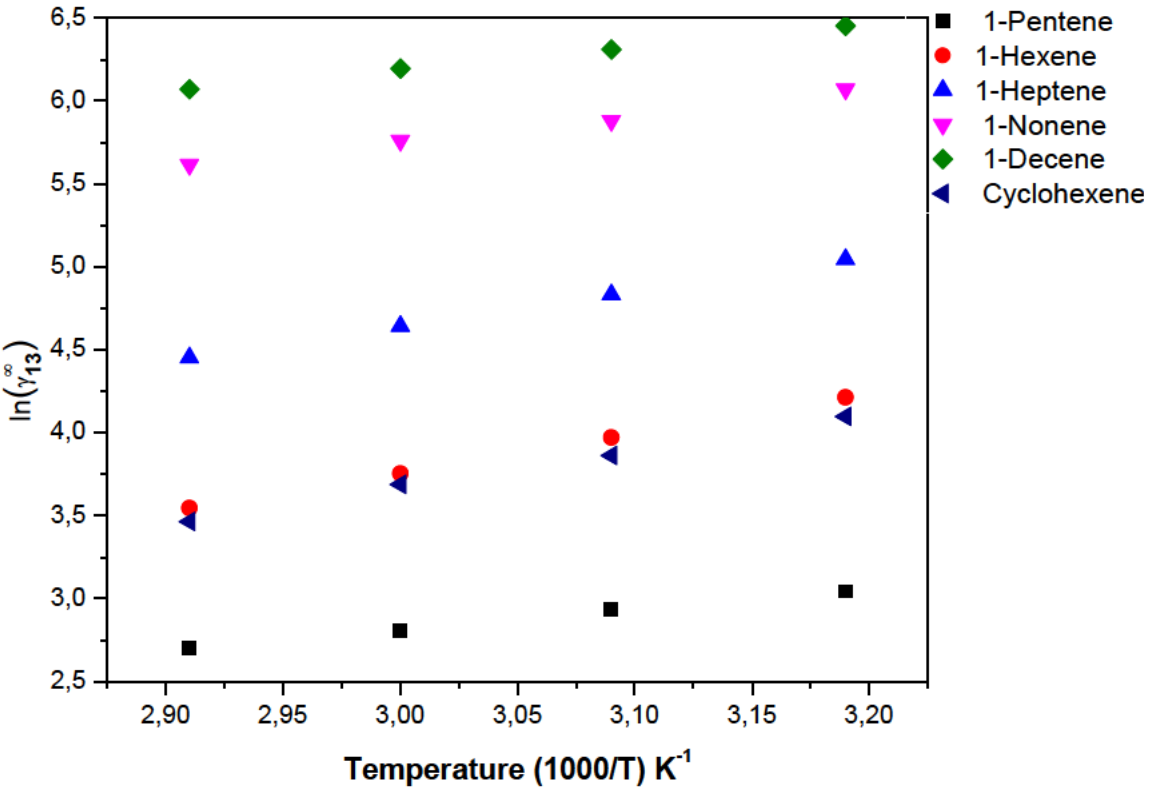

Figure 5.3. 5: Plot of $ln\,\gamma_{13}^{\infty}$ against 1000/T(K^{-1}) for the selected alkenes in DES3 [BDMIMBF$_4$+ EG], at different temperatures, T= (313.15 – 343.15) K.

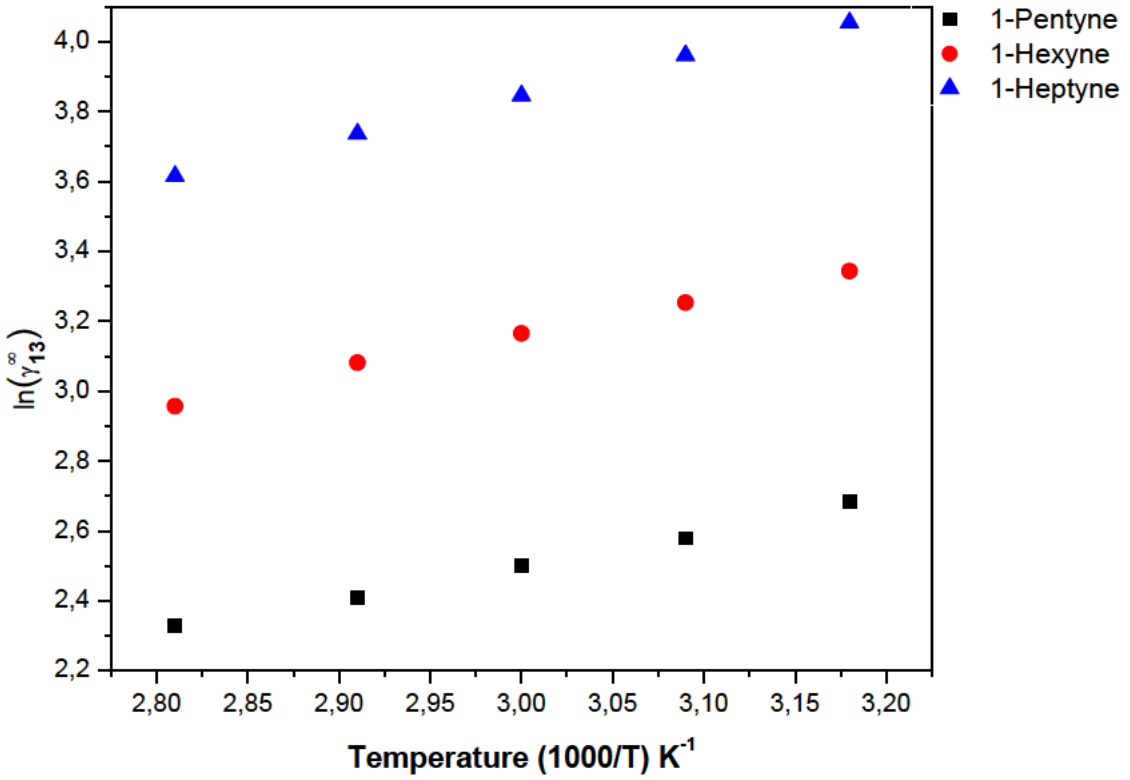

Figure 5.3. 6: Plot of $\ln \gamma_{13}^{\infty}$ against 1000/T(K^{-1}) for the selected alkynes in DES3 [BDMIMBF$_4$ + EG] at different temperatures, *T*= (313.15 – 343.15) K.

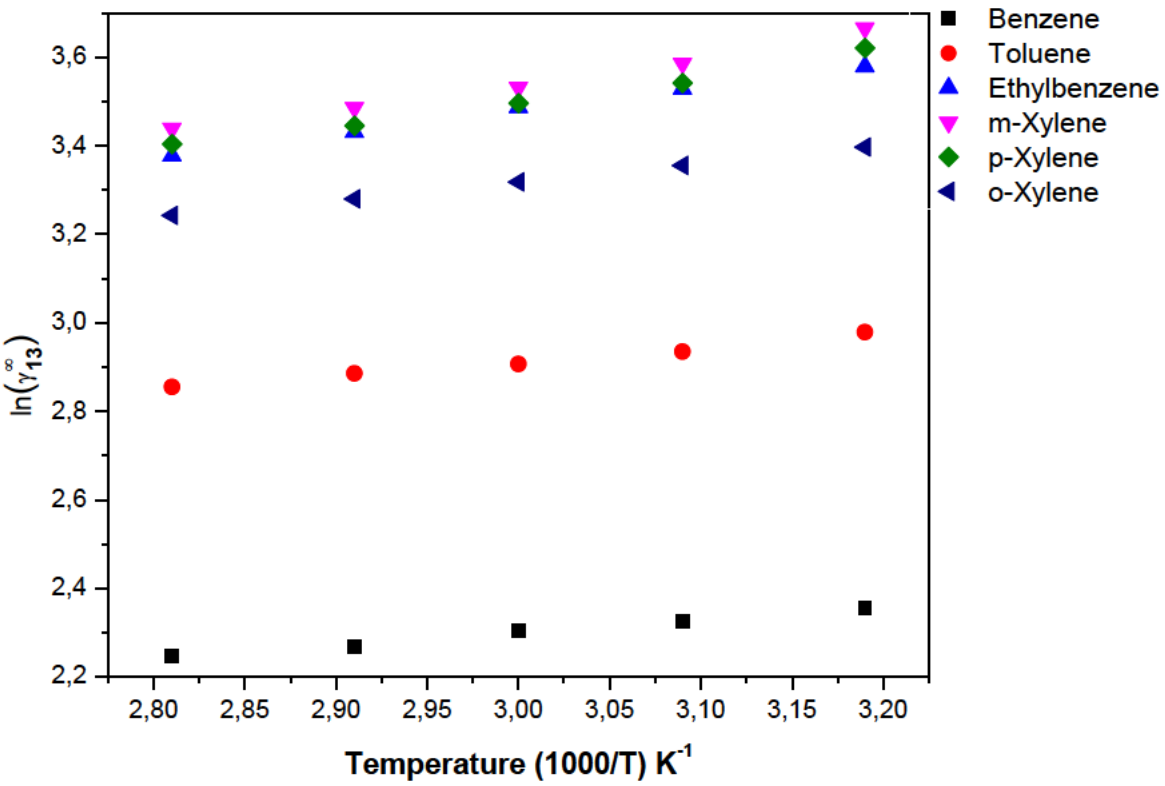

Figure 5.3. 7: Plot of $\ln \gamma_{13}^{\infty}$ against 1000/T(K^{-1}) for the selected alkenes in DES3 [BDMIMBF$_4$ + EG] at different temperatures, *T*= (313.15 – 343.15) K.

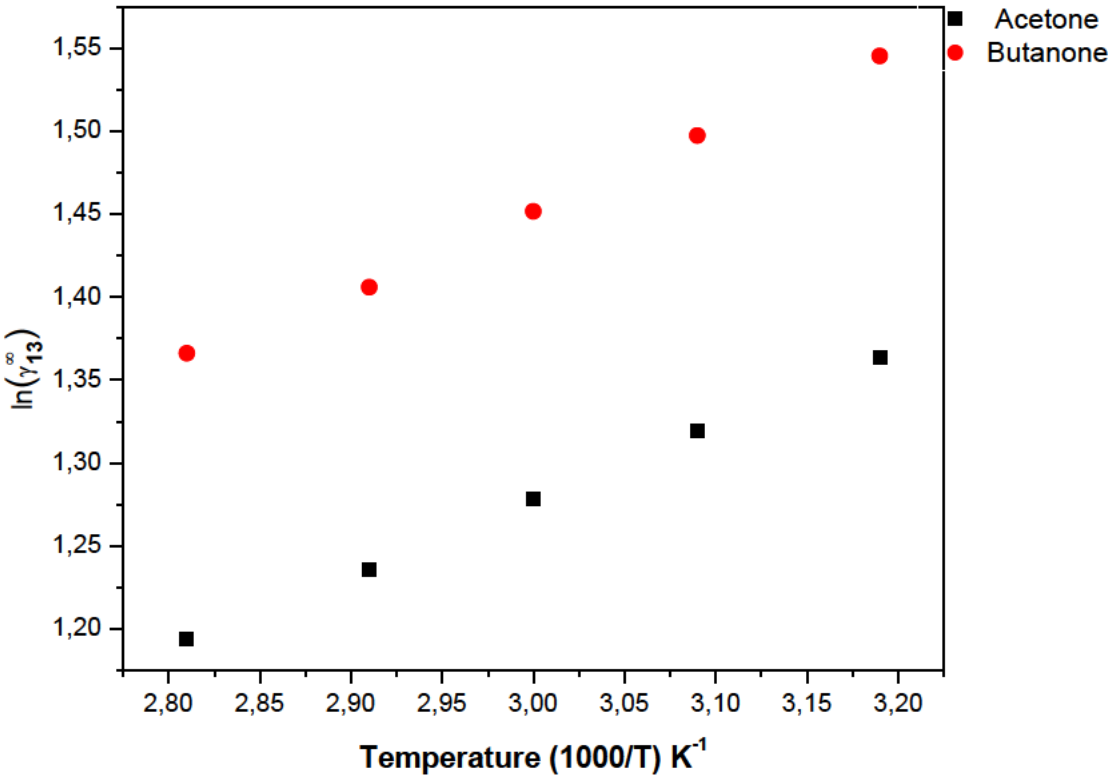

Figure 5.3. 8: Plot of $\ln \gamma_{13}^{\infty}$ against 1000/T(K^{-1}) for the selected ketones in DES3 [BDMIMBF$_4$ + EG] at different temperatures, T= (313.15 – 343.15) K.

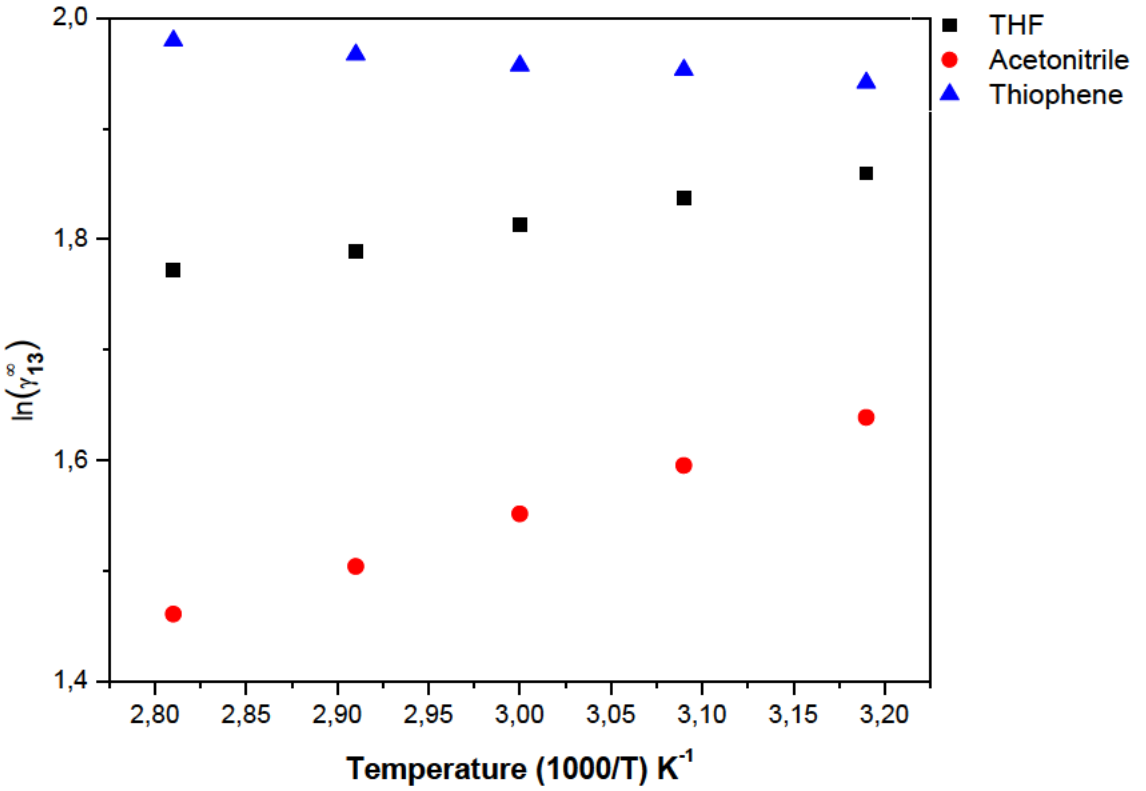

Figure 5.3. 9: Plot of $\ln \gamma_{13}^{\infty}$ against 1000/T(K^{-1}) for the selected THF, acetonitrile and thiophene in DES3 [$BDMIMBF_4$ + EG] at different temperatures, *T*= (313.15 – 343.15) K.

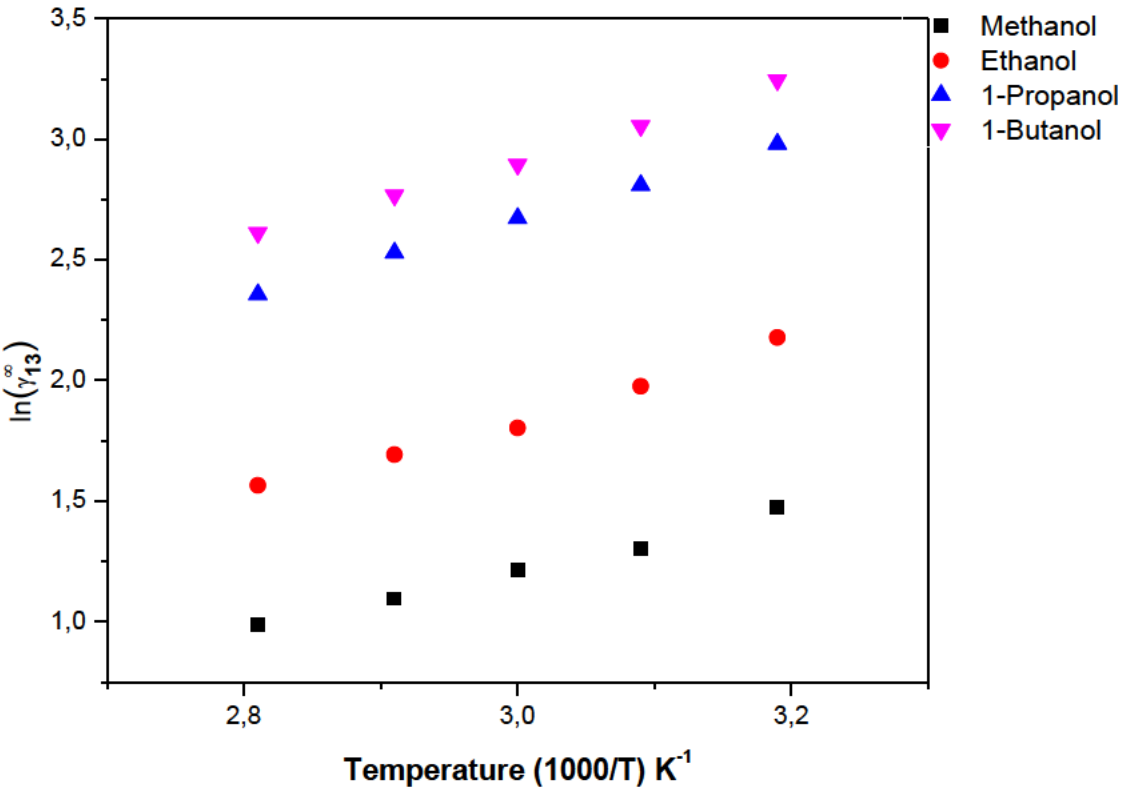

Figure 5.3. 10: Plot of $\ln \gamma_{13}^{\infty}$ against 1000/T(K^{-1}) for the selected alcohols in DES3 [BDMIMBF$_4$ + EG] at different temperatures, *T*= (313.15 – 343.15) K.

5.4 DES4: 1-butyl-2,3-dimethylimidazolium tetrafluoroborate + diethylene glycol

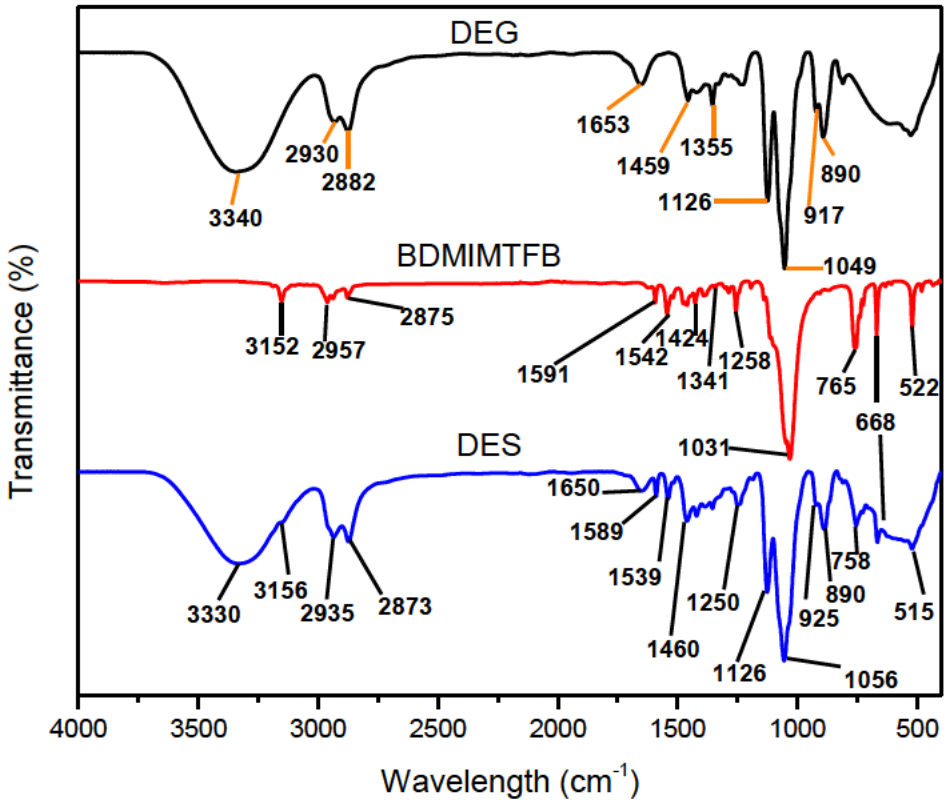

Figure 5.4. 1: FT-IR spectra of diethylene glycol (DEG), 1-butyl-2,3-dimethylimidazolium tetrafluoroborate (BDMIMTFB), and DES ($BDMIMTBF_4$+ DEG).

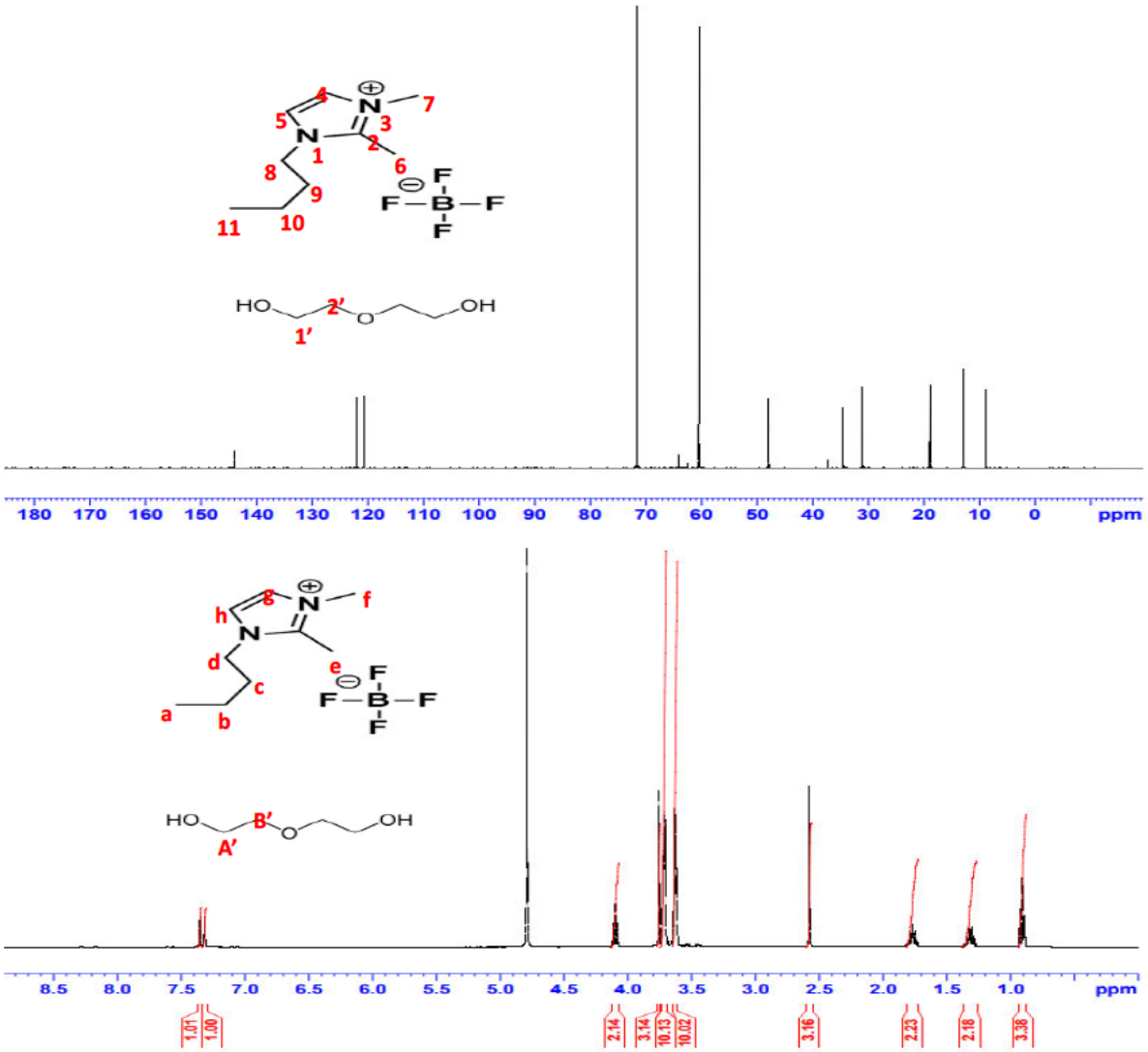

Figure 5.4. 2: (a) ^{13}C-NMR spectra, (b) ^{1}H-NMR spectra of DES (BDMIMTBF$_4$+ DEG).

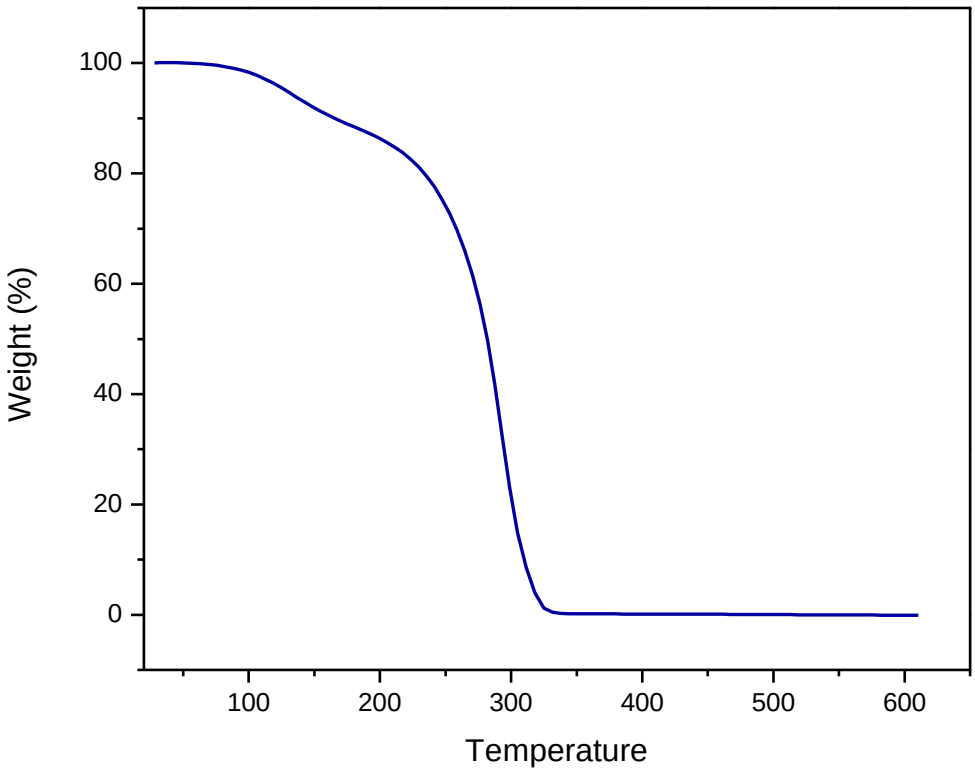

Figure 5.4. 3: Thermogravimetric analysis (TGA) curves of DES ($BDMIMTBF_4$ + DEG).

Table 5.4. 1: Activity coefficients at infinite dilution for the solutes in deep eutectic solvent [1-butyl-2,3-dimethylimidazolium tetrafluoroborate + diethylene glycol] at temperatures *T* = (313.15 - 353.15) K.

.

Average γ_{13}^{∞} values					
Solutes	*T* = 313.15 K	*T* = 323.15 K	*T* = 333.15 K	*T* = 343.15 K	*T* = 353.15 K
2,2-dimethylbutane	29.97	25.31	22.5	19.50	17.71
Pentane	18.18	15.58	13.7	12.94	12.02
Hexane	55.94	45.87	38.2	31.07	25.16
Heptane	140.20	109.36	82.6	67.75	55.34
Octane	303.04	241.01	194.5	150.06	125.06
n-Nonane	584.26	470.16	367.4	306.96	252.62
n-Decane	1054.23	862.52	711.4	577.15	476.19
1-Pentene	16.77	14.92	12.8	11.52	10.46
1-Hexene	69.43	55.86	41.7	32.92	24.80
1-Heptene	127.11	100.44	77.0	61.35	47.39
1-Nonene	411.68	336.68	284.1	236.45	200.15
1-Decene	618.27	539.32	440.0	365.46	313.74
Cyclohexene	80.89	64.74	49.4	37.53	27.99
Cyclohexane	74.10	60.07	50.9	40.66	31.73
Cyclooctane	331.98	257.79	205.8	161.51	134.99
1-Pentyne	12.71	11.55	10.6	9.44	8.52
1-Hexyne	23.69	20.41	19.2	16.95	15.46
1-Heptyne	48.98	43.47	38.3	33.52	30.25
Benzene	16.36	15.47	14.6	14.26	13.69
Toluene	31.85	29.41	27.7	26.07	24.56
Ethylbenzene	55.18	52.17	49.8	46.92	44.80
m-Xylene	61.90	58.22	54.7	52.77	48.95
p-Xylene	57.46	54.54	52.1	49.17	45.64
o-Xylene	47.58	44.88	42.4	39.94	38.24
Methanol	4.58	3.95	3.36	2.93	2.55
Ethanol	7.91	6.80	5.79	4.90	4.26
2-Propanol	17.47	15.93	14.02	11.94	10.56
1-Butanol	25.54	23.29	20.67	18.10	15.55
THF	7.22	6.98	6.72	6.55	6.40
Acetonitrile	7.65	6.88	6.22	5.75	5.34
Thiophene	8.24	8.42	8.62	8.80	8.97
Acetone	4.09	3.90	3.74	3.60	3.46
2-butanone	5.66	5.27	4.96	4.67	4.45

[a]Standard uncertainties u are u(γ_{13}^{∞}) = 0.05, u(T) = 0.02 K, u(BDMIMBF$_4$: DEG) = 0.005.

Table 5.4. 2: Partial molar excess properties, enthalpies ($\Delta H_1^{E,\infty}$), Gibbs free energies ($\Delta G_1^{E,\infty}$), and entropies ($T_{ref}\Delta S_1^{E,\infty}$) for the various organic solutes in DES4 [BDMIMBF$_4$ + DEG], at the temperature, T = 323.15 K.

Solutes	$\Delta H_1^{E,\infty}$/kJ .mol^{-1}	$\Delta G_1^{E,\infty}$/kJ.mol^{-1}	$T_{ref}\Delta S_1^{E,\infty}$/kJ.mol^{-1}
2,2-dimethylbutan	12.10	8.68	3.42
Pentane	9.37	7.38	1.99
Hexane	18.27	10.28	7.99
Heptane	21.55	12.61	8.93
Octane	20.65	14.74	5.91
n-Nonane	19.37	16.53	2.84
n-Decane	18.31	18.16	0.15
1-Pentene	11.08	7.26	3.82
1-Hexene	23.78	10.81	12.97
1-Heptene	22.68	12.38	10.29
1-Nonene	16.53	15.63	0.90
1-Decene	16.05	16.90	-0.85
Cyclohexene	24.49	11.20	13.29
Cyclohexane	19.15	11.00	8.15
Cyclooctane	20.89	14.92	5.97
1-Pentyne	9.20	6.57	2.63
1-Hexyne	9.57	8.10	1.46
1-Heptyne	11.26	10.14	1.13
Benzene	4.05	7.36	-3.31
Toluene	5.90	9.09	-3.18
Ethylbenzene	4.81	10.63	-5.82
m-Xylene	5.22	10.92	-5.70
p-Xylene	5.18	10.74	-5.57
o-Xylene	5.10	10.22	-5.12
Methanol	13.53	3.56	9.97
Ethanol	14.37	5.16	9.21
2-Propanol	11.89	7.75	4.13
1-Butanol	11.41	8.89	2.51
THF	2.79	5.22	-2.43
Acetonitrile	8.30	5.18	3.12
Thiophene	-1.97	5.73	-7.70
Acetone	3.80	3.65	0.15
2-butanone	5.56	4.46	1.09

[a]Standard uncertainties u are u(γ_{13}^{∞}) = 0.05, u(T) = 0.02 K, u(BDMIMBF$_4$: DEG) = 0.005

Table 5.4. 3: Selectivity and Capacity at Infinite Dilution of Various Solvents for Common Industrial Separation Problems at T = 313.15 K.

Solvent abbreviation	S_{ij}^{∞}			K_j^{∞}			ref
	Cyclohexane/methanol	Heptane/ Ethanol	Toluene/Benzene	Methanol	Ethanol	Benzene	
([BDMIM] BF4 + DEG) 1:3	16.17	17.72	1.91	0.213	0.1264	0.0611	This work
[EMIM Cl_4Al] [DEG] 1:4	111.1	217.1	1.69	5.26	3.703	0.503	(Kabane *et al.* 2023)
[EMPYR] Br + 1,6-HDO]	2.44	2.99	1.128	1.020	0.926	0.613	(Manyoni and Redhi 2022a)
[BMIM][BF4]	39.68	130.9	1.833	0.819	0.524	0.463	(Revelli *et al.* 2009)
[BMIM+][BF4 -]	31.72	60.36	1.70	0.826	0.524	0.411	(Foco *et al.* 2006)
NMP	5.025	14.73	---	0.51	0.763	---	(Krummen and Gmehling 2004)

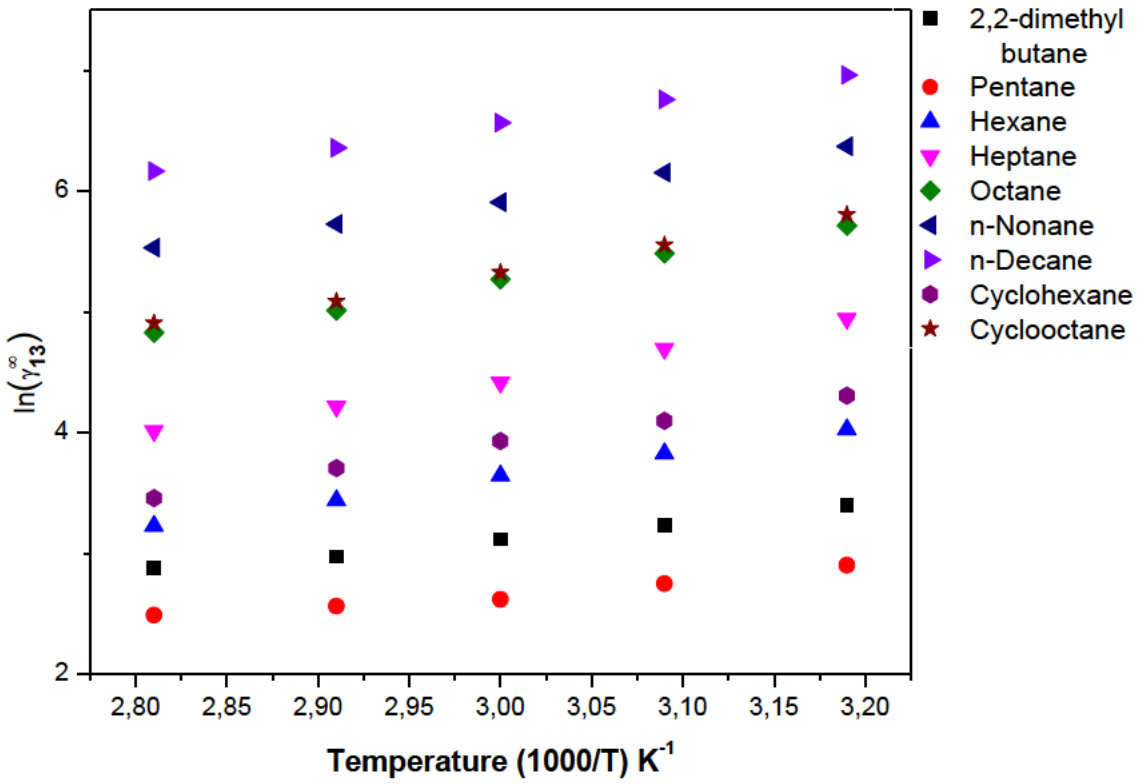

Figure 5.4. 4: Plot of $\ln \gamma_{13}^{\infty}$ against 1000/T(K^{-1}) for the selected alkanes in DES4 [$BDMIMBF_4$ + DEG] at different temperatures, *T*= (313.15 – 343.15) K.

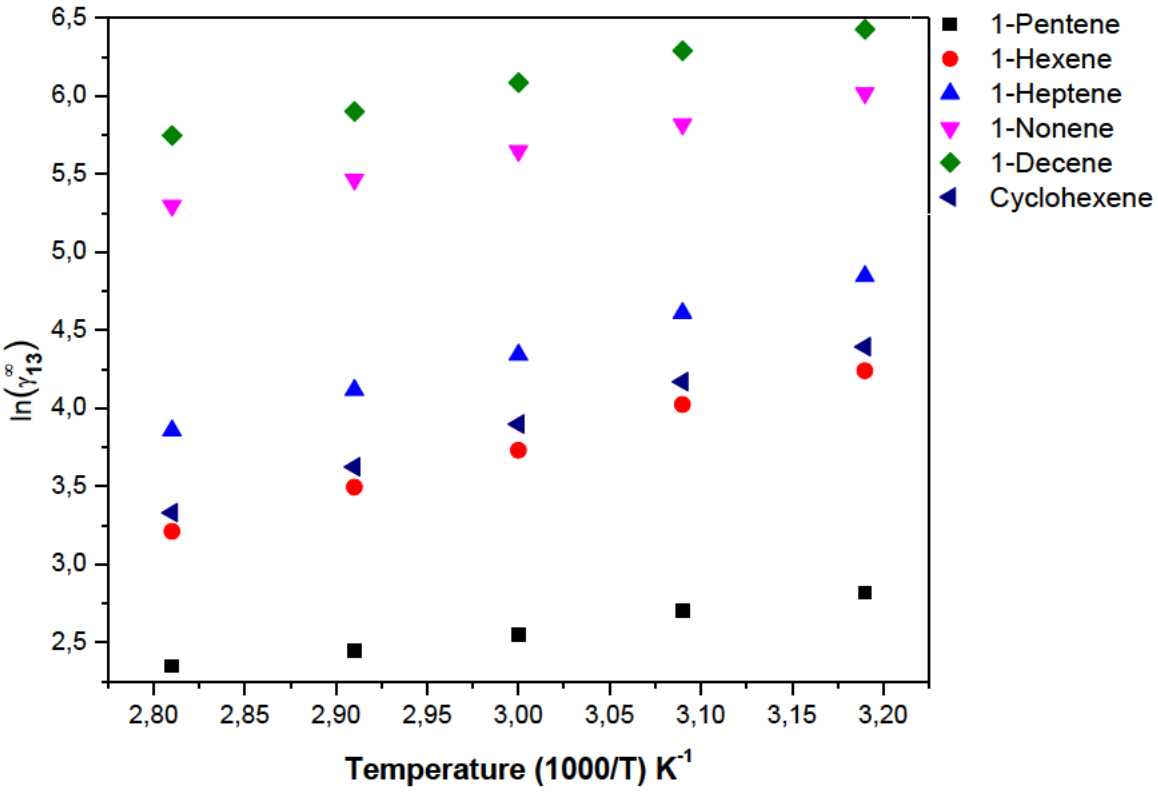

Figure 5.4. 5: Plot of $\ln \gamma_{13}^{\infty}$ against 1000/T(K^{-1}) for the selected alkenes in DES4 [BDMIMBF$_4$ + DEG] at different temperatures, *T*= (313.15 – 343.15) K.

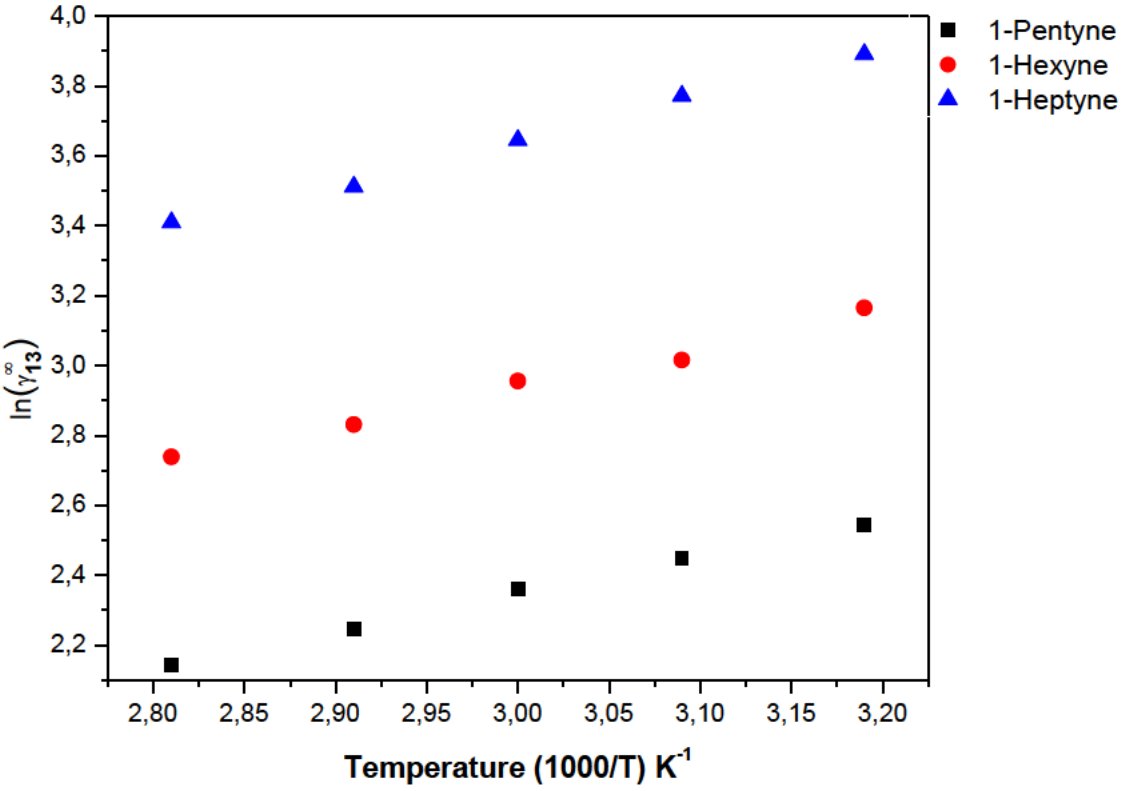

Figure 5.4. 6: Plot of $\ln \gamma_{13}^{\infty}$ against 1000/T(K^{-1}) for the selected alcohols in DES4 [BDMIMBF$_4$ + DEG] at different temperatures, *T*= (313.15 – 343.15) K.

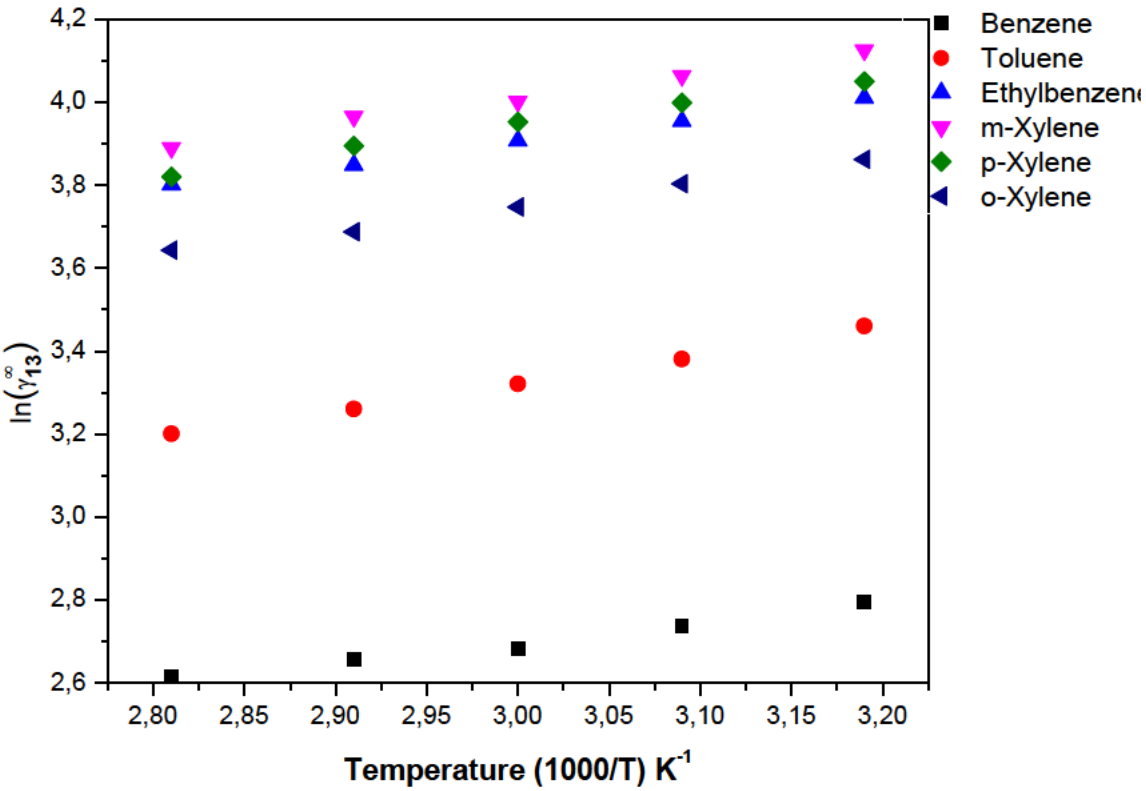

Figure 5.4. 7: Plot of $\ln \gamma_{13}^{\infty}$ against 1000/T(K^{-1}) for the selected aromatic hydrocarbons in DES4 [BDMIMBF$_4$ + DEG] at different temperatures, *T*= (313.15 – 343.15) K.

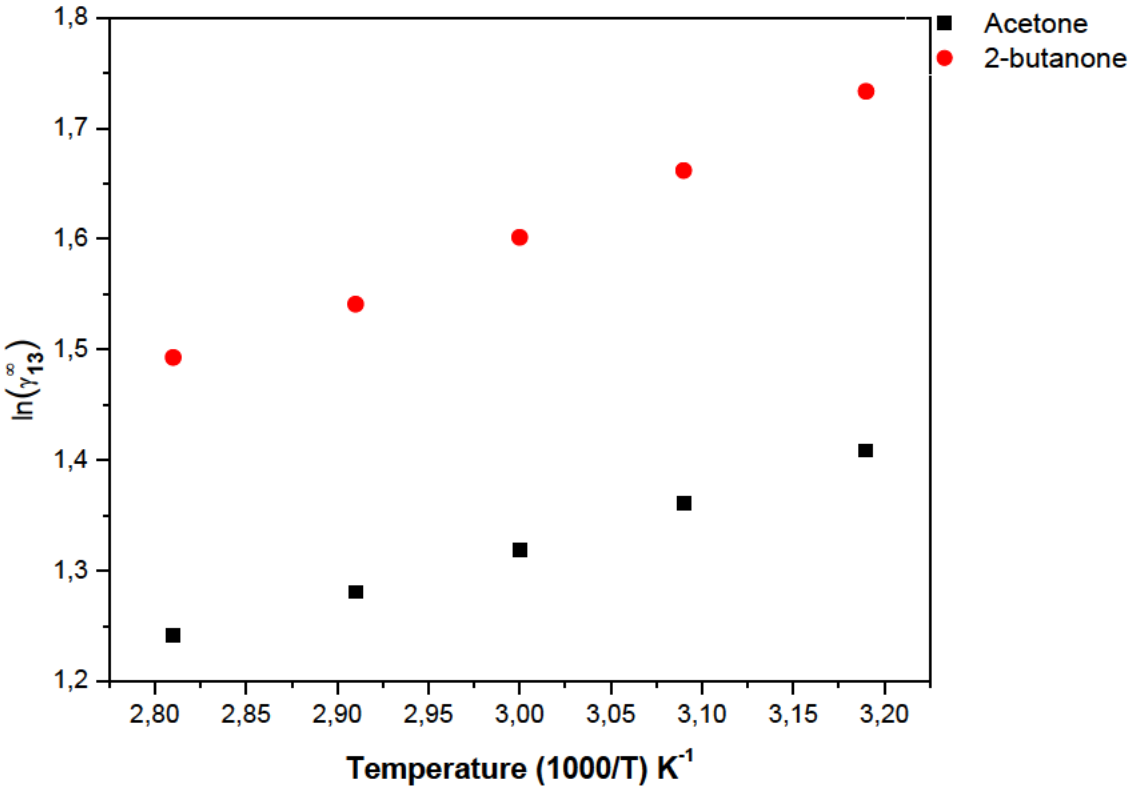

Figure 5.4. 8: Plot of $\ln \gamma_{13}^{\infty}$ against 1000/T(K^{-1}) for the selected ketones in DES4 [BDMIMBF$_4$+ DEG] at different temperatures, *T*= (313.15 – 343.15) K.

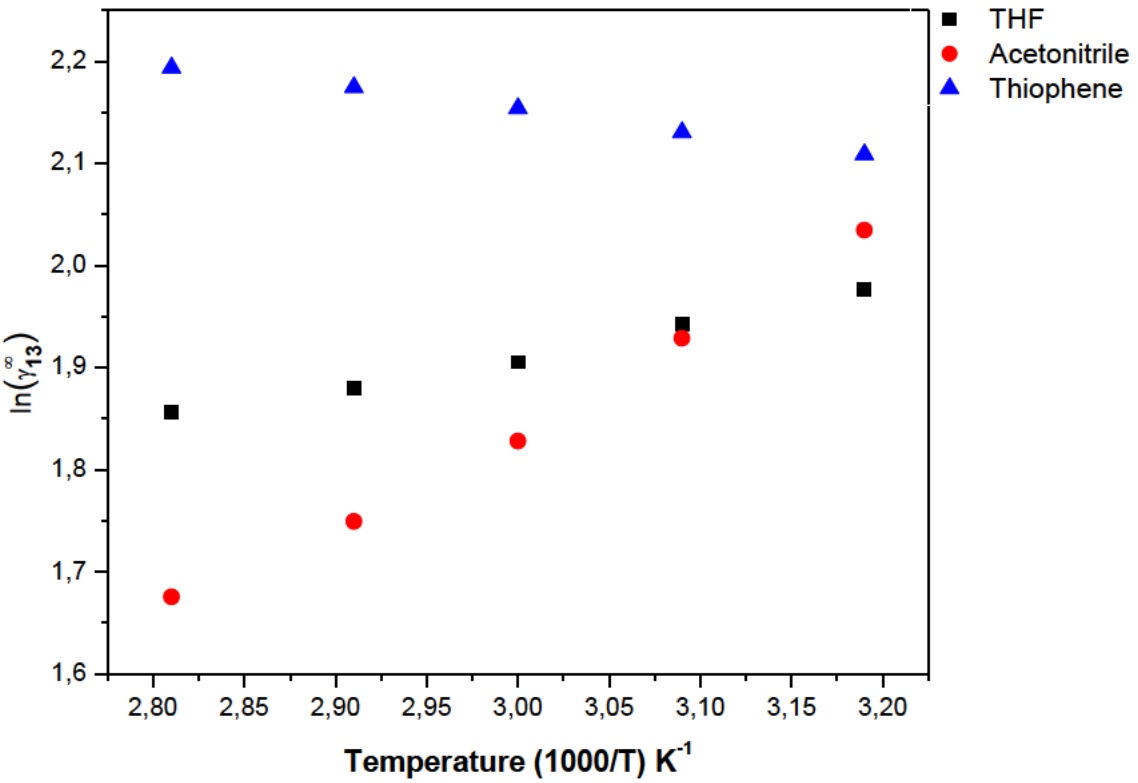

Figure 5.4. 9: Plot of $\ln \gamma_{13}^{\infty}$ against 1000/T(K^{-1}) for the selected THF, acetonitrile and thiophene in DES4 [$BDMIMBF_4$ + DEG] at different temperatures, *T*= (313.15 – 343.15) K.

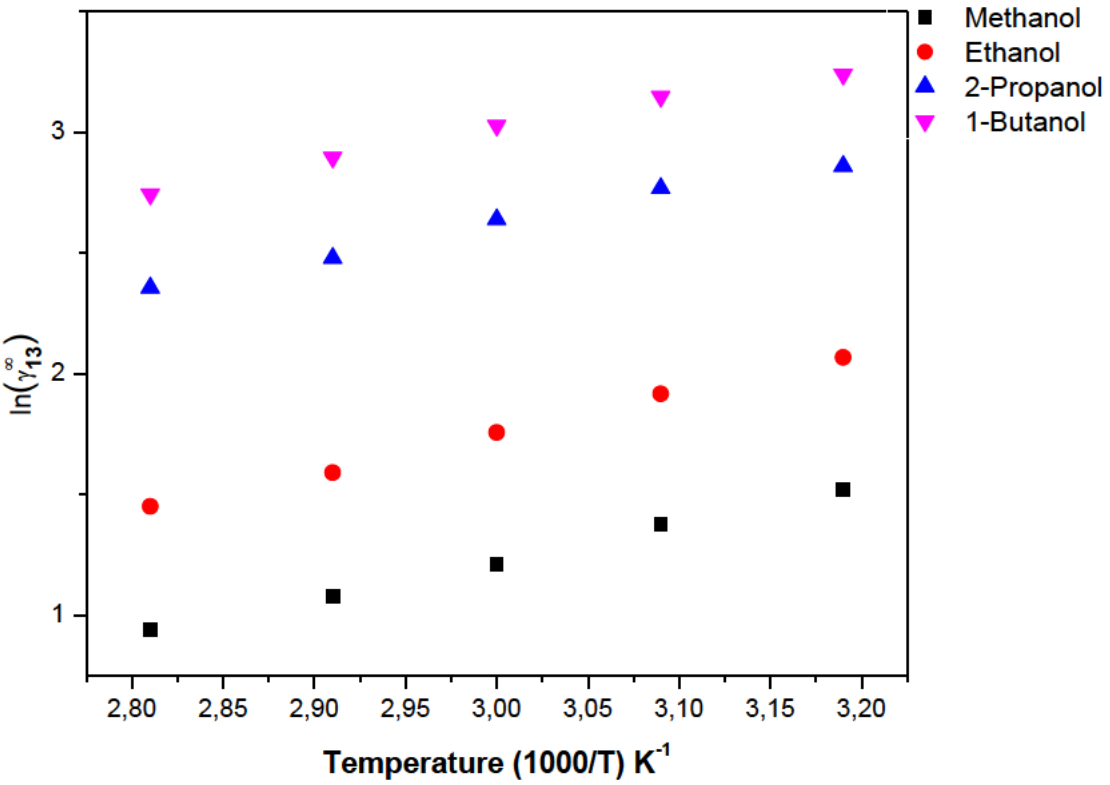

Figure 5.4. 10: Plot of $\ln \gamma_{13}^{\infty}$ against 1000/T(K^{-1}) for the selected alcohols in DES4 [BDMIMBF$_4$ + DEG] at different temperatures, *T*= (313.15 – 343.15) K.

5.5 DES 5 (1-butyl-1-methylpyrolidinium bromide + ethylene glycol) + acetic acid binary mixture.

CHARACTERIZATION OF DES5 USING FTIR, TGA, AND NMR (^{13}C)

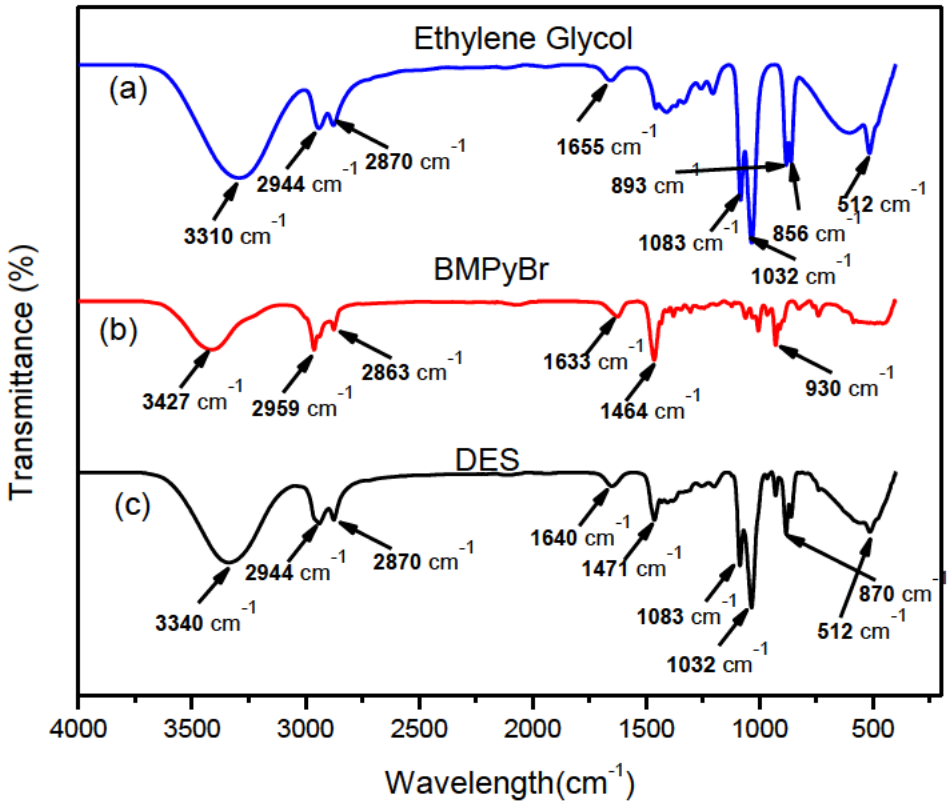

Figure 5.5. 1: (a) FT-IR spectra of ethylene glycol (EG) (blue curve), (b) 1butyl-1-methylpyrolidinium bromide (BMPyBr) (red curve), and (c) DES (EG + BMPyBr) (black curve).

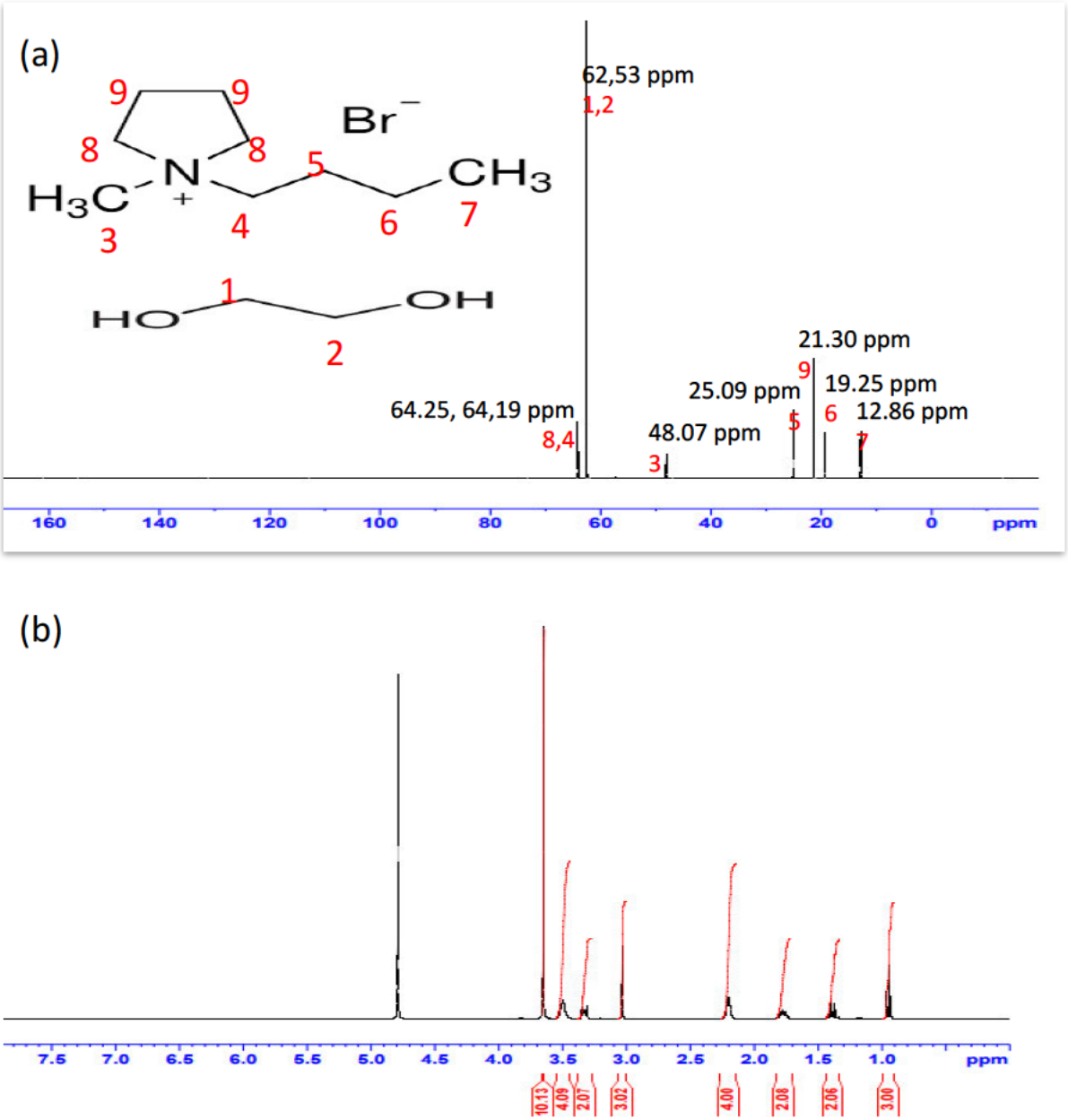

Figure 5.5. 2: (a) ^{13}C-NMR spectra, (b) ^{1}H-NMR spectra of DES (BMPyBr + EG).

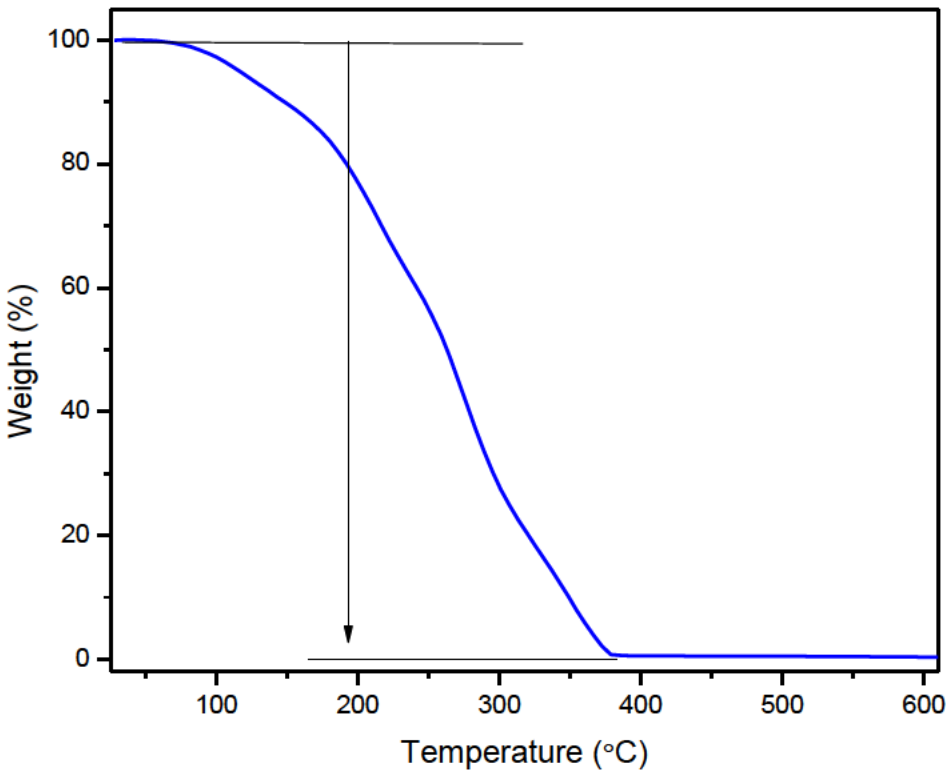

Figure 5.5. 3: Thermogravimetric analysis (TGA) curves of DES (BMPyBr + EG).

Table 5.5. 1: Densities (ρ), speed of sound (u), and refractive indices (nD) of DES(BMPrBr + EG) + acetic acid binary mixture at T= 293.15K - 313.15K and at p = 0.1 MPa.

x_1	ρ (g/cm^3)	u (m/s)	nD
	293.15 K		
0	1.0513	1164.62	1.3746
0.0900	1.1082	1401.66	1.4178
0.1048	1.1144	1440.59	1.4244
0.2049	1.1331	1521.36	1.4379
0.3049	1.1446	1569.04	1.4472
0.4052	1.1517	1620.32	1.4538
0.5048	1.1571	1650.77	1.4591
0.6047	1.1609	1675.52	1.4633

0.7053	1.1642	1693.33	1.4657
0.8050	1.1664	1708.00	1.4675
0.9053	1.1685	1720.24	1.4690
1	1.1699	1729.48	1.4697
		298.15 K	
0	1.0457	1147.42	1.3731
0.0900	1.1019	1387.28	1.4166
0.1048	1.1089	1426.35	1.4231
0.2049	1.1286	1507.99	1.4369
0.3049	1.1402	1561.92	1.4463
0.4052	1.1475	1608.08	1.4528
0.5048	1.1534	1647.22	1.4583
0.6047	1.1574	1663.71	1.4624
0.7053	1.1608	1679.47	1.4645
0.8050	1.1630	1696.38	1.4667
0.9053	1.1652	1707.18	1.4678
1	1.1666	1718.04	1.4684
		303.15 K	
0	1.0400	1130.23	1.3717
0.0900	1.0951	1372.9	1.4154
0.1048	1.1033	1411.75	1.4223
0.2049	1.1245	1495.04	1.4359
0.3049	1.1364	1546.82	1.4446
0.4052	1.1436	1595.44	1.4520
0.5048	1.1497	1626.97	1.4574
0.6047	1.1539	1651.56	1.4616
0.7053	1.1574	1667.89	1.4638
0.8050	1.1596	1684.48	1.4658
0.9053	1.1618	1697.79	1.4671
1	1.1632	1706.33	1.4678

308.15 K			
0	1.0344	1113.12	1.3704
0.0900	1.0902	1358.57	1.4144
0.1048	1.0985	1393.77	1.4197
0.2049	1.1202	1481.82	1.4350
0.3049	1.1325	1534.68	1.4436
0.4052	1.1403	1582.91	1.4512
0.5048	1.1463	1610.28	1.4569
0.6047	1.1504	1639.40	1.4608
0.7053	1.1539	1655.40	1.4630
0.8050	1.1562	1672.57	1.4651
0.9053	1.1584	1682.32	1.4669
1	1.1598	1694.24	1.4687
313.15 K			
0	1.0288	1096.06	1.3690
0.0900	1.0848	1344.35	1.4135
0.1048	1.0934	1375.74	1.4187
0.2049	1.1151	1468.63	1.4340
0.3049	1.1282	1519.19	1.4425
0.4052	1.1364	1570.47	1.4504
0.5048	1.1427	1603.05	1.4556
0.6047	1.1468	1627.27	1.4601
0.7053	1.1503	1645.89	1.4622
0.8050	1.1527	1660.64	1.4644
0.9053	1.1550	1671.12	1.4661
1	1.1565	1682.44	1.4686

Table 5.5. 2: Change in refractive indices, ΔnD, excess molar volume, V_m^E, isentropic compressibilities, k_s, deviation in isentropic compressibilities, Δk_s, and intermolecular free lengths, L_f, of DES(BMPyrBr + EG) + acetic acid binary mixture at T= 293.15K - 313.15K and at p = 0.1 MPa.

x_1	ΔnD	V_m^E ($cm^{-3}.mol^{-1}$)	k_s (Kg-1.m.s2.Pa-1)	Δk_s ($m^3.mol^{-1}.Pa^{-1}$)	Lf (10^{-7} m)
			293.15 K		
0	0	0	70.12	0	1.7104
0.0900	0.0346	-0.9135	45.92	-20.45	1.3842
0.1048	0.0399	-1.0733	43.23	-22.53	1.3430
0.2049	0.0438	-0.9534	38.12	-23.48	1.2611
0.3049	0.0436	-0.8770	35.48	-21.96	1.2167
0.4052	0.0406	-0.7165	33.07	-20.21	1.1745
0.5048	0.0365	-0.6239	31.71	-17.43	1.1502
0.6047	0.0311	-0.4775	30.68	-14.31	1.1313
0.7053	0.0240	-0.4121	29.95	-10.86	1.1178
0.8050	0.0163	-0.2525	29.38	-7.28	1.1072
0.9053	0.0083	-0.1630	28.91	-3.59	1.0983
1	0	0	28.57	0	1.0918
			298.15 K		
0	0	0	72.63	0	1.7567
0.0900	0.0349	-0.8167	47.15	-21.55	1.4154
0.1048	0.0400	-1.0253	44.32	-23.74	1.3722
0.2049	0.0442	-0.9395	38.96	-24.73	1.2866
0.3049	0.0441	-0.8377	35.94	-23.39	1.2358

0.4052	0.0410	-0.6771	33.69	-21.26	1.1965
0.5048	0.0370	-0.6271	31.95	-18.67	1.1651
0.6047	0.0316	-0.5039	31.21	-15.05	1.1516
0.7053	0.0241	-0.4447	30.54	-11.34	1.1391
0.8050	0.0168	-0.2651	29.87	-7.65	1.1267
0.9053	0.0084	-0.1814	29.44	-3.72	1.1185
1	0	0	29.03	0	1.1108
			303.15 K		
0	0	0	75.26	0	1.8046
0.0900	0.0350	-0.6762	48.44	-22.70	1.4477
0.1048	0.0405	-0.9616	45.47	-24.99	1.4027
0.2049	0.0445	-0.9687	39.78	-26.10	1.3120
0.3049	0.0435	-0.8688	36.77	-24.53	1.2614
0.4052	0.0413	-0.6651	34.35	-22.37	1.2191
0.5048	0.0371	-0.6465	32.85	-19.31	1.1923
0.6047	0.0317	-0.5302	31.77	-15.83	1.1724
0.7053	0.0243	-0.4671	31.05	-11.94	1.1592
0.8050	0.0167	-0.2796	30.39	-8.05	1.1467
0.9053	0.0083	-0.1812	29.85	-3.99	1.1366
1	0	0	29.52	0	1.1302
			308.15 K		
0	0	0	78.01	0	1.8539
0.0900	0.0351	-0.6735	49.69	-24.00	1.4796
0.1048	0.0389	-0.9727	46.85	-26.13	1.4367
0.2049	0.0444	-0.9843	40.65	-27.53	1.3382
0.3049	0.0432	-0.9064	37.48	-25.89	1.2851
0.4052	0.0409	-0.7589	34.99	-23.57	1.2417

0.5048	0.0368	-0.7013	33.64	-20.15	1.2174
0.6047	0.0309	-0.5596	32.34	-16.65	1.1936
0.7053	0.0232	-0.4932	31.62	-12.55	1.1803
0.8050	0.0155	-0.2959	30.91	-8.47	1.1670
0.9053	0.0075	-0.1851	30.50	-4.07	1.1591
1	0	0	30.03	0	1.1503
			313.15 K		
0	0	0	80.90	0	1.9048
0.0900	0.0355	-0.6405	51.00	-25.36	1.5124
0.1048	0.0392	-0.9539	48.31	-27.30	1.4721
0.2049	0.0445	-0.9085	41.57	-29.01	1.3655
0.3049	0.0431	-0.8745	38.40	-27.14	1.3124
0.4052	0.0410	-0.7568	35.67	-24.81	1.2649
0.5048	0.0363	-0.7272	34.05	-21.43	1.2358
0.6047	0.0308	-0.5861	32.92	-17.52	1.2152
0.7053	0.0229	-0.4897	32.08	-13.29	1.1996
0.8050	0.0152	-0.3094	31.45	-8.90	1.1877
0.9053	0.0069	-0.2125	31.00	-4.31	1.1791
1	0	0	30.54	0	1.1704

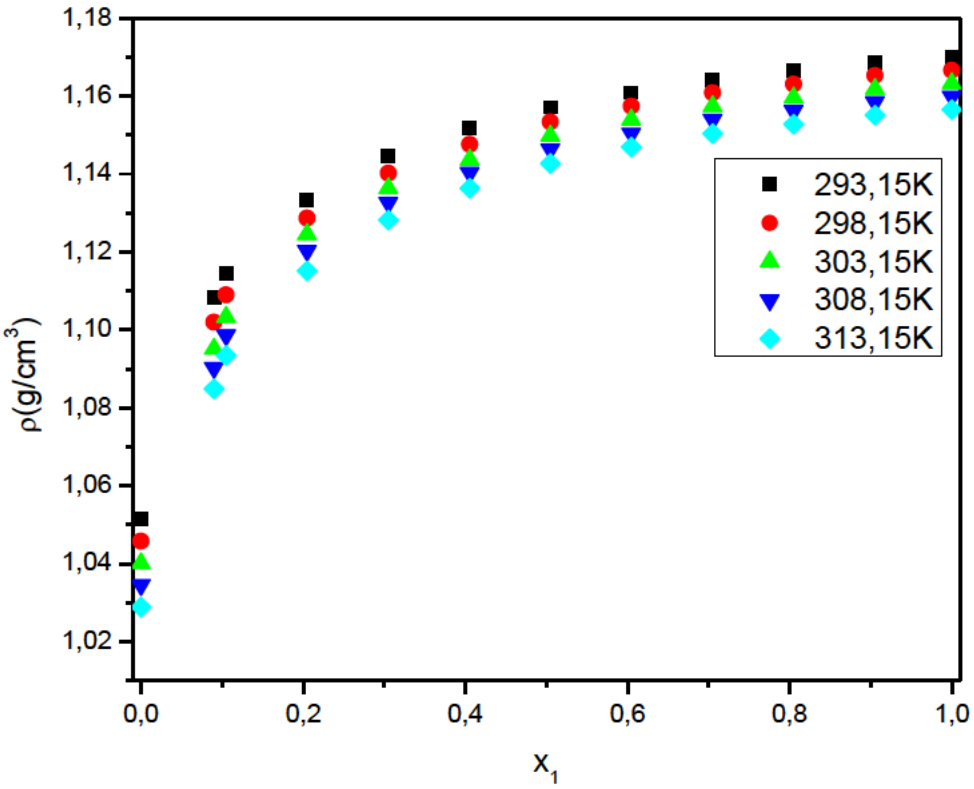

Figure 5.5. 4: Densities of the binary mixtures of DES (BMPRLBr + EG) + acetic acid) at T = 293.15 K - 313.15 K.

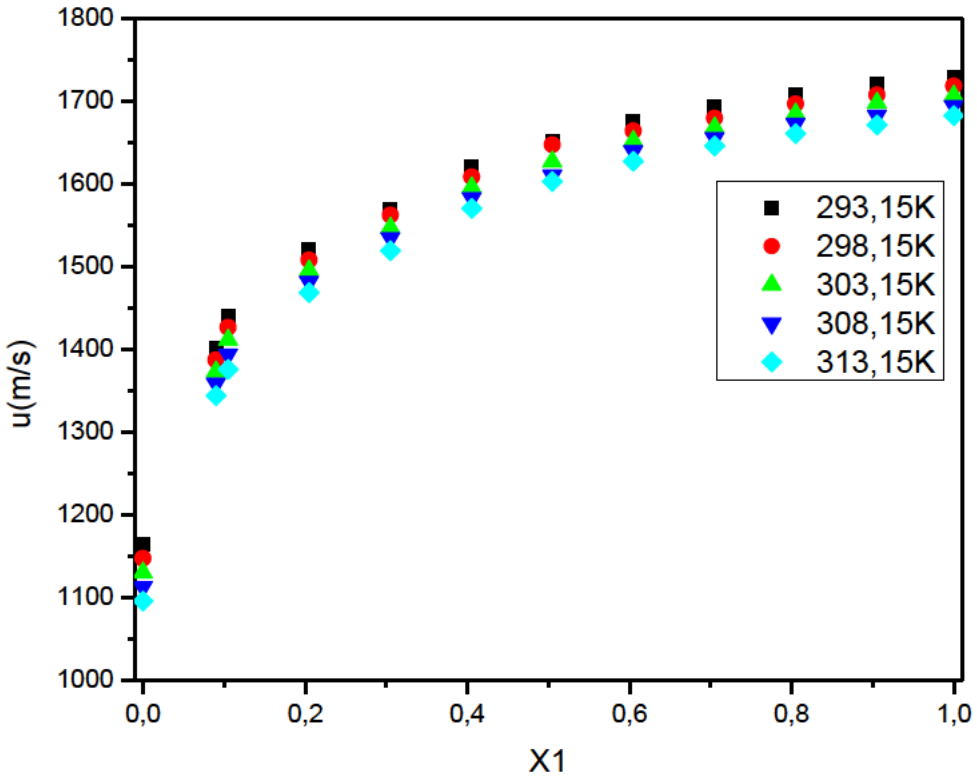

Figure 5.5. 5: Speed of sound of the binary mixtures of {DES (BMPyrBr + EG) + acetic acid} at *T* = 293.15 K - 313.15 K.

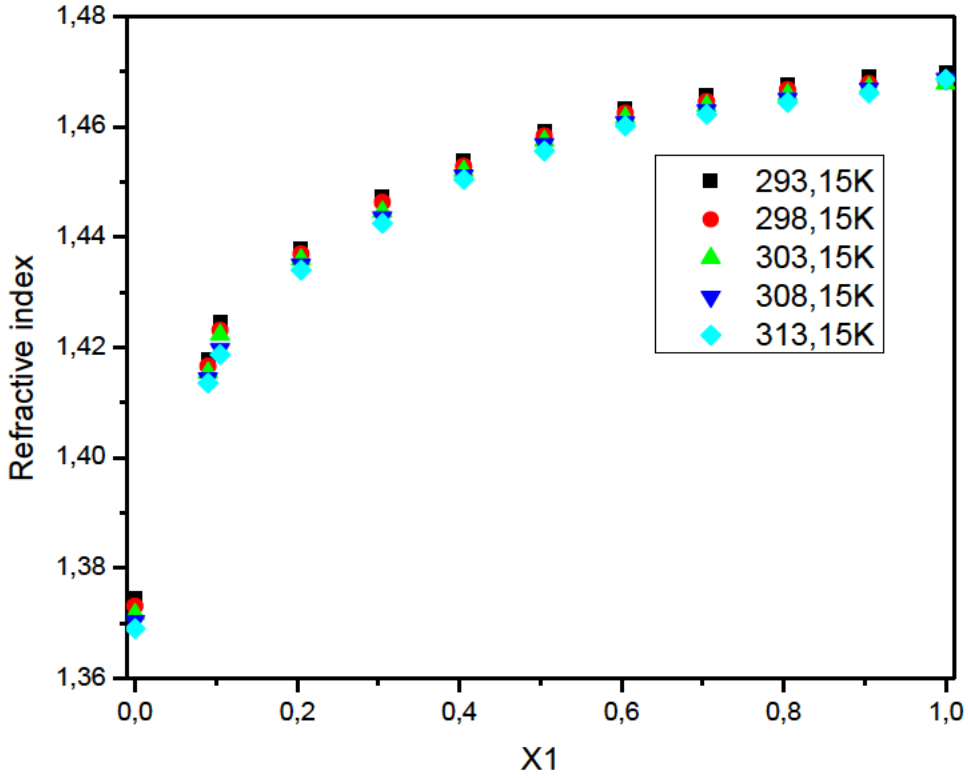

Figure 5.5. 6: Refractive indices of the binary mixtures of {DES (BMPyrBr + EG) + acetic acid} at *T* = 293.15 K - 313.15 K.

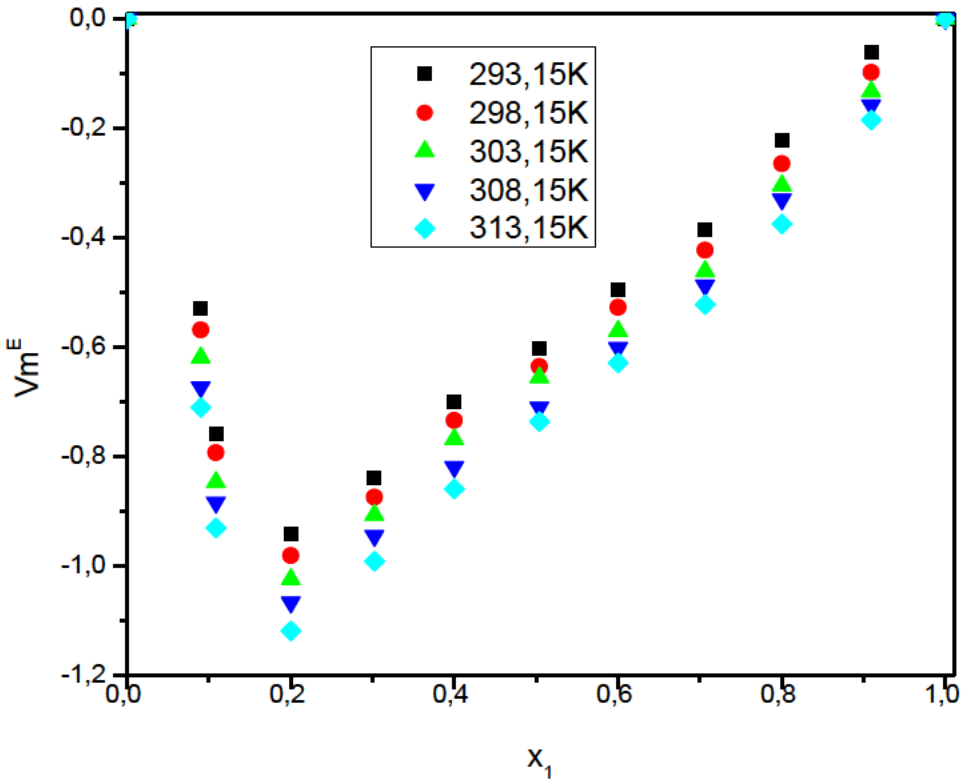

Figure 5.5. 7: Excess molar volume (V_m^E) of the prepared mixtures for {DES (BMPyrBr + EG) + acetic acid} at T = (293.15 - 313.15) K.

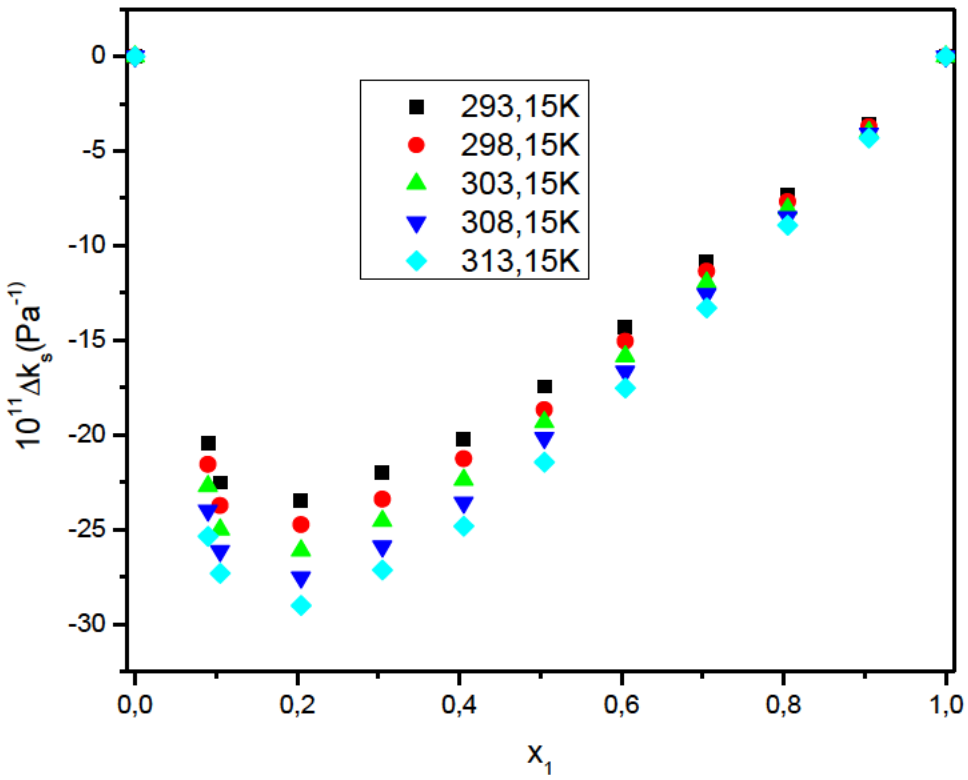

Figure 5.5. 8: Deviation in isentropic compressibility (Δk_S) of the binary mixtures of {DES (BMPyrBr + EG) + acetic acid} expressed in mole fraction of DES (BMPyrBr + EG) at T = (293.15, 298.15, 303.15, 308.15 and 313.15) K.

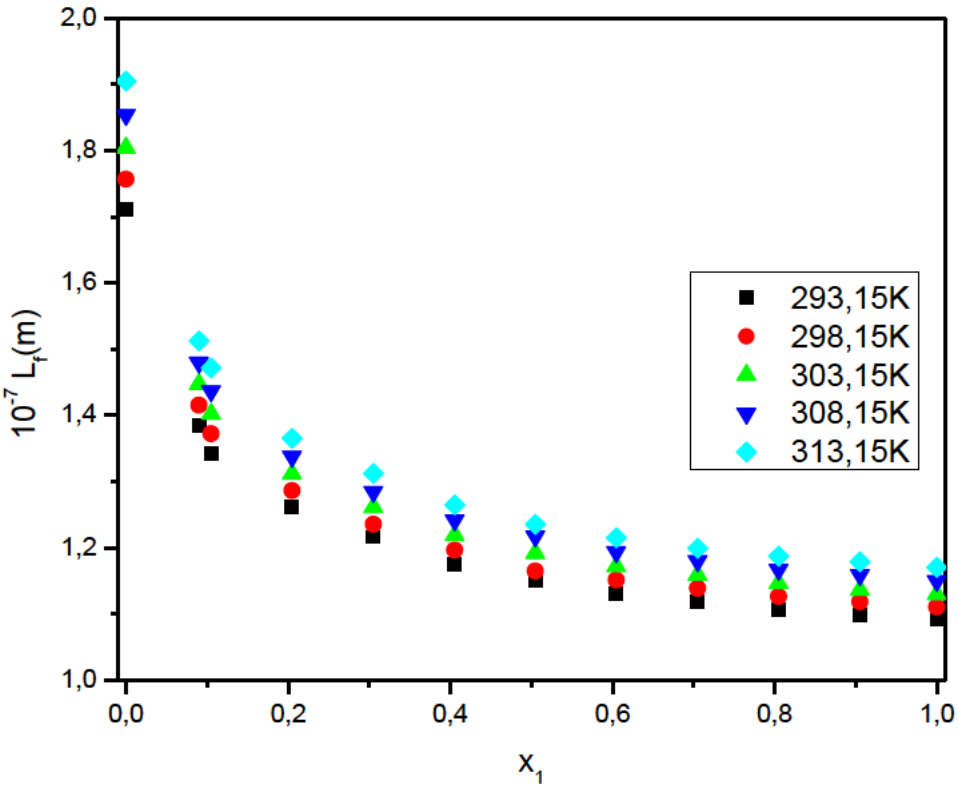

Figure 5.5. 9: Intermolecular free length (L_f), of the binary mixtures of {DES (BMPyrBr + EG) + acetic acid} given as a function of mole fraction of DES at T = (293.15, 298.15, 303.15, 308.15 and 313.15) K.

5.6 DES5 (1-butyl-1-methylpyrolidinium bromide + ethylene glycol) + ethanol binary mixture.

Table 5.6. 1: Densities (ρ), speed of sound (u), and refractive indices (nD) of DES (BMPyrBr + EG) + ethanol binary mixture at T= (293.15K - 313.15) K and at p = 0.1 MPa.

x1	ρ (g/cm^3)	u (m/s)	nD
	293.15 K		
0	0.7928	1169.31	1.3634
0.0928	0.9429	1347.42	1.4102
0.1007	0.9771	1411.09	1.4211
0.2009	1.0264	1474.75	1.4347
0.3008	1.0668	1538.02	1.4458
0.4002	1.1001	1601.29	1.4546
0.5039	1.1235	1634.53	1.4591
0.6003	1.1366	1666.41	1.4630
0.7064	1.1470	1685.13	1.4656
0.8026	1.1563	1703.85	1.4678
0.9007	1.1624	1716.67	1.4691
1	1.1699	1729.48	1.4697
	298.15 K		
0	0.7885	1152.78	1.3619
0.0928	0.9390	1332.94	1.4097
0.1007	0.9675	1396.32	1.4203
0.2009	1.0188	1461.42	1.4343
0.3008	1.0565	1523.24	1.4448
0.4002	1.0902	1589.09	1.4537
0.5039	1.1150	1621.35	1.4585
0.6003	1.1331	1654.34	1.4622
0.7064	1.1390	1673.24	1.4645
0.8026	1.1529	1692.29	1.4670
0.9007	1.1555	1702.36	1.4681
1	1.1666	1718.04	1.4686
	303.15 K		
0	0.7842	1135.60	1.3602
0.0928	0.9351	1318.42	1.4082
0.1007	0.9609	1381.52	1.4190
0.2009	1.0109	1447.99	1.4327
0.3008	1.0489	1508.37	1.4427
0.4002	1.0913	1576.15	1.4526
0.5039	1.1066	1608.41	1.4577
0.6003	1.1297	1642.16	1.4612
0.7064	1.1332	1660.51	1.4634
0.8026	1.1495	1680.47	1.4661
0.9007	1.1473	1690.25	1.4671
1	1.1632	1706.33	1.4678

308.15 K			
0	0.7928	1118.72	1.3589
0.0928	0.9429	1303.90	1.4074
0.1007	0.9771	1366.34	1.4177
0.2009	1.0264	1434.55	1.4318
0.3008	1.0668	1493.51	1.4417
0.4002	1.1001	1563.64	1.4519
0.5039	1.1235	1594.97	1.4563
0.6003	1.1366	1629.98	1.4604
0.7064	1.1470	1647.32	1.4627
0.8026	1.1563	1668.58	1.4654
0.9007	1.1624	1676.25	1.4661
1	1.1598	1694.24	1.4667
313.15 K			
0	0.7754	1101.94	1.3576
0.0928	0.9272	1289.44	1.4070
0.1007	0.9500	1351.42	1.4169
0.2009	1.0005	1421.07	1.4310
0.3008	1.0385	1478.24	1.4421
0.4002	1.0815	1551.07	1.4511
0.5039	1.1022	1581.36	1.4553
0.6003	1.1228	1617.79	1.4598
0.7064	1.1328	1633.27	1.4623
0.8026	1.1427	1665.38	1.4647
0.9007	1.1493	1664.32	1.4651
1	1.1565	1682.44	1.4656

Table 5.6. 2: Change in refractive indices, ΔnD, excess molar volume, V_m^E, isentropic compressibilities, k_s, deviation in isentropic compressibilities, Δk_s, and intermolecular free length, L_f of DES(BMPyrBr + EG) + ethanol binary mixture at *T*= 293.15K - 313.15K and *p* = 0.1 MPa.

x_1	ΔnD	V_m^E($cm^{-3}.mol^{-1}$)	k_s ($Kg^{-1}.m.s^2.Pa^{-1}$)	ΔK_s ($m^3.mol^{-1}.Pa^{-1}$)	L_f (10^{-7} m)
293.15 K					
0	0	0	92.24	0	1.9617
0.0928	0.0369	-0.6229	58.41	-27.92	1.5610
0.1007	0.0469	-0.7450	51.39	-34.43	1.4642
0.2009	0.0499	-0.8367	44.79	-34.65	1.3670
0.3008	0.0504	-0.8653	39.62	-33.47	1.2856
0.4002	0.0486	-0.8887	35.44	-31.31	1.2160
0.5039	0.0421	-0.9269	33.31	-26.85	1.1788
0.6003	0.0357	-0.8991	31.68	-22.34	1.1496
0.7064	0.0271	-0.6838	30.69	-16.56	1.1316
0.8026	0.0190	-0.4425	29.78	-11.35	1.1147
0.9007	0.0099	-0.1962	29.19	-5.70	1.1035

1	0	0	28.57	0	1.0918
			298.15 K		
0	0	0	95.42	0	2.0136
0.0928	0.0378	-0.6468	59.93	-29.33	1.5957
0.1007	0.0476	-0.7689	53.00	-35.73	1.5007
0.2009	0.0509	-0.8713	45.95	-36.12	1.3973
0.3008	0.0508	-0.8974	40.79	-34.66	1.3164
0.4002	0.0490	-0.9233	36.32	-32.53	1.2423
0.5039	0.0428	-0.9512	34.11	-27.85	1.2039
0.6003	0.0362	-0.9234	32.24	-23.33	1.1704
0.7064	0.0272	-0.7163	31.35	-17.16	1.1542
0.8026	0.0194	-0.4774	30.28	-11.85	1.1343
0.9007	0.0100	-0.2211	29.86	-5.76	1.1263
1	0	0	29.03	0	1.1108
			303.15 K		
0	0	0	98.88	0	2.0684
0.0928	0.0380	-0.6698	61.51	-30.92	1.6314
0.1007	0.0479	-0.7835	54.52	-37.37	1.5359
0.2009	0.0508	-0.8947	47.17	-37.76	1.4287
0.3008	0.0501	-0.9269	41.90	-36.11	1.3464
0.4002	0.0493	-0.9528	36.88	-34.23	1.2633
0.5039	0.0432	-0.9640	34.92	-29.00	1.2293
0.6003	0.0364	-0.9414	32.82	-24.42	1.1917
0.7064	0.0271	-0.7387	32.00	-17.87	1.1767
0.8026	0.0195	-0.4999	30.80	-12.40	1.1544
0.9007	0.0099	-0.2636	30.50	-5.90	1.1489
1	0	0	29.52	0	1.1302
			308.15 K		
0	0	0	100.78	0	2.1071
0.0928	0.0384	-0.6864	62.37	-31.83	1.6577
0.1007	0.0479	-0.7970	54.81	-38.83	1.5540
0.2009	0.0512	-0.9226	47.34	-39.22	1.4441
0.3008	0.0503	-0.9538	42.02	-37.47	1.3606
0.4002	0.0498	-0.9709	37.17	-35.28	1.2797
0.5039	0.0430	-0.9910	34.98	-30.14	1.241495
0.6003	0.0367	-0.9580	33.11	-25.19	1.2078
0.7064	0.0276	-0.7487	32.12	-18.67	1.1896
0.8026	0.0199	-0.5149	31.06	-12.93	1.1697
0.9007	0.0101	-0.2911	30.61	-6.44	1.1614
1	0	0	30.03	0	1.1503
			313.15 K		
0	0	0	106.19	0	2.1824
0.0928	0.0393	-0.7197	64.86	-34.31	1.7055
0.1007	0.0484	-0.8085	57.63	-40.94	1.6077
0.2009	0.0516	-0.9769	49.49	-41.50	1.4898
0.3008	0.0520	-0.9951	44.06	-39.37	1.4057

0.4002	0.0502	-1.0204	38.43	-37.48	1.3128
0.5039	0.0432	-0.9888	36.27	-31.79	1.2755
0.6003	0.0373	-0.7512	34.02	-26.75	1.2353
0.7064	0.0284	-0.7614	33.09	-19.66	1.2182
0.8026	0.0204	-0.5268	31.55	-13.92	1.1895
0.9007	0.0102	-0.3086	31.40	-6.64	1.1868
1	0	0	30.54	0	1.1704

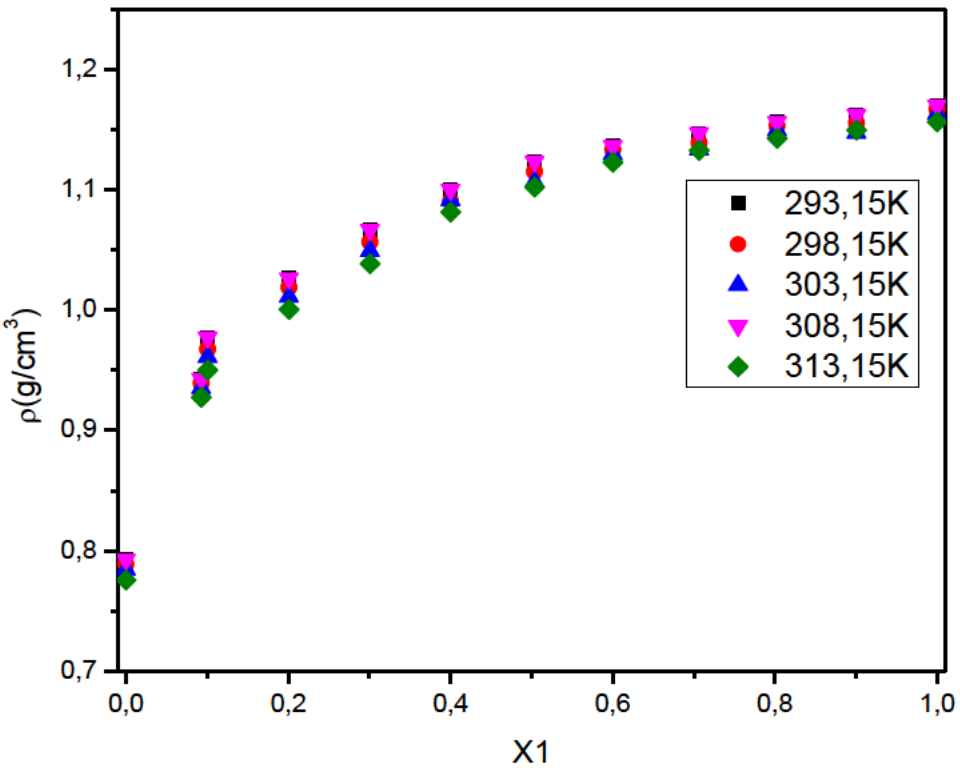

Figure 5.6. 1: Density of the binary mixtures of {DES (BMPyrBr + EG) + ethanol} at *T* = (293.15 K - 313.15) K.

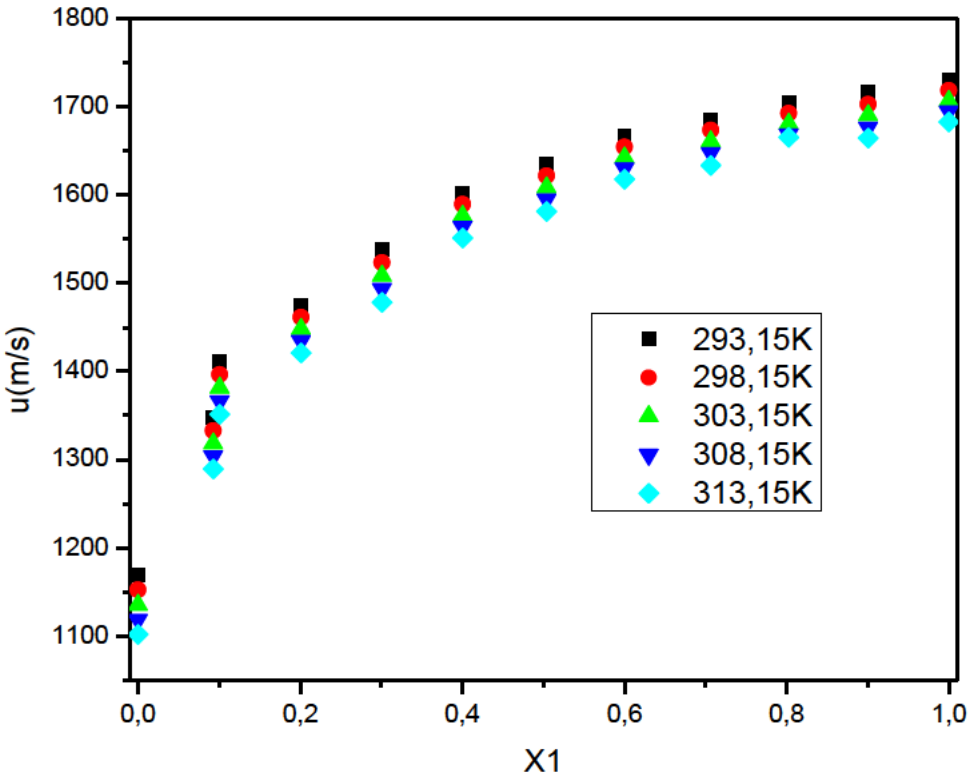

Figure 5.6. 2: Speed of sound of the binary mixtures of {DES (BMPyrBr + EG) + acetic acid} at *T* = (293.15 K - 313.15) K.

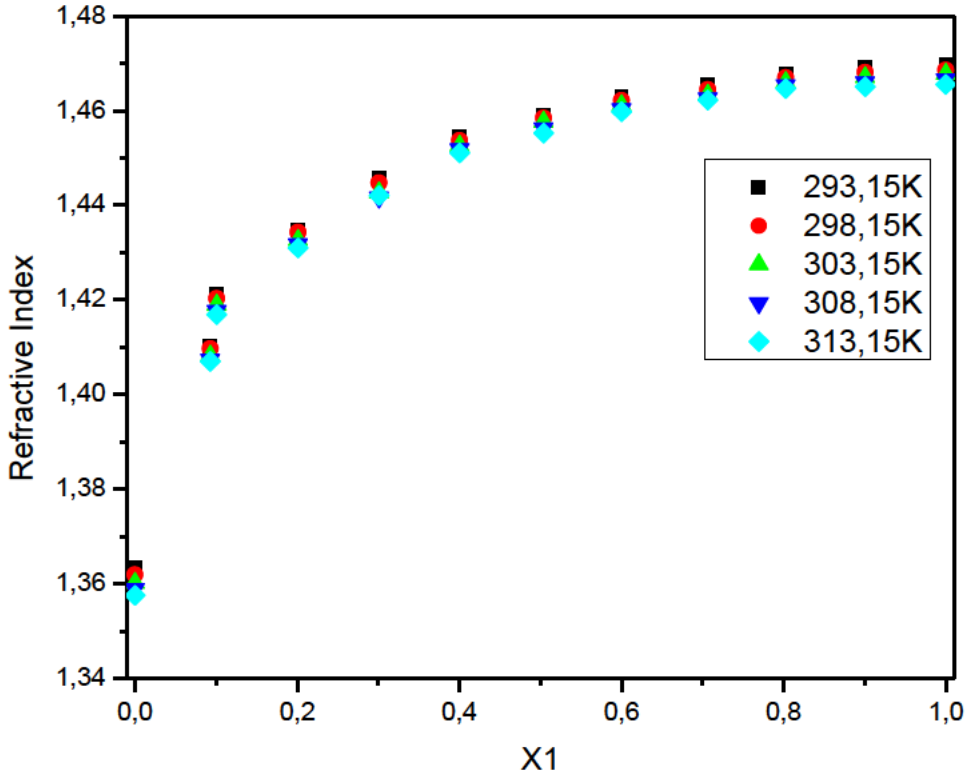

Figure 5.6. 3: Refractive indices of the binary mixtures of {DES (BMPyrBr + EG) + ethanol} at *T* = (293.15 K - 313.15) K

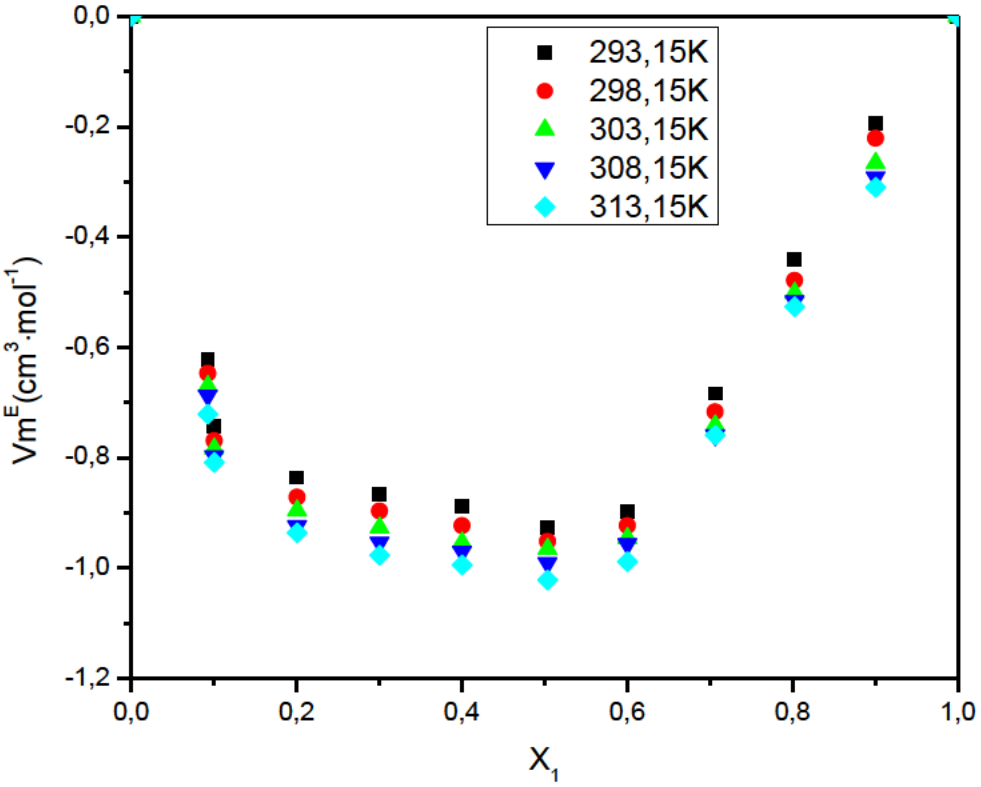

Figure 5.6. 4: Excess molar volume (V_m^E) of the miscible prepared mixtures of {DES (BMPyrBr + EG) (x_1) + ethanol (x_2)} as a function of mole fraction of ionic liquid at *T* = (293.15, 298.15, 303.15, 308.15 and 313.15) K.

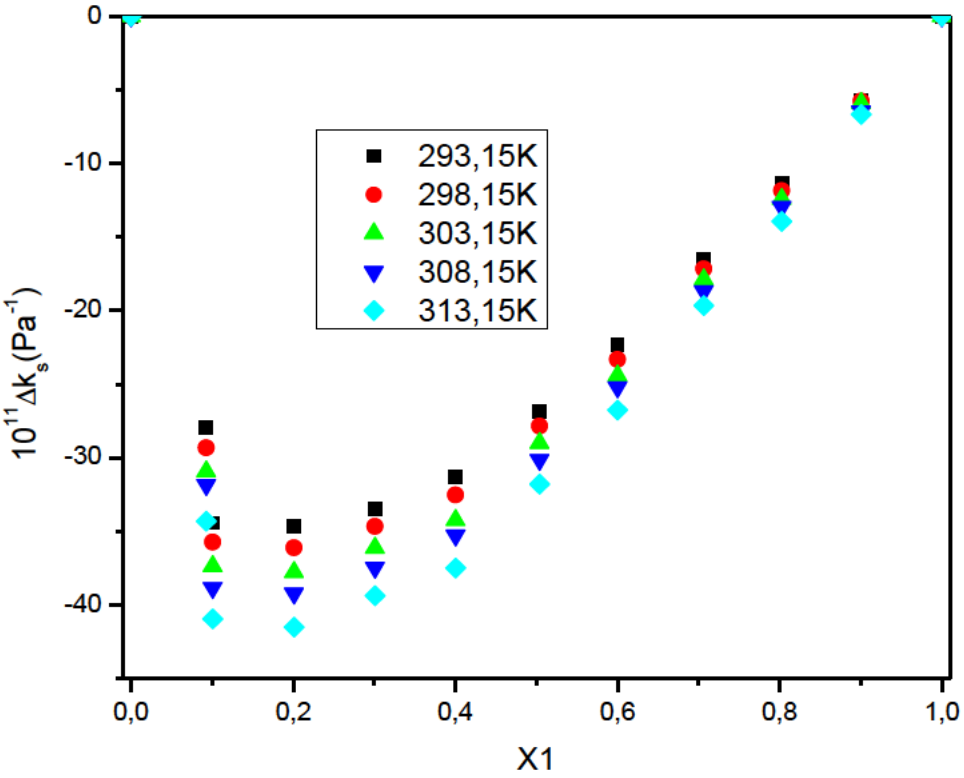

Figure 5.6. 5: Deviation in isentropic compressibilities (Δk_S) of the binary mixtures of {DES (BMPyrBr + EG) + ethanol} expressed in mole fraction of DES (BMPyrBr + EG) at T = (293.15, 298.15, 303.15, 308.15 and 313.15) K.

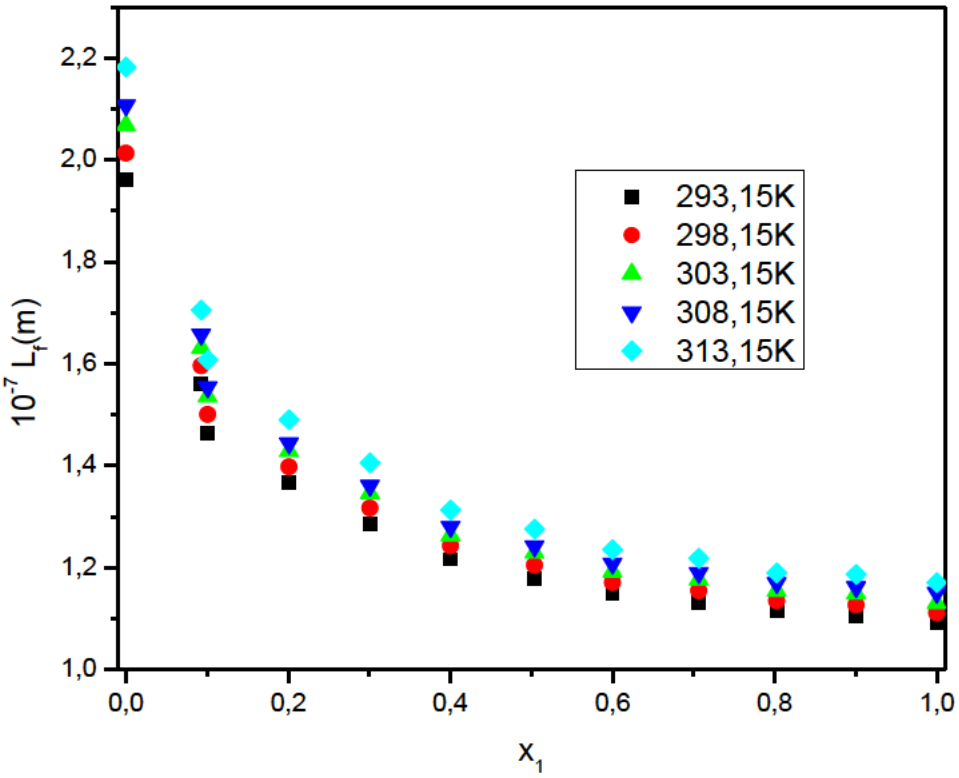

Figure 5.6. 6: Intermolecular free length (L_f), of the binary mixtures of {DES (BMPyrBr + EG) + ethanol} given as a function of mole fraction of DES at T = (293.15, 298.15, 303.15, 308.15 and 313.15) K.

5.7 DES6 (1-butyl-3-methylimidazolium chloride + ethylene glycol) + acetic acid binary mixture.

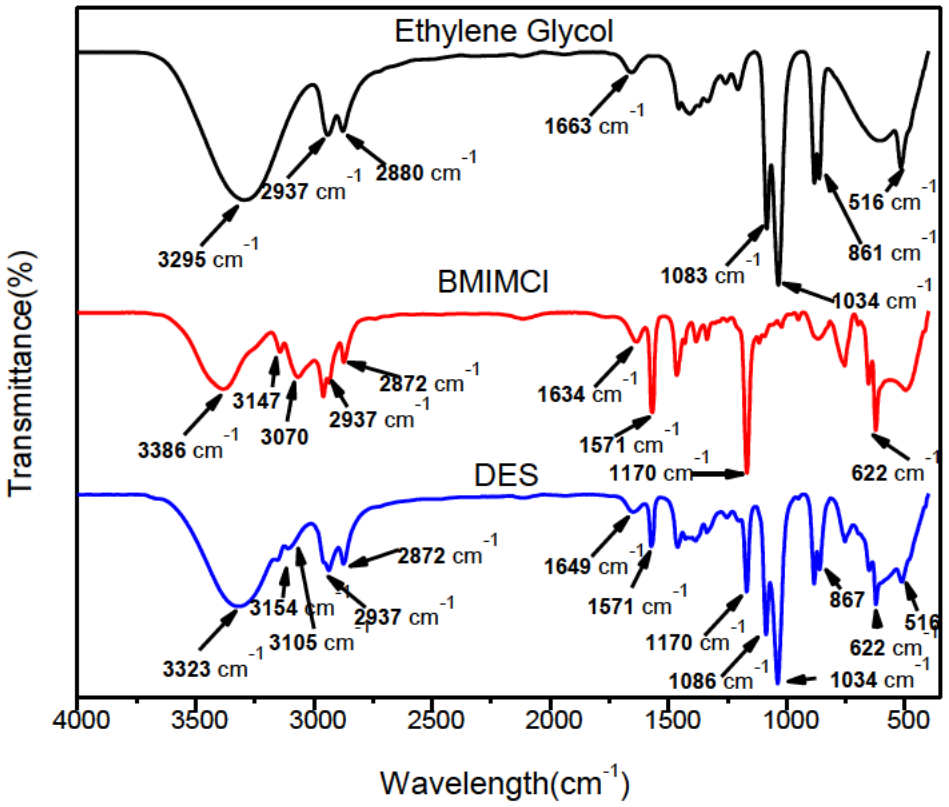

Figure 5.7. 1: FT-IR spectra of ethylene glycol (EG) (black curve), 1butyl-3-methylimidazolium chloride (BMIMCl) (red curve), and DES (EG + BMIMCl) (blue curve).

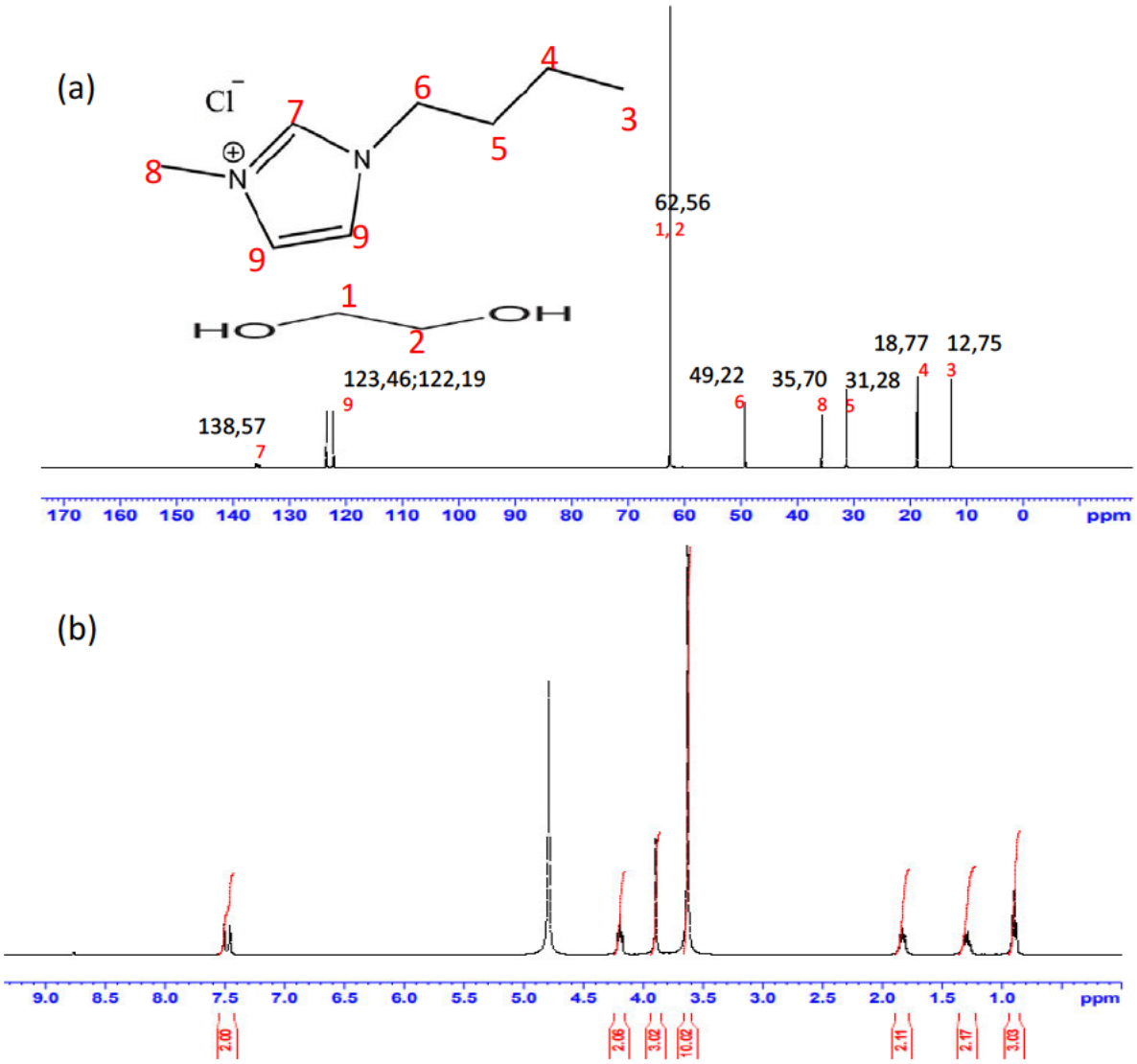

Figure 5.7. 2: (a) ^{13}C-NMR spectra, (b) ^{1}H-NMR spectra of DES (BMIMCl + EG).

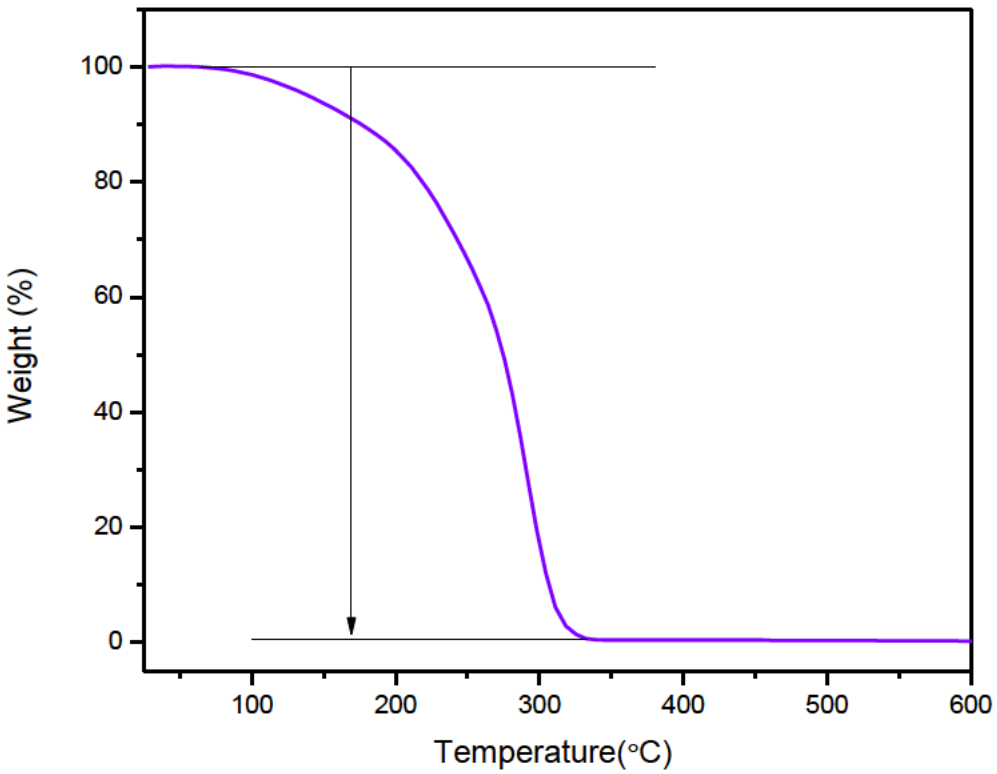

Figure 5.7. 3: Thermogravimetric analysis (TGA) curves of DES (BMPyBr + EG).

Table 5.7. 1: Densities (ρ), speed of sound (u), and refractive indices (nD) of DES (BMIMCl + EG) + acetic acid binary mixture at *T*= 293.15K -313.15K and *p* = 0.1 MPa.

x1	ρ (g/cm^3)	u (m/s)	nD
293.15 K			
0	1.0512	1164.62	1.3704
0.0878	1.0782	1401.66	1.4115
0.0995	1.0805	1460.85	1.4254
0.2011	1.0829	1521.36	1.4379
0.2999	1.0843	1570.84	1.4496
0.3977	1.0852	1620.32	1.4538
0.4913	1.0857	1647.92	1.4566
0.5975	1.0862	1675.52	1.4633
0.6980	1.0865	1691.76	1.4654
0.7985	1.0870	1708	1.4675
0.8905	1.0879	1718.74	1.4681
1	1.0895	1729.48	1.4697
298.15 K			
0	1.0456	1147.42	1.3731
0.0878	1.0738	1387.28	1.4166
0.0995	1.0754	1446.35	1.4244
0.2011	1.0788	1507.99	1.4369
0.2999	1.0803	1557.35	1.4486
0.3977	1.0817	1608.08	1.4528
0.4913	1.0826	1634.62	1.4556
0.5975	1.0832	1663.71	1.4624
0.6980	1.0832	1678.42	1.4644
0.7985	1.0837	1696.38	1.4667
0.8905	1.0850	1705.32	1.4676
1	1.0863	1718.04	1.4684
303.15 K			
0	1.0400	1130.23	1.3717
0.0878	1.0682	1372.9	1.4154
0.0995	1.0702	1431.25	1.4233
0.2011	1.0741	1495.04	1.4359
0.2999	1.0762	1543.63	1.4475
0.3977	1.0782	1595.44	1.452
0.4913	1.0794	1621.24	1.4546
0.5975	1.0799	1651.56	1.4616
0.6980	1.0796	1665.32	1.4634
0.7985	1.0805	1684.48	1.4658
0.8905	1.0820	1691.25	1.4665
1	1.0831	1706.33	1.4678
308.15 K			
0	1.0343	1113.12	1.3704
0.0878	1.0637	1358.57	1.4144
0.0995	1.0655	1412.38	1.4224
0.2011	1.0693	1481.82	1.435
0.2999	1.0717	1530.32	1.4466

0.3977	1.0746	1582.91	1.4512
0.4913	1.0756	1608.51	1.4537
0.5975	1.0762	1639.4	1.4608
0.6980	1.0760	1651.47	1.4624
0.7985	1.0772	1672.57	1.4651
0.8905	1.0784	1678.67	1.4656
1	1.0799	1694.24	1.4667
	313.15 K		
0	1.0287	1096.06	1.3690
0.0878	1.0592	1344.35	1.4135
0.0995	1.0614	1399.65	1.4215
0.2011	1.0644	1468.63	1.4340
0.2999	1.0677	1517.25	1.4455
0.3977	1.0710	1570.47	1.4504
0.4913	1.0724	1585.35	1.4527
0.5975	1.0740	1627.27	1.4600
0.6980	1.0728	1642.35	1.4615
0.7985	1.0740	1660.64	1.4644
0.8905	1.0753	1668.34	1.4640
1	1.0767	1682.44	1.4656

Table 5.7. 2: Change in refractive index, Δn, excess molar volume, V_m^E, isentropic compressibility, k_s, deviation in isentropic compressibility, Δk_s, and intermolecular free length, L_f , of DES(BMIMCl + EG) + ethanol binary mixture at *T*= 293.15K - 313.15Kb and *p* = 0.1 MPa.

x_1	Δn	V_m^E($cm^{-3}.mol^{-1}$)	ks ($Kg^{-1}.m.s^2.Pa^{-1}$)	ΔKs ($m^3.mol^{-1}.Pa^{-1}$)	L_f (10^{-7} m)
			293.15 K		
0	0	0	70.13	0	1.7067
0.0878	0.0323	-0.9956	47.20	-19.45	1.4003
0.0995	0.0451	-1.1189	43.36	-22.83	1.3421
0.2011	0.0475	-0.9320	39.89	-22.30	1.2872
0.2999	0.0494	-0.7471	37.37	-20.92	1.2459
0.3977	0.0439	-0.5631	35.09	-19.34	1.2073
0.4913	0.0374	-0.3628	33.91	-16.83	1.1868
0.5975	0.0335	-0.1441	32.79	-13.76	1.1670
0.6980	0.0256	0.0856	32.15	-10.43	1.1557
0.7985	0.0178	0.2328	31.53	-7.09	1.1444
0.8905	0.0092	0.2289	31.11	-3.88	1.1368
1	0	0	30.68	0	1.1289
			298.15 K		
0	0	0	72.63	0	1.7529
0.0878	0.0351	-1.0334	48.38	-20.60	1.4307
0.0995	0.0418	-1.0982	44.44	-24.06	1.3712
0.2011	0.0446	-0.9428	40.76	-23.53	1.3131
0.2999	0.0469	-0.7297	38.16	-22.03	1.2706
0.3977	0.0417	-0.5925	35.74	-20.40	1.2297
0.4913	0.0356	-0.4430	34.56	-17.70	1.2092
0.5975	0.0323	-0.2253	33.35	-14.51	1.1878

0.6980	0.0247	0.0574	32.76	-10.93	1.1773
0.7985	0.0175	0.2221	32.06	-7.47	1.1646
0.8905	0.0096	0.1288	31.69	-4.03	1.1578
1	0	0	31.18	0	1.1486
			303.15 K		
0	0	0	75.26	0	1.8007
0.0878	0.0352	-0.9830	49.66	-21.77	1.4627
0.0995	0.0420	-1.0668	45.61	-25.32	1.4017
0.2011	0.0448	-0.9059	41.64	-24.85	1.3394
0.2999	0.0469	-0.7185	38.99	-23.20	1.2960
0.3977	0.0420	-0.6202	36.43	-21.50	1.2528
0.4913	0.0356	-0.5105	35.24	-18.62	1.2322
0.5975	0.0324	-0.2557	33.94	-15.28	1.2093
0.6980	0.0246	0.1268	33.39	-11.46	1.1995
0.7985	0.0173	0.2119	32.61	-7.87	1.1853
0.8905	0.0092	0.0596	32.30	-4.16	1.1797
1	0	0	31.70	0	1.1687
			308.15 K		
0	0	0	78.02	0	1.8499
0.0878	0.0355	-1.0126	50.93	-23.07	1.4946
0.0995	0.0424	-1.0748	47.04	-26.42	1.4365
0.2011	0.0452	-0.8436	42.58	-26.22	1.3667
0.2999	0.0473	-0.6425	39.84	-24.45	1.3219
0.3977	0.0425	-0.6495	37.13	-22.68	1.2762
0.4913	0.0359	-0.4617	35.93	-19.60	1.2554
0.5975	0.0328	-0.2101	34.57	-16.10	1.2314
0.6980	0.0247	0.1682	34.07	-12.00	1.2224

0.7985	0.0178	0.2021	33.18	-8.29	1.2063
0.8905	0.0094	0.1749	32.90	-4.35	1.2013
1	0	0	32.25	0	1.1894
			313.15 K		
0	0	0	80.91	0	1.9007
0.0878	0.0360	-1.0458	52.23	-24.45	1.5272
0.0995	0.0428	-1.1347	48.09	-28.03	1.4653
0.2011	0.0455	-0.7867	43.55	-27.68	1.3945
0.2999	0.0475	-0.6432	40.68	-25.79	1.3477
0.3977	0.0429	-0.6767	37.85	-23.92	1.3000
0.4913	0.0362	-0.5517	37.09	-20.17	1.2870
0.5975	0.0332	-0.4831	35.16	-17.00	1.2529
0.6980	0.0250	0.1280	34.55	-12.77	1.2421
0.7985	0.0182	0.1916	33.76	-8.73	1.2278
0.8905	0.0089	0.1136	33.40	-4.66	1.2213
1	0	0	32.80	0	1.2103

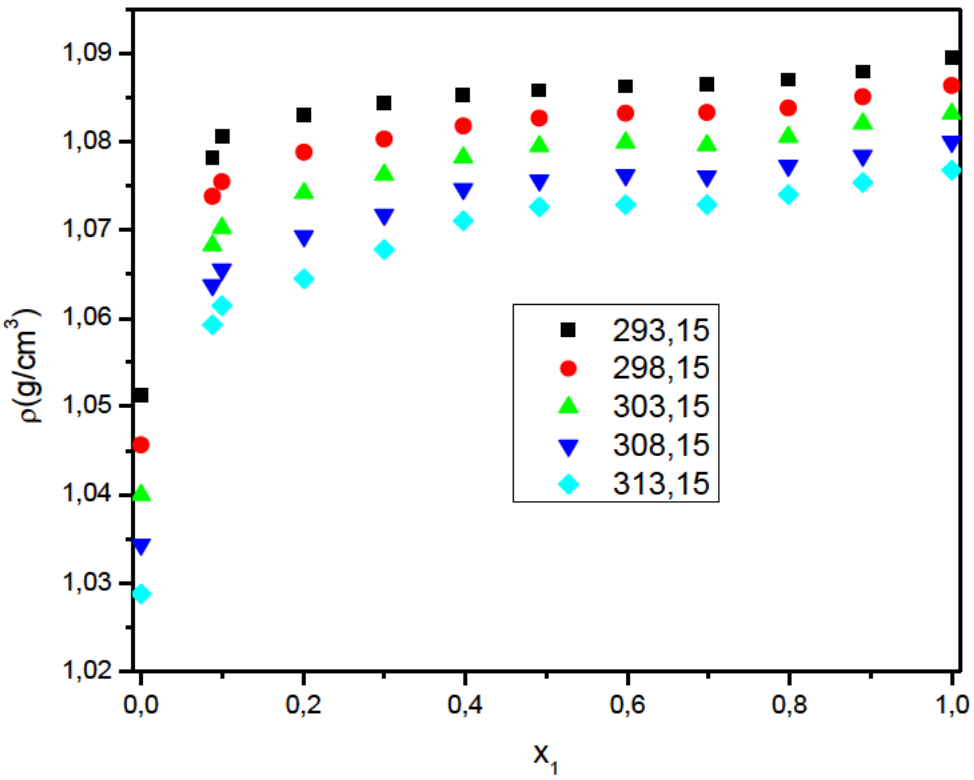

Figure 5.7. 4: Densities of the binary mixtures of {DES (BMIMCl + EG) + acetic acid} at *T* = 293.15 K - 313.15 K.

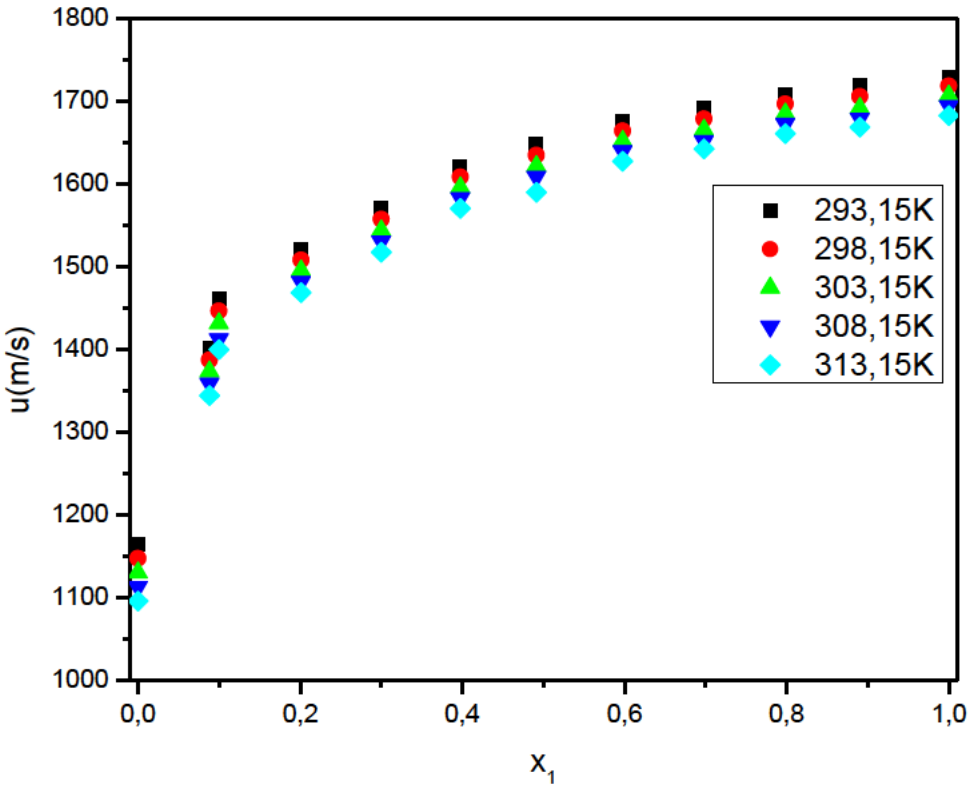

Figure 5.7. 5: Speed of sound of the binary mixtures of {DES (BMIMCl + EG) + acetic acid} at *T* = 293.15 K - 313.15 K.

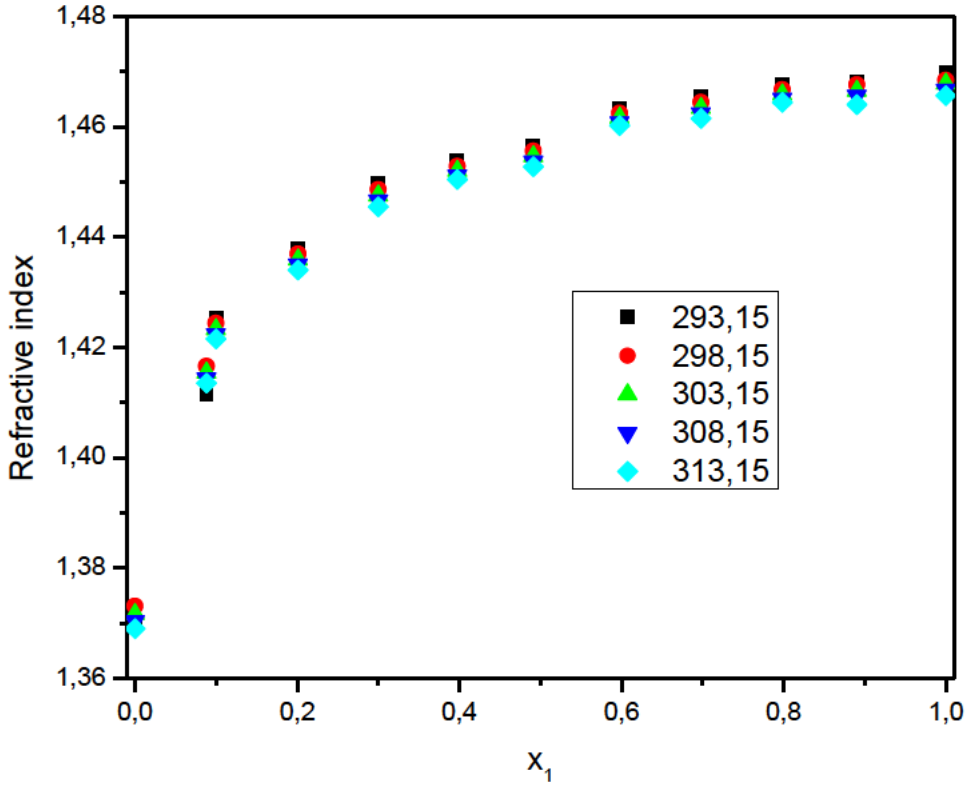

Figure 5.7. 6: Refractive indices of the binary mixtures of {DES (BMIMCl + EG) + acetic acid} at *T* = 293.15 K - 313.15 K.

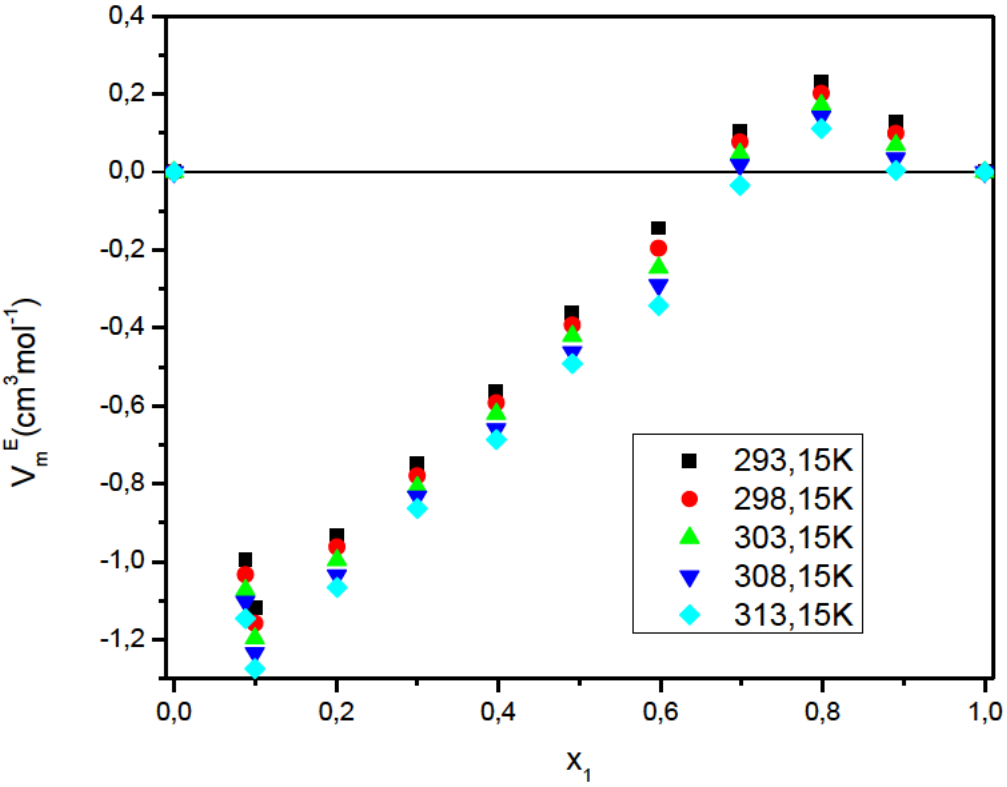

Figure 5.7. 7: Excess molar volumes (V_m^E) of the prepared mixtures for {DES (BMIMCl + EG) + acetic acid} at T = (293.15 - 313.15) K.

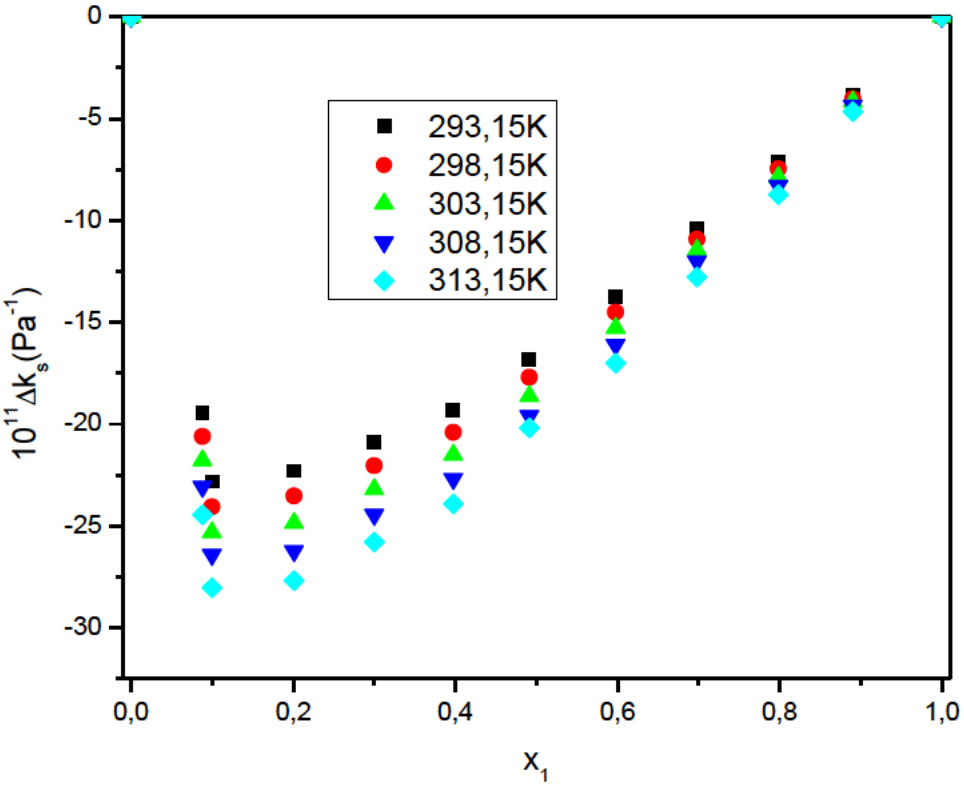

Figure 5.7. 8: Deviation in isentropic compressibility of the prepared mixtures for {DES (BMIMCl + EG) + acetic acid} at *T* = (293.15 - 313.15) K.

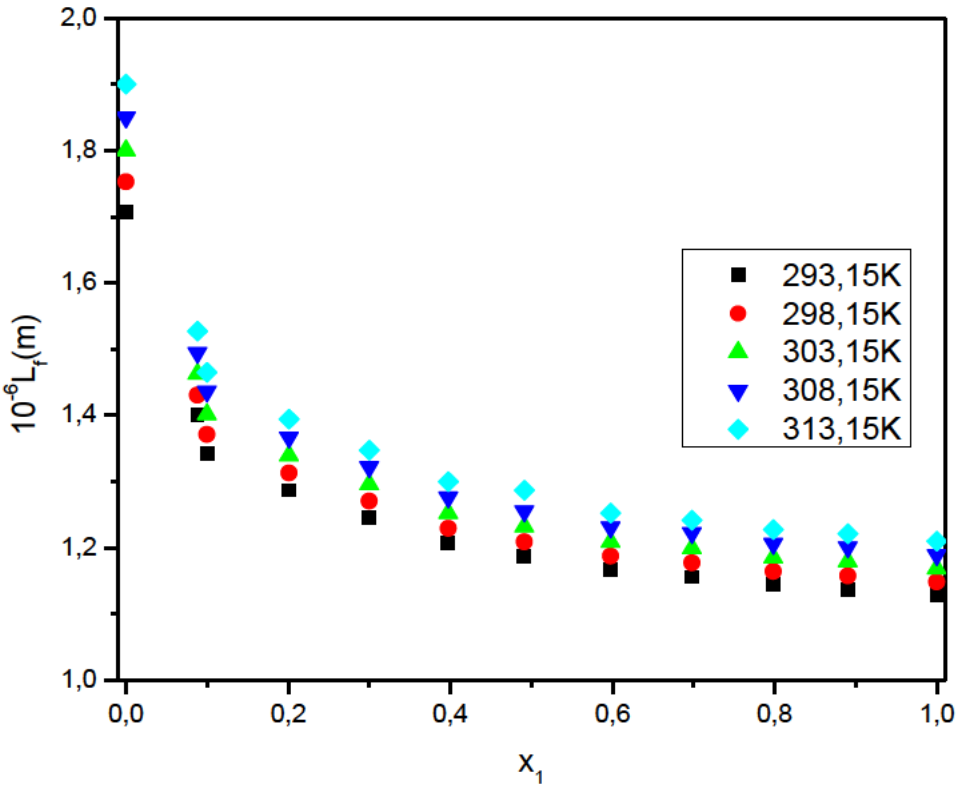

Figure 5.7. 9: Intermolecular free length (L_f), of the binary mixtures of {DES (BMIMCl + EG) + ethanol} given as a function of mole fraction of DES at T = (293.15, 298.15, 303.15, 308.15 and 313.15) K.

5.8 DES6 (1butyl-3-methylimidazolium chloride + ethylene glycol) + ethanol

Table 5.8. 1: Densities (ρ), speed of sound (u), and refractive indices (nD) of DES(BMIMCl + EG) + ethanol binary mixture at T = 293.15K -313.15K and p = 0.1 MPa.

x1	ρ (g/cm^3)	u (m/s)	nD
	293.15 K		
0	0.8049	1169.31	1.3634
0.0900	0.9150	1347.42	1.4102
0.1000	0.9319	1411.09	1.4225

0.2000	0.9786	1474.75	1.4347
0.3000	1.0032	1538.02	1.4447
0.4000	1.0368	1601.29	1.4546
0.5000	1.0502	1634.53	1.4588
0.6001	1.0640	1666.41	1.4630
0.7000	1.0763	1685.13	1.4654
0.8000	1.0857	1703.85	1.4678
0.9006	1.0875	1716.67	1.4688
1	1.0895	1729.48	1.4697
		298.15 K	
0	0.8004	1152.78	1.3619
0.0900	0.9099	1332.94	1.4097
0.1000	0.9280	1396.32	1.4182
0.2000	0.9720	1461.42	1.4343
0.3000	0.9987	1523.24	1.4432
0.4000	1.0330	1589.09	1.4537
0.5000	1.0453	1621.35	1.4573
0.6001	1.0607	1654.34	1.4622
0.7000	1.0737	1673.24	1.4639
0.8000	1.0826	1692.29	1.4670
0.9006	1.0840	1702.36	1.4673
1	1.0863	1718.04	1.4686
		303.15 K	
0	0.7959	1135.60	1.3602
0.0900	0.9050	1318.42	1.4082
0.1000	0.9257	1381.52	1.4167
0.2000	0.9656	1447.99	1.4327
0.3000	0.9960	1508.37	1.4417
0.4000	1.0291	1576.15	1.4526
0.5000	1.0417	1608.41	1.4558

0.6001	1.0574	1642.16	1.4612
0.7000	1.0673	1660.51	1.4624
0.8000	1.0793	1680.47	1.4661
0.9006	1.0799	1690.25	1.4690
1	1.0831	1706.33	1.4678
		308.15 K	
0	0.7914	1118.72	1.3589
0.0900	0.9003	1303.90	1.4074
0.1000	0.9201	1366.34	1.4154
0.2000	0.9600	1434.55	1.4318
0.3000	0.9872	1493.51	1.4402
0.4000	1.0238	1563.64	1.4519
0.5000	1.0329	1594.97	1.4543
0.6001	1.0541	1629.98	1.4604
0.7000	1.0590	1647.32	1.4615
0.8000	1.0761	1668.58	1.4654
0.9006	1.0716	1676.25	1.4658
1	1.0799	1694.24	1.4667
		313.15 K	
0	0.7868	1101.94	1.3576
0.0900	0.8958	1289.44	1.4070
0.1000	0.9131	1351.42	1.4139
0.2000	0.9536	1421.07	1.4310
0.3000	0.9851	1478.24	1.4387
0.4000	1.0185	1551.07	1.4511
0.5000	1.0317	1581.36	1.4528
0.6001	1.0508	1617.79	1.4598
0.7000	1.0578	1633.27	1.4600
0.8000	1.0729	1665.38	1.4647
0.9006	1.0707	1664.32	1.4650

1	1.0767	1682.44	1.4656

Table 5.8. 2: Change in refractive indices, Δn, excess molar volume, VmE, isentropic compressibilities, k_s, deviation in isentropic compressibilities, Δk_s, and intermolecular free length, L_f of DES(BMIMCl + EG) + ethanol binary mixture at T= 293.15 K - 313.15 K and p = 0.1 MPa.

x_1	Δn	V_m^E ($cm^{-3}.mol^{-1}$)	ks ($Kg^{-1}.m.s^2.Pa^{-1}$)	ΔKs ($m^3.mol^{-1}.Pa^{-1}$)	Lf (10^{-7} m)
			293.15K		
0	0	0	90.85	0	1.9468
0.0900	0.0372	3.7836	60.19	-25.24	1.5846
0.1000	0.0484	4.0058	53.88	-30.95	1.4993
0.2000	0.0500	5.5126	46.98	-31.83	1.4000
0.3000	0.0494	5.8226	42.13	-30.66	1.3258
0.4000	0.0486	4.1318	37.61	-29.16	1.2526
0.5000	0.0422	3.2883	35.63	-25.12	1.2193
0.6001	0.0358	1.4074	33.84	-20.90	1.1882
0.7000	0.0275	-0.3537	32.71	-16.01	1.1682
0.8000	0.0193	-3.3040	31.72	-10.99	1.1504
0.9006	0.0096	-1.0409	31.20	-5.46	1.1408
1	0	0	30.68	0	1.1314
			298.15K		
0	0	0	94.00	0	1.9985
0.0900	0.0381	4.0514	61.85	-26.49	1.6211
0.1000	0.0456	4.3131	55.26	-32.45	1.5323
0.2000	0.0510	5.8258	48.16	-33.27	1.4305
0.3000	0.0492	6.1254	43.15	-32.00	1.3540
0.4000	0.0491	4.4211	38.33	-30.53	1.2762
0.5000	0.0420	3.5214	36.39	-26.20	1.2434
0.6001	0.0362	1.7520	34.44	-21.85	1.2097
0.7000	0.0273	0.0065	33.26	-16.76	1.1888
0.8000	0.0197	-3.0075	32.25	-11.49	1.1706
0.9006	0.0093	-0.7492	31.83	-5.59	1.1629
1	0	0	31.18	0	1.1511
			303.15K		

0	0	0	97.42	0	2.0531
0.0900	0.0383	4.3245	63.56	-27.93	1.6584
0.1000	0.0457	4.6304	56.59	-34.24	1.5649
0.2000	0.0509	6.1233	49.39	-34.88	1.4618
0.3000	0.0492	6.4770	44.12	-33.57	1.3817
0.4000	0.0493	4.7251	39.11	-32.01	1.3009
0.5000	0.0417	3.8002	37.10	-27.45	1.2670
0.6001	0.0364	2.0050	35.06	-22.91	1.2317
0.7000	0.0268	0.3449	33.98	-17.44	1.2125
0.8000	0.0198	-2.7981	32.80	-12.04	1.1914
0.9006	0.011892	-0.4476	32.41	-5.82	1.1842
1	0	0	31.70	0	1.1713
			308.15K		
0	0	0	100.96	0	2.1090
0.0900	0.0387	4.6003	65.32	-29.44	1.6964
0.1000	0.0457	4.9399	58.21	-35.87	1.6014
0.2000	0.0513	6.4210	50.61	-36.60	1.4932
0.3000	0.0489	6.7288	45.41	-34.93	1.4144
0.4000	0.0498	5.0950	39.94	-33.52	1.3266
0.5000	0.0414	4.1255	38.05	-28.54	1.2948
0.6001	0.0368	2.2948	35.70	-24.02	1.25415
0.7000	0.0271	0.6559	34.79	-18.07	1.2381
0.8000	0.0202	-2.4508	33.37	-12.62	1.2125
0.9006	0.0098	-0.1487	33.20	-5.87	1.2095
1	0	0	32.25	0	1.1921
			313.15K		
0	0	0	104.66	0	2.1666
0.0900	0.0396	4.9359	67.13	-31.06	1.7352
0.1000	0.0454	5.2032	59.96	-37.51	1.6399
0.2000	0.0517	6.7134	51.92	-38.36	1.5260
0.3000	0.0486	7.0226	46.45	-36.65	1.4433
0.4000	0.0502	5.3263	40.80	-35.11	1.3528
0.5000	0.0411	4.4051	38.75	-29.97	1.3184
0.6001	0.0373	2.5470	36.35	-25.18	1.2769

0.7000	0.0267	0.9498	35.43	-18.92	1.2607
0.8000	0.0206	-2.1620	33.60	-13.57	1.2276
0.9006	0.0101	0.1645	33.71	-6.23	1.2297
1	0	0	32.80	0	1.2130

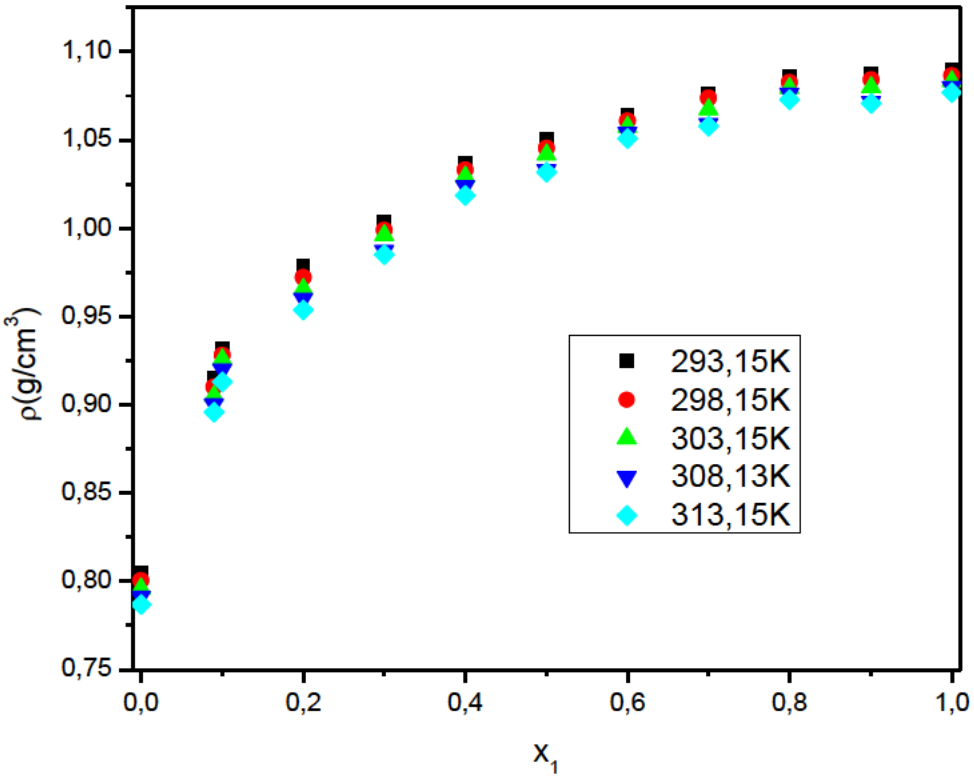

Figure 5.8. 1: Densities of the binary mixtures of {DES (BMIMCl + EG) + ethanol} at *T* = 293.15 K - 313.15 K.

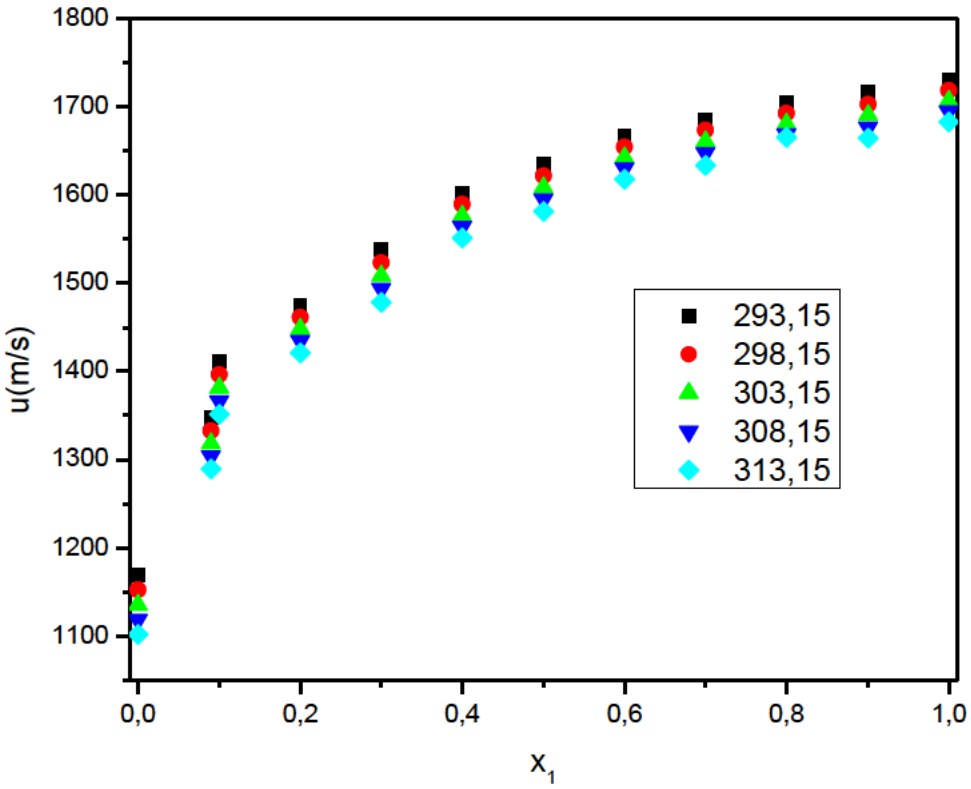

Figure 5.8. 2: Speed of sound of the binary mixtures of {DES (BMIMCl + EG) + ethanol} at *T* = 293.15 K - 313.15 K.

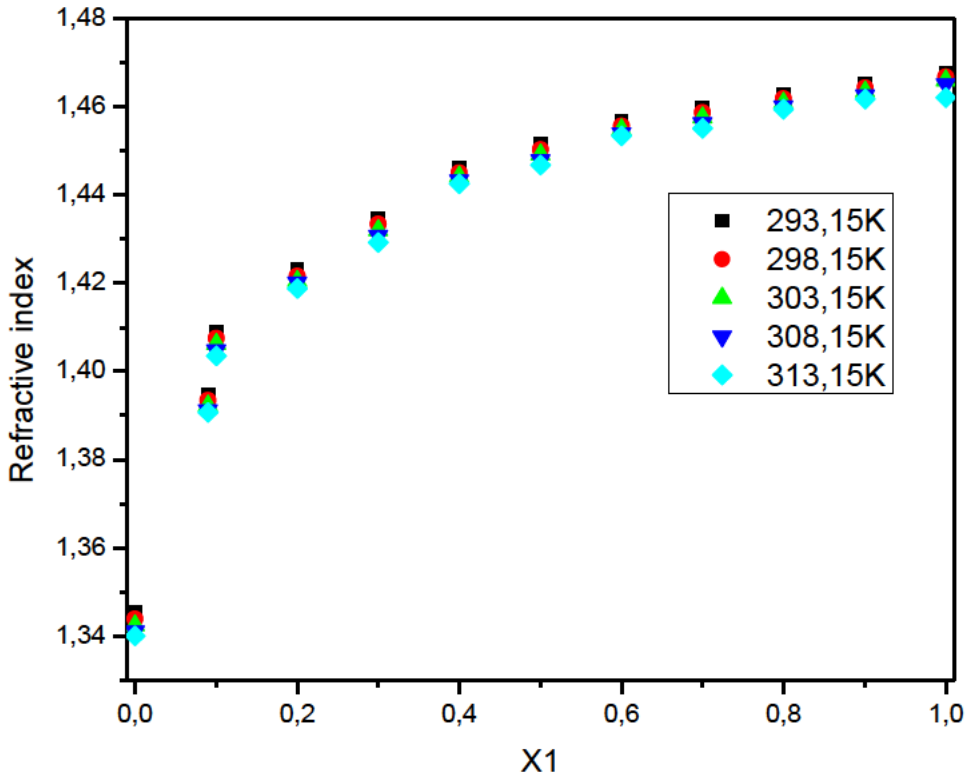

Figure 5.8. 3: Refractive indices of the binary mixtures of {DES (BMIMCl + EG) + ethanol} at *T* = 293.15 K - 313.15 K.

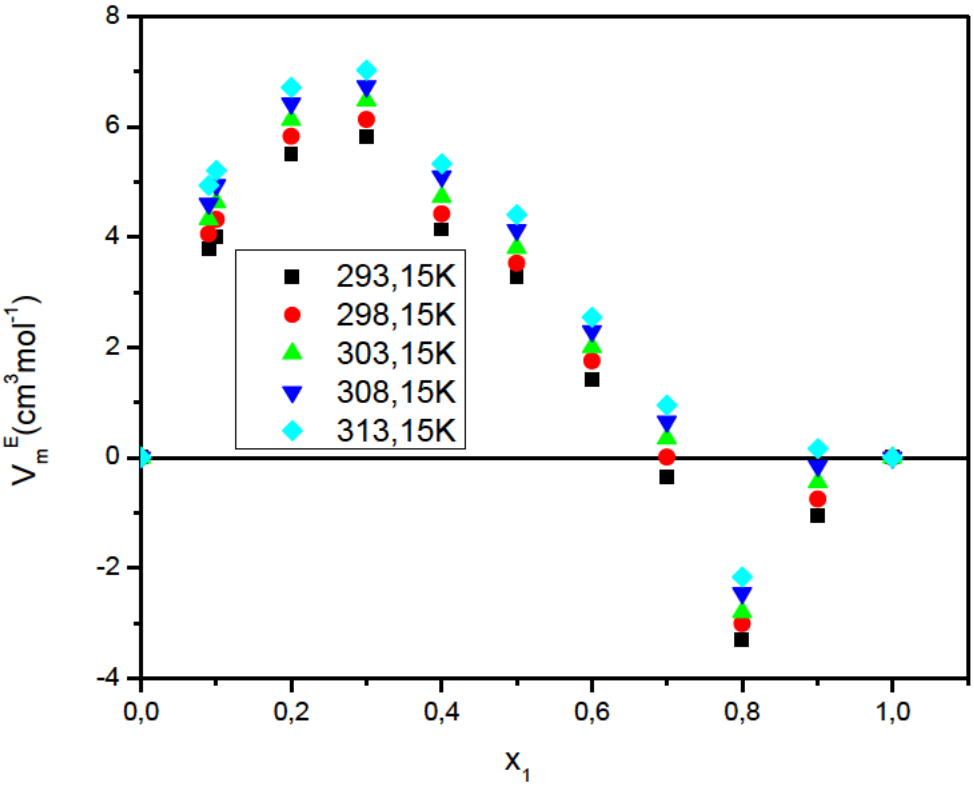

Figure 5.8. 4: Excess molar volume (V_m^E) of the prepared mixtures for {DES (BMIMCl + EG) + ethanol} at T = (293.15 - 313.15) K.

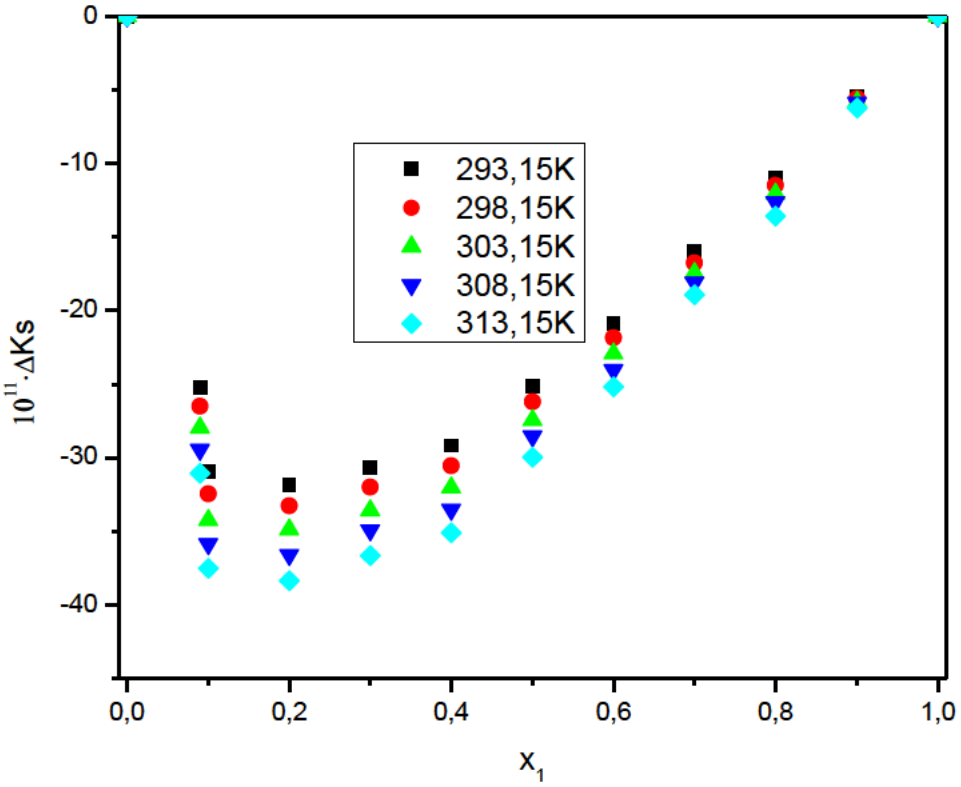

Figure 5.8. 5: Deviation in isentropic compressibilities of the prepared mixtures for {DES (BMIMCl + EG) + ethanol} at *T* = (293.15 - 313.15) K.

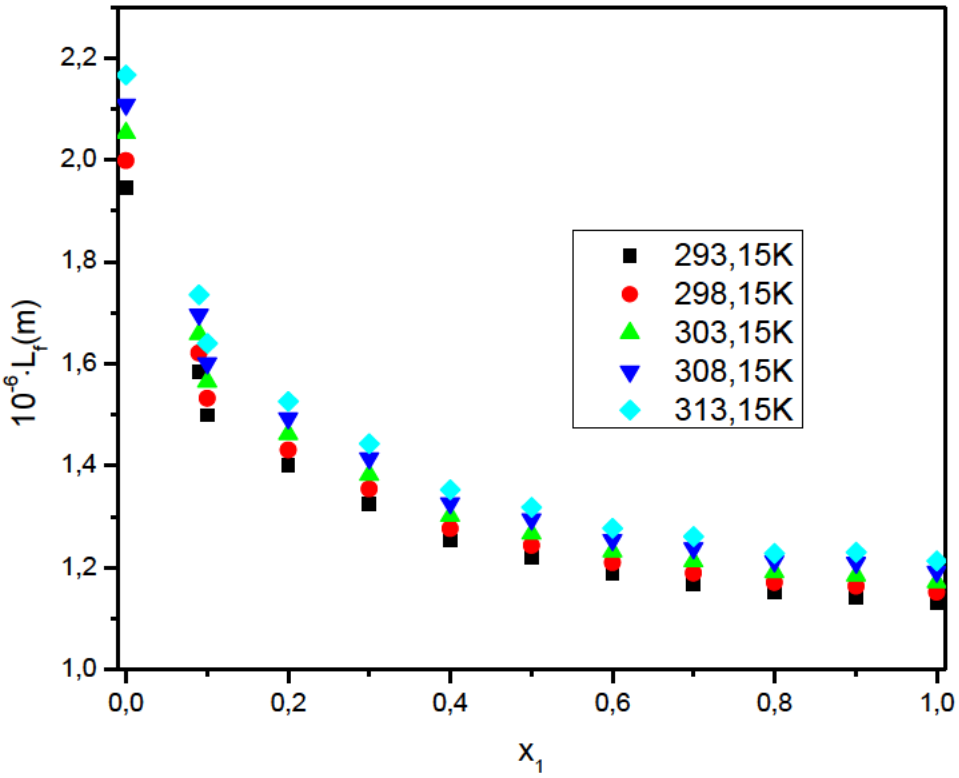

Figure 5.8. 6: Intermolecular free length (L_f), of the binary mixtures of {DES (BMIMCl + EG) + ethanol} given as a function of mole fraction of DES at T = (293.15, 298.15, 303.15, 308.15 and 313.15) K.

5.9 Correlations

Table 5.9 1: Root mean square deviation, σ, obtained from the Lorentz-Lorenz expression, for ρ and n for the binary mixtures at T = (298.15, 303.15, 308.15, 313.15 and 318.15) K.

	293.15 K	298.15 K	303.15 K	308.15 K	313.15 K
DES (BMPRLBr + EG) + acetic acid					
ρ/(g·cm-3)	0.0046	0.0055	0.0059	0.0041	0.0044
n	0.0759	0.0755	0.0750	0.0739	0.0733
DES (BMPRLBr + EG) + ethanol.					
ρ/(g·cm-3)	0.5613	0.5560	0.4771	0.5648	0.5476
n	0.3471	0.3478	0.3472	0.3461	0.3465
DES (BMIMCl + EG) + acetic acid					
ρ/(g·cm-3)	0.0096	0.0085	0.0085	0.0092	0.0095
n	0.1380	0.1390	0.1385	0.1383	0.1380
DES (BMIMCl + EG) + ethanol					
ρ/(g·cm-3)	0.0101	0.3383	0.0102	0.0122	0.0128
n	0.1348	0.3868	0.1329	0.1325	0.1323

CHAPTER 6: DISCUSSIONS

6.1 Characterization of deep eutectic solvents.

6.1.1 Fourier Transform Infrared (FTIR)Spectroscopy analysis.

To confirm the formation of deep eutectic solvents. ATR-FTIR analysis was conducted as the combination mechanism as the structure of the prepared deep eutectic solvents is unknown, hence FTIR was used for characterization. The FTIR spectra of ethylene glycol, BDMIMCl, and prepared DES is presented in Figure 5.1.1. The IR spectra of the prepared DES and its constituents are analysed to confirm the presence and the identify functional groups in constituents and DES prepared. Figure 5.1.1 shows FTIR spectra of ethylene glycol, 1-butyl-2.3-dimethylimidazolium chloride (BDMIMCl) and DES1. The spectra of ethylene glycol show a peak centred at 3310 cm^{-1} (v-OH), 2944 and 2870 cm^{-1} for (v-CH) stretching, C-O stretch at 1655 cm^{-1}. In the fingerprint region. peak centred at 1083 and 1032 cm^{-1}. The rocking vibration of -CH_2- group at 856 cm^{-1}, The C-C peak at 512 cm^{-1}which signify the aliphatic alcohol. The BDMIMCl shows the following absorption bands FTIR spectra: NH secondary amine stretching at 3395 cm^{-1}, CH aliphatic stretch at (2957, 2935, and 2873) cm^{-1}, C=N and C=C stretch at 1653 cm^{-1}, imidazole ring stretches at 1591 cm^{-1}, and HC-C and HCN at 1251cm^{-1}.

Figure 5.2.1 shows the FTIR spectra of DES2 (1-butyl-2.3-dimethylimidazolium chloride + diethylene glycol). This DES has the same HBA as DES1 which shows the same peaks noted for DES1. The difference is noted for the HBD which in this DES is diethylene glycol. For the diethylene glycol FTIR spectra. the following peaks are noted. for O-H stretching at 3338 cm^{-1}. symmetric and asymmetric stretch of the -CH_2- groups at (2876 and 2932) cm^{-1}. In the fingerprint region, we detected CCC, COC stretch at 1230 cm^{-1}, C-O symmetric and asymmetric stretching vibrations occurring at (1123 and 1054) cm^{-1}, respectively. Additionally, the COH and -OC_2H_4 groups were observed at (923 and 892) cm^{-1}. For the DES2, the FTIR spectra shows that there is a mixture of shifts to longer and shorter wavelength. The shifts of the fingerprint region C-O symmetric and asymmetric stretching at (1123 and 1054) cm^{-1} to (1078 and 1031) cm^{-1}, and COH and -OC_2H_4 groups observed at (923 and 892) cm^{-1} shifted to (882 and 861) cm^{-1}. This shows that there is a change in bond strength that leads to reduced molecular vibrations.

Figure 5.3.1 shows the FTIR spectra of the DES3 prepared from (1-butyl-2,3-dimethylimisazolium tetrafluoroborate + ethylene glycol). The spectra show the individual constituents and the prepared DES3. The ethylene spectra are same as the one used in DES1 (Figure 5.1.1). The FTIR spectra of 1-butyl-2,3-dimethylImisazolium tetrafluoroborate shows peaks centred at 3152 cm^{-1} for N-H on the imidazolium ring, CH at 2957 cm^{-1} of the butyl chain, CN at 1035 cm^{-1} (sharp peak). and the BF_4 stretch at 522 cm^{-1}. This is in agreement with the previously reported work (Sharma. Bhagour and Sharma 2012; Kumar and Katal 2018). The DES3 spectra shows that there has been a shift on peak centred at 3294 cm^{-1} on ethylene to 3367 cm^{-1} on the DES spectra, 3152 cm^{-1} on the BDMIMTFB to 3159 cm^{-1} on DES, which correspond to the OH stretch on and NH stretch on BDMIM BF_4, respectively. The shifts are associated with increased bond strength or a change in the molecular environment that leads to enhanced molecular vibrations. This shows that there has been formation of the strong hydrogen bond between the two constituents of the DES.

Figure 5.4.1 shows the FTIR spectra of the prepared DES4 (1-butyl-2,3-dimethylimidazolium tetrafluoroborate + diethylene glycol), the pure salt of 1-butyl-2.3-dimethylimidazolium tetrafluoroborate as HBA, and pure diethylene glycol as HBD. The spectrum of pure salt is discussed in detail in the DES3 (Figure 5.3.1) which is the same as in this DES4 as well as the HBD (diethylene glycol) on DES2 (Figure 5.2.1). The DES prepared results show the shift of the OH stretch of diethylene glycol from 3340 cm^{-1} to 3330 cm^{-1} and shift of the NH stretch of the BDMIMTFB from (3152 to 3156) cm^{-1}. There is a noticeable shift of the BF_4 stretch of the BDMIMTFB from (522 to 515) cm^{-1}, which signify decrease in bond strength of the BF_4 bond. This could be attributed to the hydrogen bond forming between the hydrogen atom of the DEG and the nitrogen atom of the $BDMIM^+$.

6.1.2 Nuclear Magnetic Resonance Spectrometer (NMR)

Figure 5.1.2 shows the ^{13}C-NMR and the ^{1}H-NMR for the prepared DES (1-butyl-2,3-dimethylimidazolium chloride + ethylene glycol). The ^{13}C-NMR signal shows the C atoms, the H_3C- (9) of the butyl chain at 8.85 ppm, the three -CH_2- (8.7. and 6) at (18.89. 31.01. and 47.90) ppm, respectively. The -CH_3 (10) bonded to the imidazolium ring at 12.82 ppm. -CH_3 (11) bonded to the N of the imidazolium ring at 34.54ppm and

the two -CH_2- of the ethylene glycol at 62.53 ppm, the two -CH-(4.5) in the imidazolium ring at (122.03 and 120.63) ppm, and the -C- (2) in the imidazolium ring at 144.02 ppm. This shows that the hydrogen bond between the H atom of ethylene glycol occur at the N (1) sandwiched between the -CH-(5) and -CH2-(6). The corresponding ^{1}H-NMR is also analysed which confirms the structure of DES1.

The prepared DES was characterised by ^{13}C-NMR and ^{1}H-NMR spectra (Figure 5.2.2). The 13C- NMR shows the C atoms assigned to correct position on the spectrum, -CH_3 (11) at 5.59 ppm, -CH_3 (7) attached to the imidazolium ring through the C- atom at 12.85ppm, the three -CH_2- (10. 9 and 8) at (18.95. 31.10. and 47.68) ppm, respectively. The -CH_3 (6) bonded to the N atom if the imidazolium ring at 34.45 ppm, the two -CH- (4.5) at (122.12 and 120.70) ppm. The -C- (2) in the imidazolium ring at 144.20 ppm. The two -CH_2- on the diethylene glycol at 62.68 ppm. The proton NMR spectra showed signal of the (-CH_3) methyl in butyl at 0.84 ppm (H4'), the three -CH_2- at 1.341 ppm (H3'), 1.780 ppm (H2'), and 4.103 ppm (H1'). The -CH- is observed for the imidazole ring at 7.362 ppm (H5) and 7.405 ppm (H4). The proton pf the methyl group associated with N and C of the imidazole ring at 3.693 ppm (H1") and 3.715 ppm (H1"'), respectively. These signals correspond with the BDMIMCl. The other signals which correspond to the DEG are visible for the two -CH_2- protons at 3.710 ppm (Hb), 3.693 ppm (Hc), proton on OH- at 4.121 ppm (Ha). It can be established that the obtained product was deep eutectic solvent composed from DEG and BDMIMCl.

Figure 5.3.2 shows the NMR spectras of the prepared DES (1-butyl-2,3-dimethylimidazolium tetrafluoroborate + ethylene glycol), the ^{13}C-NMR spectrum corresponds to the C atoms, -CH_3 (9) of the butyl chain at 8.58 ppm, -CH_3 (10) attached to the C atom on the imidazolium ring, the three -CH_2- (8.7. and 6) at (18.88. 31.01. and 60.49) ppm, respectively. The following was also observed on the NMR, -CH_3 (11) attached to the N in the imidazolium ring at 47.84 ppm, the two -CH- (4 and 5) in the imidazolium chloride at (122.07 and 120.65) ppm, respectively. The -C- (2) in the imidazolium ring at 144.10 ppm, and the two -CH_2- (1'. 2') of the ethylene glycol at 62.58 ppm, [There are two peaks unaccounted for which are at 71.63 and 60.49 ppm]. The peak at 60.49 ppm can be attributed to carbonyl atom (C=O) and the peak at 71.63 ppm could be from the alkyl carbon. The spectra correspond with the ^{1}H NMR

which shows that there is a hydrogen bonding between the N1 and hydrogen of the ethylene glycol.

Figure 5.4.2 shows the NMR spectra of the prepared DES (1-butyl-2,3-dimethylimidazolium tetrafluoroborate + ethylene glycol). The ^{13}C NMR shows the spectra of $-CH_3$ (11) of the alkyl chain at 8.82 ppm, three $-CH_2$ (10. 9. and 8) of the alkyl chain at (18.88. 31.01. and 47.89) ppm, respectively. The two $-CH_3$ (6 and 7) at (12.81 and 34.52) ppm, where (60 is bonded to the -C- in the imidazolium ring while (7) is bonded to N in the imidazolium ring. The -CH- (4 and 5) in the imidazolium ring at (122.02 and 120.67) ppm. and the two $-CH_2$- (1') of the diethylene glycol at 60.44ppm and the two $-CH_2$-O- (2') of the diethylene glycol at 71.61 ppm. The ^1H NMR also confirms the structure of the prepared DES with interactions due to hydrogen bonding.

6.1.3 Thermogravimetric analysis

Thermogravimetric analysis (TGA) is a thermal analysis technique used to study the changes in mass of a sample as a function of temperature. The analysis monitors the change of a sample as the temperature increases in a controlled environment. The mass changes occurring are due to processes such as decomposition. oxidation or desorption. The TGA is important in this work to determine the thermal stability of the prepared DESs.

The thermogravimetric analysis of DES1 (1-butyl-2,3-dimethylimidazolium chloride + ethylene glycol) has shown that upon applying heat from 28°C to 600°C. The onset temperature which is the temperature value where a measurable weight loss is observed (noted by a horizontal line at the top on Figure 5.1.3). We noted a predominant mass loss of approximately 100% at temperatures exceeding 90°C, and an undetermined residue of 0.32% is detected at 316°C. The TGA curve shows a one-step decomposition with the most decomposition occurring at 300°C (evident by the steep curve). The curve shows that the DES decomposes at relatively high temperature which suggest thermal stability of the DES, as most of the DES decomposes at a temperature above 300°C. When compared to the constituents (BDMIMCl), the curve shows an onset temperature of 260°C and end at 360°C (Fox *et al.* 2005; Muhammad 2016), which shows higher thermal stability. The ethylene

glycol TGA curve shows first weight loss at 65°C up to 170°C (Pantoja-Espinoza *et al.* 2021), which could have had a much influence on the TGA curve of the DES1.

Figure 5.2.3 shows the TGA curve of the prepared DES (1-butyl-2,3-dimethylimidazolium chloride + diethylene glycol). The TGA curve shows a two-step decomposition. The first step onset temperature of DES shows a measurable decomposition at 140°C to 247°C and correspond to 44% weight loss. The second step of degradation start at 400°C to 503°C with 45% weight loss. The two step decomposition was influenced by diethylene glycol as reported on literature (Lecomte and Liggat 2006). Figure 5.3.3 shows the DES (1-butyl-2,3-dimethylimidazolium tetrafluoroborate + ethylene glycol). The curve shows one step decomposition starting at 99°C to 332°C with weight loss of 90%. Figure 5.4.3 shows the decomposition of DES (1-butyl-2,3-dimethylimidazolium tetrafluoroborate + diethylene glycol). The curve shows a two-step decomposition starting at 72°C to 250°C with 43% weight loss. The second step start at 339°C to 500°C showing 53% weight loss. The reminder of 1.26% weight remained at the end of the decomposition.

Activity coefficients at infinite dilution

The measure of the non-ideal behaviour of a solute when partitioning in a solvent is referred to as measurement of activity coefficients at infinite dilution. The measurements are done as the concentration of the solute approaches zero which extrapolate the infinite dilution part. The information provided by these measurements evaluate the extent of interactions occurring between molecules of the solute and solvent. The interactions normally determined are either solute-solute or solute-solvent interactions depending on the type of solute and solvent investigated. Gas-liquid chromatography is a commonly used technique to investigate the measurement of activity coefficients at infinite dilution. The experimental measurements give data to understand the solutes' behaviour in the various solvents investigated and used for the pre-screening of the extracting solvents.

6.2 Deep eutectic solvent (BDMIMCl + EG or DEG)

6.2.1 Activity Coefficients at Infinite Dilution

Table 5.1.1 shows the activity coefficients at infinite dilution for the prepared DES (BDMIMCl and EG). The alkanes have the highest γ_{13}^{∞} with the highest being n-decane

437.08 at 313.15 K. The high γ_{13}^{∞} value results from weak solute-solvent interactions occurring between the alkanes and the DES. The aliphatic hydrocarbons γ_{13}^{∞} values follow a pattern alkane > alkenes > alkynes. The γ_{13}^{∞} have shown to be increasing as the alkyl chain length of the compound increases. The cyclic hydrocarbons have shown to have lower γ_{13}^{∞} values when compared to the aliphatic counterparts, this is due to the stronger interactions between the cyclic hydrocarbons and the imidazolium ring (Gutel *et al.* 2009). The alkynes have shown to have the lowest γ_{13}^{∞} values amongst all the hydrocarbons, this is attributed by the presence of the triple bond present between two carbon atoms, where the pi-π-electrons on the alkyne interact with the pi electrons of $BDMIM^{+}$ ion. The aromatic hydrocarbons have shown relatively low γ_{13}^{∞} when compared to alkanes, this is due to the presence of the delocalized pi-electrons on the benzene ring which forms an electron cloud above and below the benzene ring and the addition of methyl group on the benzene ring increases the electron density. The ketones have shown to have the lowest γ_{13}^{∞} values when compared to the other solutes investigated. The γ_{13}^{∞} values for acetonitrile, THF and thiophene were also investigated and proven to be low which a shows strong intermolecular forces between these solute molecules and the solvent. The alcohols show lower γ_{13}^{∞} values and in agreement with the ethylene based DESs (Nkosi, Tumba and Ramsuroop 2018; Manyoni, Kabane and Redhi 2022; Manyoni and Redhi 2022). Figures 5.1.4 – 5.1.10 shows that as the alkyl length of the solute changes, the γ_{13}^{∞} values increases. Alkanes, alkenes, cyclic hydrocarbons, aromatic hydrocarbons showed that as the temperature increase, the γ_{13}^{∞} decreases, this results from a rise in dipole-dipole forces with an increase in the number of carbons, leading to an augmentation in electron presence. For alcohols, THF, acetonitrile, thiophene and ketones, the increase in temperature leads to an increase in the γ_{13}^{∞} values, because of the enhanced intermolecular forces among solute molecules and the solvent.

The deep eutectic solvent prepared from 1-butyl-2,3-dimethylimidazolium chloride as hydrogen bond acceptor (HBA) and diethylene glycol as the hydrogen bond donor (HBD) was evaluated for possible application in separation problems. This preparation was at a molar ratio of 1:2. The average activity coefficients at infinite dilution at infinite dilution (γ_{13}^{∞}) values for the prepared DES are presented in Table 5.2.1. The natural logarithmic of γ_{13}^{∞} are presented in Figure 5.2.4 to 5.2.10 as a function of temperature (1000/T K^{-1}) for all the investigated solutes grouped based on their functional groups.

The Figure 5.2.4 – 5.2.6 represent the natural logarithm of γ_{13}^{∞} for the alkanes, alkenes, alkynes which shows that as the temperature increase the γ_{13}^{∞} values decreases. This is because as temperature increase the solutes start to move faster in the column and hence not interact much with the column's stationary phase. In addition, as the temperature increases, the shape of molecules in the DES changes and the polarity of its bonds, which reveals that at higher temperatures, the prepared DES is becoming less polar at higher temperature and non-polar compounds interact more with the DES. There is also a notable increase in γ_{13}^{∞} values, as the number of carbon atoms increases, there is an increase in the molecule or size, covering more surface which in turn increases the solvation. Among the aliphatic hydrocarbons, the alkynes have shown to have lower γ_{13}^{∞} values which is due to the presence of triple bond between the carbon atoms leading to an increased polarity, making the alkynes more soluble in solvents as compared to the other aliphatic hydrocarbons. For the aromatic hydrocarbons, Figure 5.2.7, which also shows the same pattern regarding the length of the alkyl chain, this impact shows that as the length increase, the γ_{13}^{∞} values increases and the temperature on γ_{13}^{∞} values shows the inverse proportionality. The γ_{13}^{∞} values for the aromatic hydrocarbon have shown to be lower than those of alkanes and alkenes, due to the hydrogen cloud above and below the benzene ring which shows lower binding energies. The ketones shows that the γ_{13}^{∞} values increases as chain length increase, and the molecular interactions result from the presence of dipole-dipole forces between the DES and the solute leading to weaker interactions. For the THF, acetonitrile and thiophene, the γ_{13}^{∞} values decrease in this order: THF> acetonitrile> thiophene. Thiophene has shown much lower activity coefficients at infinite dilutions which suggest much more interactions with the stationary phase, this may be attributed to the presence of two lone electron pairs on the sulphur atom. The natural logarithm of γ_{13}^{∞} for the alcohols, are presented on Figure 5.2.10, which shows that as the length of the alcohol molecule increases, the γ_{13}^{∞} values also increase. For the investigation of alcohols, the retention times were very high showing a much higher interaction occurring in the column between the DES and the alcohols which led to much lower γ_{13}^{∞} values. The interaction may be attributed to the presence of oxygen lone pairs on the diethylene glycol, which may have interacted through a hydrogen bond with the solutes.

6.2.2 Thermodynamic Functions at Infinite Dilution

The partial excess molar properties, specifically the enthalpies, entropies and Gibbs free energies at infinite dilution, were calculated using the temperature-dependent relationship of $\ln(\gamma_{13}^{\infty})$. The change in enthalpy exposes the separation of bonds, which is linked to the dissolution of a substance in the deep eutectic mixture. This involves the attraction between the solvent and solute, encompassing the endothermic process of breaking bonds between the solvent and solute.

Table 5.1.2 shows the partial excess molar properties, including (enthalpies, entropies and Gibbs free energies) at infinite dilution at temperature T = 323.15 K. The alkanes, alkenes, cyclic hydrocarbons, alkynes, aromatic hydrocarbons showed positive excess enthalpies. This shows that there is an exothermic dissolution. For alcohols, ketones, acetonitrile, THF, and thiophene shows negative enthalpies which represent the greater energy from solute-solvent interactions. Furthermore, this indicates that the investigated deep eutectic solvents (DESs) exhibit strong hydrophilic characteristics, particularly when mixed with solutes having negative enthalpy values.

The Gibbs free energy was investigated for all the solutes and revealed negative values for the alcohols, ketones, acetonitrile, THF, and thiophene, which shows the spontaneity of the process. The other solutes showed positive values for the Gibbs free energies, which suggest weaker interactions with these solutes (Kabane and Redhi 2020). The entropy value signifies how the solute molecules arrange themselves around the solvent during the interactions, it is commonly referred to as the level of disorder, where the positive entropy shows more disorder in the system, while the negative entropy value show less disorder in the system. The entropy values were also investigated which showed the arrangement of the solutes in the column as their atoms interact with the solvent, showing negative entropy values of solutes (ethanol, propanol, THF, acetonitrile, thiophene and ketones) which show less disorder of the molecules when interacting with the solvent.

The average activity coefficients at infinite dilution (γ_{13}^{∞}) values were used to determine the partial excess molar properties, enthalpies, entropies, and Gibbs free energies. These properties were calculated using the temperature-dependent relationship of $\ln(\gamma_{13}^{\infty})$. The change in enthalpy exposes the separation of bonds. which is linked to the dissolution of a substance in the deep eutectic mixture. This involves the attraction

between the solvent and solute. encompassing the endothermic process of breaking bonds between the solvent and solute. Table 5.2.2 shows the enthalpies, Gibbs free energies, and entropies at infinite dilution at temperature T=323.15 K. All solutes have positive excess enthalpies, except for thiophene. This shows that there is an endothermic dissolution. There are attractive forces between thiophene and DES molecules in the mixture. These forces may include van der Waals forces, dipole-dipole interactions, and hydrogen bonding. Furthermore, this indicates that the investigated deep eutectic solvent (DES) exhibit strong hydrophilic characteristics when separating thiophene.

The Gibbs free energy was investigated for all the solutes and showed positive values, which shows the spontaneity of the process. The entropy values were also investigated which showed the arrangement of the solutes in the column as their atoms interact with the solvent. With the exception of 1-nonene, 1-decene, m-xylene, tetrahydrofuran (THF), thiophene, and acetone, all calculated entropy values are positive.

6.2.3 Selectivities and Capacities

The main purpose of this work and infinite dilution activity coefficients values is to evaluate the performance of the prepared DES (BDMIMCl+EG) as a separating solvent for industrial extraction processes. Equations 3.20 and 3.21 were used to calculate the selectivity and capacity values tabulated in Table 5.1.3. The results tabulated are also compared with the previously used DESs and ionic liquids with similar HBA or HBD. The commonly applied solvents in the industry such as sulfolane and N-methyl-2-pyrrolidinone (NMP) are also compared to the investigated DES. The investigated DES was used to separate the mixtures of cyclohexane/benzene, hexane/thiophene, as well as cyclohexane/ethanol. The cyclohexane/benzene mixture is important for various industrial processes and applications due to the distinct properties and uses of these two chemicals, it is a commonly found mixture in crude oil refining. The hexane/ thiophene mixture is crucial as hexane and thiophene can be present in crude oil, and to produce low-sulphur fuels, the separation of thiophene from hydrocarbons like hexane is important to meet environmental regulations and produce cleaner fuels. For the mixture of cyclohexane/ethanol are commonly used as solvents in the production of adhesives, coatings, and sealants. Also, in biofuel production, ethanol is a key component, hence, its separation from cyclohexane is

essential to ensure the purity and compliance of ethanol with fuel quality standards, contributing to the production of clean and efficient biofuels. The separation parameters were monitored at temperature of 313.15 K, the results showed that the prepared DES have low capacity to separate cyclohexane/benzene, despite being highly selective for this azeotropic mixture. The capacity and selectivity values for the other two industrial separation problems (hexane/thiophene and cyclohexane/ethanol) at selectivities (159 and 92) and capacities (2 and 5) were high when compared to the previously used solvents, which showed that the DES is well performing as an entrainer.

The efficacy of the DES (BDMIMCl + DEG) as a solvent for addressing issues related to chemical separation. The selectivity and capacity values were calculated using Equations 3.20 and 3.21, and the results are presented in Table 5.2.3 alongside with the literature values for DESs with similar cation or anion, as well as currently employed solvents in extraction processes. To gauge the effectiveness of the investigated solvent, selectivity, and capacity data for other significant industrial solvents such as sulfolane and N-methyl-2-pyrrolidinone (NMP) are also included for comparison. Selectivity measures a solvent's ability to selectively separate desired components in a separation process, while capacity indicates the quantity of material that can be processed in the separation process. Considering these factors are crucial for designing and optimizing separation processes.

The results tabulated in Table 5.2.3 are also compared with the previously used DESs and ionic liquids with similar HBA or HBD, such as [BMIMCl][Gly] and [EMIMCl4Al][DEG] with selectivity values of 9 and 17, respectively. The commonly applied solvents in the industry such as sulfolane and N-methyl-2-pyrrolidinone (NMP) are also compared to the investigated DES. The investigated DES was used to separate the mixtures of heptane/toluene, pentane/benzene, as well as heptane/ethanol. The separation parameters were monitored at temperature of 313.15 K, the results showed that the prepared DES will have low capacity to separate cyclohexane/benzene despite being highly selective for the azeotropic mixture. The capacity and selectivity values for the other two potential separation problems were high when compared to the previously used solvents. which showed that the DES is well performing as an entrainer.

6.3 Deep eutectic solvent (BDMIMBF4 + EG or DEG)

6.3.1 Activity coefficients at infinite dilution

A deep eutectic solvent was prepared using 1-butyl-2,3-dimethylimidazolium tetrafluoroborate as the hydrogen bond acceptor (HBA) and ethylene glycol as the hydrogen bond donor (HBD) at a molar ratio of 1:3. The corresponding average activity coefficients at infinite dilution (γ_{13}^{∞}) for this prepared DES are detailed in Table 5.3.1. In Figures 5.3.4 to 5.3.10, the natural logarithms of γ_{13}^{∞} are illustrated as a function of temperature (1000/T in K) for all investigated solutes categorized based on their functional groups. Specifically, Figure 5.3.4 to 5.3.6 depict the natural logarithm of γ_{13}^{∞} for alkanes, alkenes, and alkynes, revealing a decrease in γ_{13}^{∞}values with increasing temperature. This phenomenon arises because, with increasing temperature, solutes exhibit higher mobility within the column, reducing their molecular interactions with the stationary phase of the column. Additionally, there is a noticeable rise in γ_{13}^{∞}values as the number of carbon atoms increases, corresponding to an increase in molecular size. This larger size results in greater surface coverage, subsequently enhancing solvation. Among aliphatic hydrocarbons, alkynes exhibit lower γ_{13}^{∞} values due to the presence of triple bonds between carbon atoms, leading to higher polarity. This increased polarity makes alkynes more soluble in the solvents compared to other aliphatic hydrocarbons. In the case of aromatic hydrocarbons, as illustrated in Figure 5.3.7, a similar trend is observed concerning the increase in γ_{13}^{∞} values with the lengthening of the alkyl chain. The temperature and γ_{13}^{∞} values exhibit an inverse proportionality. Notably, the γ_{13}^{∞} values for aromatic hydrocarbons are lower than those for alkanes and alkenes. This difference is attributed to the presence of a hydrogen cloud above and below the benzene ring as well as delocalized electrons. The behaviour of ketones indicates that γ_{13}^{∞} values increase with the lengthening of the alkyl chain. The presence of dipole-dipole forces between the DES and the solute contributes to lower interactions. Regarding THF, acetonitrile, and thiophene, the order of decreasing γ_{13}^{∞} values is THF > acetonitrile > thiophene. Thiophene exhibits significantly lower activity coefficients at infinite dilution, suggesting more interactions with the stationary phase, likely due to the presence of two lone electron pairs on the sulphur atom. For alcohols, illustrated in Figure 5.3.10, the natural logarithm of γ_{13}^{∞} indicates an increase in γ_{13}^{∞} values with the lengthening of the alcohol molecule. In the

investigation of alcohols, high retention times were observed, signifying substantial interaction in the column between the DES and alcohols, resulting in lower γ_{13}^{∞} values. This strong interaction may be attributed to the presence of ethylene glycol, possibly engaging in hydrogen bonding with the solutes.

This deep eutectic solvent was prepared using 1-butyl-2,3-dimethylimidazolium tetrafluoroborate as the hydrogen bond acceptor (HBA) and diethylene glycol as the hydrogen bond donor (HBD) at a molar ratio of 1:3. The corresponding average activity coefficients at infinite dilution (γ_{13}^{∞}) for this prepared DES are detailed in Table 5.4.1. In Figures 5.4.4 to 5.4.10, the natural logarithms of γ_{13}^{∞} are illustrated as a function of temperature for all investigated solutes. Figure 5.4.4 to 5.4.6 depict the natural logarithm of γ_{13}^{∞} for alkanes, alkenes, and alkynes, revealing a direct inverse relation between γ_{13}^{∞} values and temperature. This phenomenon arises because, with increasing temperature, solutes move faster within the column, reducing interaction with the stationary phase of the column and shorten the retention time. Additionally, there is a noticeable rise in γ_{13}^{∞} values as the number of carbon atoms increases, corresponding to an increase in molecular size. This larger size results in greater surface area, subsequently enhancing solvation. Among aliphatic hydrocarbons, alkynes exhibit lower γ_{13}^{∞} values due to the presence of triple bonds between carbon atoms. This increased polarity makes alkynes more soluble in the solvents when compared to other aliphatic hydrocarbons. In the case of aromatic hydrocarbons, as illustrated in Figure 5.4.7, a similar trend is observed concerning the increase in γ_{13}^{∞} values with the lengthening of the alkyl chain. The temperature and γ_{13}^{∞} values exhibit an inverse proportionality. Notably, the γ_{13}^{∞} values for aromatic hydrocarbons are lower than those of alkanes and alkenes. This difference is attributed to the presence of a hydrogen cloud above and below the benzene ring. The behaviour of ketones indicates that γ_{13}^{∞} values increase with the lengthening of the alkyl chain. The presence of dipole-dipole forces between the DES and the solute contributes to lower interactions. For THF, acetonitrile, and thiophene, the order of decreasing γ_{13}^{∞} values, thiophene > acetonitrile > THF. The observation that thiophene exhibits different behaviour compared to other solutes is indeed an interesting point. Which was also observed in literature (Domańska and Marciniak 2009; Marciniak and Wlazło 2015; Arumugam *et al.* 2020). For alcohols, illustrated in Figure 5.4.10. the natural logarithm of γ_{13}^{∞} indicates an increase in γ_{13}^{∞} values with the lengthening of the alcohol molecule.

In the investigation of alcohols. higher values of γ_{13}^{∞} were noted. This shows weaker interactions with the DES.

6.3.2 Thermodynamic Functions at Infinite Dilution

The study utilized average activity coefficients at infinite dilution (γ_{13}^{∞}) values to calculate partial excess molar properties, including enthalpy, entropy, and Gibbs free energy. These properties were determined using the temperature-dependent relationship of ln (γ_{13}^{∞}). The change in enthalpy reflects the separation of bonds. indicating the dissolution of a substance in the deep eutectic mixture. This process involves the endothermic breaking of bonds between the solvent and solute, demonstrating the attractive forces between them.

Table 5.3.2 presents enthalpies, Gibbs free energies, and entropies at infinite dilution at a temperature of *T*=323.15 K. With the exception of thiophene, all solutes exhibit positive excess enthalpies, indicating an endothermic dissolution process. This suggests strong attractive forces, potentially including van der Waals forces, dipole-dipole interactions, and hydrogen bonding between thiophene and the deep eutectic solvent (DES). The positive Gibbs free energy values for all solutes imply the spontaneity of the process. However, for some solutes (alcohols and ketones), positive Gibbs free energy values suggest stronger interactions, indicating a spontaneous process.

Entropy values were also investigated, revealing the arrangement of solutes in the column as their atoms interact with the solvent. With the exception of 1-nonene, 1-decene, alkynes, aromatic hydrocarbons, tetrahydrofuran (THF), thiophene, and acetonitrile, all calculated entropy values are positive. This signifies a predominantly favourable arrangement of solutes in the column and reflects the hydrophilic characteristics of the investigated DES.

Table 5.4.2 presents enthalpies, Gibbs free energies, and entropies at infinite dilution at a temperature of *T* = 323.15 K. Apart from thiophene, all solutes exhibit positive excess enthalpies, indicating an endothermic dissolution process. This suggests strong attractive forces, hydrogen bonding between thiophene and the deep eutectic solvent (DES). The positive Gibbs free energy values for all solutes imply the

spontaneity of the process. Gibbs free energy values were all positive for the solutes, suggesting weaker interactions, indicating a less spontaneous process.

Entropy values were also investigated, revealing the arrangement of solutes in the column as their atoms interact with the solvent. Apart from 1-decene, aromatic hydrocarbons, tetrahydrofuran (THF), and thiophene, all calculated entropy values are positive. This signifies a predominantly favourable arrangement of solutes in the solvent and reflects the hydrophilic characteristics of the investigated DES.

6.3.3 Selectivity and Capacities

The γ_{13}^{∞} values obtained for DES3 (1-butyl-2,3-dimethylimidazolium tetrafluoroborate + ethylene glycol) were used to determine the selelectivity and capacity for the separation of (hexene/toluene), (hexane/acetone) and (heptane/ethanol). The results of the selectivity and capacity are tabulated on Table 5.3.3 and are compared with the previously used DESs and ionic liquids with similar HBA or HBD. The commonly applied solvents in the industry such as N-methyl-2-pyrrolidinone (NMP) is also compared to the investigated DES3. The results showed that the prepared DES have low capacity to separate hexene/toluene despite being highly selective for their azeotropic mixture. The capacity and selectivity values for the (hexane/acetone and heptane/ethanol) separation problems were relatively comparable with the previously used solvents, which showed that the DES is a promising entrainer for hexane/acetone separation and heptane/ethanol separation. The presence of HBD make it easier for the separation of heptane/ethanol, as the solvent can easily accommodate ethanol due to the hydroxyl group found in ethylene glycol.

The DES4 (1-butyl-2,3-dimethylimidazolium tetrafluoroborate + diethylene glycol) was used to investigate its possible use as an entrainer by determining the selectivity and capacity for the separation of (Cyclohexane/methanol), (Heptane/Ethanol), and (Toluene/Benzene). These values were computed from γ_{13}^{∞} values, Table 5.4.3 shows the results, where the currently investigated DES is compared to the previously used solvents for separations. For the separation of cyclohexane/methanol, the DES shows relatively low selectivity and capacity values at 16.17 and 0.2, respectively. Although it shows higher selectivity as compared to the highly used solvent NMP. For the separation of heptane and ethanol, the same capacity and selectivities were noted as

they were low. For the separation of toluene/benzene, it shows a relatively high selectivity at 1.91 and low capacity. This shows that DES4 is a promising entrainer for the separation of toluene/benzene. The separation of toluene and benzene is common in several industries, particularly in those that involve the production and processing of petrochemicals and chemicals. The separation is crucial because toluene and benzene are valuable industrial solvents and feedstocks and having them in pure form is essential for various processes (Li *et al.* 2021).

6.4 Influence of increasing the length of HBD (EG to DEG) with same HBA

The effect of increasing the chain length of the hydrogen bond donor (HBD) from ethylene glycol (EG) to diethylene glycol (DEG) while keeping the hydrogen bond acceptor (HBA) constant on the deep eutectic solvents (DESs) on activity coefficients at infinite dilution was investigated. As the length of the HBD increased, transitioning from EG to DEG, the activity coefficients at infinite dilution of the DES was examined to assess how this change impacted the solute-solvent interactions.

Looking at DES1 and DES2, the following was noted for the alkanes as the change of HBD affected the values of activity coefficients in a way that the values for the HBD (ethylene glycol) has proven to be lower than those of HBD (diethylene glycol, this particular effect of using different extended chain length of HBD (ethylene and diethylene glycol) on DES for separation was noticed for the solutes, to give an example n-decane γ_{13}^{∞} = 437.08 for DES1 and γ_{13}^{∞} = 732.24 for the DES2 at *T* = 353.15 K. This could be attributed to the molar ratio of HBA to HBD (1:2) in DES2 as compared to DES1(1:3). For the alkenes the opposite is noticed with the n-Decene of DES1 at γ_{13}^{∞} = 417 while it is at γ_{13}^{∞} = 239 for the DES2. For cyclic hydrocarbons it showed a more similar activity values although for alkynes the values were higher for the DES2. For alcohols the values for the DES1 showed to be much closer to zero as compared to the ones on DES2 which are much higher with the highest being for butane at γ_{13}^{∞} = 4.63. The ketones show similar behaviour as the alcohols with much lower for DES1 and much higher for DES2. For THF it shows that it interacts with the DES onto the column more the same in both the DESs with value of activity at 10.

Thiophene and acetonitrile shows similar trends with lower values for the DES1 and much higher values for DES2. When it comes to the effect of temperature on the DESs with same HBA and different HBD. We noted that for DES1, it shows a decrease in activity coefficient values as the temperature increases for all the alkanes, alkenes, alkynes, and cyclic hydrocarbon. However, for other solutes including alcohols, THF, Acetonitrile, thiophene and ketones, the opposite is true. This could be attributed to the polar property of the solutes.

For the investigation done on using the same HBA (1-butyl-2,3-dimethylimidazolium tetrafluoroborate) with different HBD (ethylene glycol and diethylene glycol) named DES3 and DES4. The results showed that as the length of the HBD increases the activity coefficients also decreases, for instance for alkanes i.e., n-decane it moved from γ_{13}^{∞} = (1231 to 1054), alkene (n-decene) from γ_{13}^{∞} = (634 to 618), alkynes (1-heptyne) from γ_{13}^{∞} = (57.67 to 48.98) and thiophene from γ_{13}^{∞} = (9.97 to 8.24). For the other solutes, it showed that the activity coefficients of the ethylene glycol-based DES were lower than those of diethylene-based DES. For instance, cyclic hydrocarbons (o-xylene) from γ_{13}^{∞} = (29.87 to 47.58), ketones (butanone) from γ_{13}^{∞} = (4.696 to 5.66), THF, and acetonitrile from γ_{13}^{∞} = (6.42. 5.15) to γ_{13}^{∞} = (7.22 and 7.65), respectively. The use of both DESs showed to have not much effect on alcohol irrespective of the HBD length used. The effect of temperature by the HBD is also investigated and showed that as the temperature increases, all the solutes activity coefficients decrease except for thiophene in both DESs.

The effect on the sets of DESs investigated in this work can be attributed to many and specific effect on the presence of the ethylene glycol or diethylene glycol based DESs. Ethylene glycol and diethylene glycol have different molecular structures in which the ethylene glycol has a shorter chain length as compared to the diethylene glycol which is also characterised by the presence of an oxygen atom between the two carbon atoms which is also depicted in the FTIR spectra. The interaction of both DESs with the solutes have shown to be different with each solute depending on whether it is a polar or non-polar solute which in turn affected the value of activity coefficients. Ethylene glycol and diethylene glycol contains a polar OH groups, because oxygen is more electronegative it tends to polarise the electron pair in the OH group towards it. Diethylene glycol have an extended chain (-CH_2) which also influence the polarity index and in turn impact the γ_{13}^{∞} values for both polar and non-polar solutes.

6.5 Effect of change in anion of the HBA with same HBD

The effect of using DES prepared from same HBD and HBA with different anions (Cl^- and BF_4^-) but same cation (1-butyl-2,3-dimethylimidazolium$^+$). There are different effects noted from using these DES with the same set of solutes when investigating the activity coefficients at infinite dilutions. The activity coefficients showed that there is a huge difference when it comes to alkanes (n-decene) which has the value of γ_{13}^{∞} = 437.08 for DES1 (with Cl^-) when compared to the value of γ_{13}^{∞} = 1231 when screening DES3 (with BF_4^-). This may show that the change in anion on the HBA plays a major role as it shows the different bonding interactions, which in turn affect the solvation property of the prepared deep eutectic solvent. For alkenes (n-decene) DES1 (γ_{13}^{∞} = 417) and Des3 (γ_{13}^{∞} = 634), for alkynes (heptyne), DES1 (γ_{13}^{∞} = 3.180) and DES3 (γ_{13}^{∞} = 57.67), for cyclic hydrocarbons (o-Xylene) DES1 (γ_{13}^{∞} = 26.59) to DES3 (γ_{13}^{∞} = 29.87), for alcohols (methanol) DES1 (γ_{13}^{∞} = 0.16) and DES3 (γ_{13}^{∞} = 4.37), for ketones (acetone) DES1 (γ_{13}^{∞} = 0.10) and DE3 (γ_{13}^{∞} = 3.91), the values for THF, acetonitrile and thiophene for DES1 are γ_{13}^{∞} = (10.19, 0.30 and 0.47), while for DES3 are γ_{13}^{∞} = (6.42, 5.15, and 9.97), respectively. This shows that the anion on the HBA plays a significant role to influence the solubility of the DES. Additionally, the change in anion affect the overall ionic strength and electrostatic interactions in the DES which impact the distribution of the solutes when partitioning through the DES onto the column. The temperature influence was only observed for the alcohols, ketones, THF and acetonitrile in both DESs, where the DES1 shows an increase with temperature while DES3 shows a decrease for all the investigated solutes.

For the DES2 and DES4 where diethylene was used as HBD, the same trend observed in the DES1 and DES3 was noted, where the HBA with anion ($chloride^-$) prove to have lower values of activity coefficients while the HBA with anion (BF_4^-) have the higher values of activity coefficients. The same trend is also noted for temperature effect (all solutes decreases) except for thiophene as the temperature increases.

6.6 Characterization of deep eutectic solvents used for thermophysical properties measurements.

6.6.1 Fourier transform infrared spectroscopy analysis.

The FTIR analysis for both the prepared DESs [(1-butyl-1-methylpyrrolidinuim bromide + ethylene glycol) and (1-butyl-3-methylimidazolium chloride + ethylene glycol) was

conducted to confirm the interaction between the hydrogen bond acceptor (HBD) and hydrogen bond donor (HBD). The attention was given to the interactions occurring between the HBD and HBA. The peaks from both pure components were monitored for any shift and new peaks on the prepared DESs (separately). For both of the prepared DESs shows the spectra of pure ethylene depicted in Figures 5.5.1 and 5.7.1 in Chapter 5. The spectra of ethylene glycol show a peak centred at 3310 cm^{-1} (-OH), (2944 and 2870) cm^{-1} for (-CH) stretching, C-O stretch at 1655 cm^{-1} was observed. In the fingerprint region, peak centred at (1083 and 1032) cm^{-1}. The rocking vibration of -CH2- group at 856 cm^{-1} is also observed. The C-C peak at 512 cm^{-1} which signifies the aliphatic alcohol. These are in agreement with literature (Krishnan 1961; Chirea *et al.* 2011). For the analysis of pure 1-butyl-1-methylpyrrolidinuim bromide, there are peaks centred at 3427 cm^{-1} (-OH stretching), 2959 cm^{-1} (CH3, CH2 stretch) of alkyl chain, 2868 cm^{-1} (CH) for the ring. The peak at 1464 cm^{-1} corresponds to the C-N stretch and the stretch at 930 cm^{-1} is a characteristic peak for the quaternary nitrogen observed (Patel and Patel 2012; Kumar and Katal 2018). For the DES (1-butyl-1-methylpyrrolidinuim bromide + ethylene glycol) the peaks noted are those present in both the pure individual components and there is no new peak formed which shows that there is only hydrogen bonding between the two components.

The spectra of pure 1-butyl-3-methylimidazolium chloride, major peaks noted are centered at 3386 cm^{-1} (NH stretch), 2872 cm^{-1} (N-CH_3), 1634 cm^{-1} (C=C stretch), the imidazolium framework vibration is noted at 1571 cm^{-1}, the CH, C-N stretch at 1170 cm^{-1} and the C-Cl vibration at 622 cm^{-1}. The spectra of the prepared DES (1-butyl-3-methylimidazolium chloride + ethylene glycol) shows several peaks present in the pure EG such (2937, 2880, 1034 and 516) cm^{-1}, with the shift of the OH stretch signifying the weakening of hydrogen bond. The peaks on the BMIMCl are as follows. (2937, 1571, 1170, and 662) cm^{-1}, which correspond to N-C, imidazolium ring, CH stretch and C-Cl stretch, respectively. The presence of the peaks on pure components and on the DES proves that the DES is formed through hydrogen bonding.

6.6.2 ^{13}C-NMR and ^{1}H-NMR spectroscopic analysis

The prepared DES (1-butyl-1-methylpyrrolidinuim bromide + ethylene glycol) was characterized by ^{13}C-NMR [Figure 5.5.2(a)]. The spectra shows the peaks corresponding to -CH_3 (7) of the butyl at 12.86 ppm, -CH_2- (6) of butyl at 19.25 ppm, -CH_2- (5) of butyl at 25.09 ppm, -CH_2- (9) of ring at 21.30 ppm, -CH_3 (3) attached to N

at 48.07 ppm, -CH_2- (4) at 64.19 ppm, -CH_2- (8) at 64.25 ppm, and -CH_2- (1.2) at 62.53 ppm correspond with the two carbons on the ethylene glycol. The corresponding ^{1}H-NMR was analysed and shows that the DES has formed and the component bond through hydrogen bonding H on the OH of ethylene glycol and N on the pyrolidinium.

The prepared DES (1-butyl-3-methylimidazolium chloride + ethylene glycol) was also characterised to confirm the interaction occurring in the DES. The ^{13}C-NMR shows the C peaks corresponding to C atoms, CH_3- (3) at 12.75 ppm, -CH2- (4) at 18.77 ppm, -CH_2- (5) at 31.28 ppm, -CH_3 (8) attached to -N- atom of the imidazolium ring at 35.70 ppm, -CH_2- (6) attaching the butyl to imidazolium ring at 49.22 ppm, two -CH_2- (1. 2) for the ethylene glycol at 62.56 ppm, -CH- (7) in the ring at 138.57 ppm and the two -CH- in the ring at (123.46 and 122.19) ppm. The carbon atoms correspond to the H atoms on Figure 5.7.2 (b), showing that the formed DES consist of hydrogen bonds between the two constituents of the DES.

6.6.3 Thermogravimetric analysis

The impact of varying temperatures on the thermal characteristics of the deep eutectic solvents was also investigated. This was to test the strength of the DES at high temperatures. Figures 5.5.3 and 5.7.3 shows the TGA curve for DES (1-butyl-1-methylpyrrolidinuim bromide + ethylene glycol) and DES (1-butyl-3-methylimidazolium chloride + ethylene glycol). The thermal stability was done over the range of temperature from room temperature of (30 to 610) ºC. The two DESs showed only one step. Although the investigated DES has not been studied before, the individual components of the DES were compared with the obtained thermal stability. This observation agrees with the results of previously reported work (Salgado *et al.* 2014). where 1-butyl-1-methylpyrrolidinium tris(pentafluoroethyl) trifluorophosphate showed degradation on one step, which is an ionic liquid with the same cation as the salt used (1-butyl-1methylpyrrolidinium$^+$). The DES (1-butyl-1-methylpyrrolidinuim bromide + ethylene glycol) shows an onset temperature at weight percentage (99%).

The thermogravimetric analysis of DES (1-butyl-3-methylimidazolium chloride + ethylene glycol) has shown that upon applying heat, a predominant mass loss of approximately 100% at temperatures exceeding 90°C was observed, and an under timed residue of 0.36% is detected at 336°C. The TGA shows a one-step decomposition. The curve shows that the DES decomposes at relatively high

temperature which suggest thermal stability of the DES, as most of the DES decomposes at a temperature above 300°C, this indicated that the DES can withstand elevated temperatures without significant degradation. The results shows that the DES has lower temperature of decomposition when compared to one constituent (1-butyl-3-methylImidazolium chloride) which has onset temperature above 200°C (Efimova. Hubrig and Schmidt 2013).

Thermophysical properties

6.7 Binary mixtures of [DES (BMPyrBr + EG) + acetic acid or ethanol] and [DES (BMIMCl +EG) + acetic acid or ethanol]

6.7.1 Measured properties

6.7.1.1 Density

The density measurements were conducted for the binary mixtures of the DES (1-butyl-1-methylpyrrolidinium bromide + ethylene glycol) and acetic acid and ethanol, respectively. The densities were measured for the pure DES, acetic acid, ethanol as well as the densities of the binary mixtures at different concentrations, these were measured over the range of temperatures of *T*= (293.15 to 313.15) K. The density for the acetic acid was comparable to the reported values on literature at T= (303.15, 308.15, and 313.15) K (Dai *et al.* 2008; Ren *et al.* 2014). The main reason for the range of temperature measurements is to evaluate the changes occurring and the behaviour of the binary mixtures. The resulted measured densities are represented in Table 5.5.1, 5.6.1, 5.7.1 and 5.8.1 and Figure (5.5.4, 5.6.1, 5.7.4 and 5.8.1) for the binary systems of DES (BMPyrBr + EG) + acetic acid, DES (BMPyrBr + EG) + ethanol, DES (BMIMCl +EG) + acetic acid, and DES (BMIMCl + EG) + ethanol, respectively. The measurements of densities have shown to decrease with an increase in temperature for all the binary systems. The densities increase as the molar ratio of the DESs (x_1) increases.

6.7.1.2 Speed of sound

The speed of sound of the binary mixtures is an important property to investigate as it helps in assessing the mixture's acoustic properties and the interaction occurring between the mixture and the sound waves. This property is essential as it gives the type of interaction occurring between the two systems mixed, it describes weather

there is a solute-solute, solute-solvent or solvent-solvent interactions occurring. The speed of sound was measured at temperatures *T* = (293.15 K to 313.15 K with an interval of 5 K) for all the investigated binary mixtures. The results of the measured speed of sound are presented in Table 5.5.1, 5.6.1, 5.7.1, and 5.8.1 and Figure 5.5.5, 5.6.2, 5.7.5 and 5.8.2. The figures show a plot of density the concentration/ mole fraction of DESs (x_1) at the stipulated temperatures, and show that as the temperature increases, the speed of sound decrease. It can be observed that as the concentration of the DESs (x_1) increases, the speed of sound increases.

6.7.1.3 Refractive index

Refractive index is an optical property which gives the type of interaction occurring in the binary mixture. Refractive index measured the amount of reduction or bending of speed of light when the light passes through the mixture in comparison to the speed of light in a vacuum. This property is of importance as it also determines the interactions occurring within the binary mixture. The refractive indices of the binary mixtures studied are presented in Table 5.5.1, 5.6.1, 5.7.1, 5.8.1 and are plotted in Figure 5.5.6, 5.6.3, 5.7.6, and 5.8.3. The refractive indices have shown to follow a pattern of decreasing as the temperature increases and increase as the molar fractions of the DESs (x1) increases.

6.7.2 Derived excess properties

6.7.2.1 Excess molar volume

The excess molar volume was calculated from the density of pure components and the binary mixtures using the equation (3.26) in chapter 3. The excess molar volumes were calculated over the temperature range of (293.15 to 313.15) K at corresponding mole fractions of DESs (x_1). The calculated results are presented on Table 5.5.2, 5.6.2, 5.7.2, 5.8.2 and represented in Figure 5.5.7, 5.6.4, 5.7.7, and 5.8.4. The calculated excess molar volume values are negative for the binary mixtures of DES (BMPyrBr + EG) and acetic acid, as well as DES (BMPyrBr + EG) and ethanol at mole fraction range (x_1 = 0 - 1) and at different temperatures. The temperature increase lead to more negative values of the excess molar volumes retaining the asymmetric shape of the profile. The asymmetry observed in the curves of binary mixtures (DES (BMPyrBr + EG) and acetic acid) results from variations in the molar volumes of the individual

components within the mixture. The presence of negative excess molar volume (V_m^E) values may be attributed to strong interactions between the acetic acid or alcohol employed on the DES (BMPyrBr + EG). This occurs because of intermolecular forces and packing, which influenced by variations in the size and shape of the molecules, and impact the excess molar volumes. For the binary mixture of DES (BMIMCl + EG) and acetic acid, the V_m^E start at the negative, with the minimum at x_1= 0.1 and transition into the positive side at x_1= 0.7 with a maximum at x_1=0.8, for all temperatures. The positive values of excess molar volumes (V_m^E) stemming from the combination of the DES (BMIMCl + EG) with acetic acid may be attributed to several factors: a reduction in the self-association of the DES, a decrease in the self-association of acetic acid through hydrogen bonding, or an effect where the larger DES (BMIMCl + EG) molecules do not fit into the network of hydrogen-bonded acetic acid. For the binary systems of DES (BMIMCl + EG) with ethanol, the opposite is true, where the curve starts on the positive side with maximum at x_1= 0.3 and minimum at x_1= 0.8. The positive values originate from the reduction of dispersive interactions between the deep eutectic solvent (DES) and ethanol, or an electrostatic misfit (slightly repulsive) between the components, the negative values result from the existence of electron donor-acceptor type interactions between the DES and ethanol. It can be concluded that in the DES rich mixture, the dispersion dominated the behaviour of the mixture.

6.7.2.2 Deviation in isentropic compressibility

The isentropic compressibility of a substance is the property that describes how substance's volume change as the pressure changes while the entropy is constant. It can also be explained in terms of speed of sound, a compound with higher density and lower compressibility will have a higher speed of sound. Conversely, a compound with lower density and higher compressibility will have a lower speed of sound. The isentropic compressibility was calculated using the equation (3.27), while the deviation in isentropic compressibility was calculated using the equation (3.28) explained in chapter 3. The calculated values for isentropic compressibilities (k_s) and deviation in isentropic compressibilities (Δk_s) for the binary mixtures of [(DES (BMPyrBr + EG)) + acetic acid or ethanol) and ((DES (BMIMCl + EG) + acetic acid or ethanol]. The results are presented in Table 5.5.2, 5.6.2, 5.7.2 and 5.8.2 for all the temperatures investigated and at different molar ratios of DES (x_1). The calculated k_s values

decrease with the increase in molar fraction of the DESs at all investigated temperatures. This phenomenon occurs due to a rise in thermal agitation. rendering the soluble liquids more susceptible to compression. The interactions observed in the binary systems resulted in a reduction of available space, causing negative Δk_s values. The negative Δk_s occurs when the calculated k_s of the mixture is lower than the values of predicted ideal mixture values. This shows that the compressibility obtained exhibit less compressibilities than expected, meaning that the mixture is less compressible. This is attributed by stronger intermolecular forces between the DESs and acetic acid or alcohols than expected, and attractive forces, such as hydrogen bonding or dipole-dipole interactions, dominate over repulsive forces between molecules. The Δk_s values are inversely proportional to temperature at the same mole fractions. The Δk_s minimum values are observed at (-23 to -28) x10^{11} Pa^{-1} for DES (BMPyrBr + EG) + acetic acid at x1=0.2, (-29 to -42) x10^{11} Pa^{-1} for DES (BMPyrBr + EG) + ethanol at x_1= 0.2, (-22 to -27) x10^{11} Pa^{-1} for DES (BMIMCl + EG) + acetic acid at x_1=0.1, and (-32 to 38) x10^{11} Pa^{-1} for DES (BMIMCl + EG) + ethanol at x_1=0.2.

6.7.2.3 Intermolecular free length

The intermolecular free length is a measure of the average distance between molecules in a substance. The intermolecular free length values were calculated using the equation (3.31) and values are given in Tables 5.5.2, 5.6.2, 5.7.2 and 5.8.2. The values of the pure ethanol and acetic acid have proven to be much higher than the pure DESs (BMPyrBr + EG and BMIMCl + EG). The intermolecular free length values decrease with an increase in molar ratio of the DESs at all temperatures. This is because as the molar fractions of DESs increase, the number of molecules of that DES in the mixture increases. This results in a higher density of molecules, leading to increased molecular crowding and a decrease in the average distance between molecules. Additionally, the molecules of the DESs may have attractive forces, with increased molar fraction of the DESs, there is more orderly arrangement of the DES molecules leading to a reduced intermolecular free length. Intermolecular free lengths were used to investigate the properties that exist in the binary mixtures that are comprised of attractive and repulsive forces, and a simple linear correlation with the mole fraction of the DESs was observed.

6.8 Predictions and correlations

6.8.1 Prediction of Densities by Lorentz-Lorenz (L-L) Equation

The Lorentz-Lorenz equation was used to predict the ideal density values. The equation used to predict the values is presented in chapter 3 on equation (3.36). The experimental values were then correlated with the predicted values to helps evaluate the performance of the DESs. The root mean square deviation (RMSD), a measure of the average differences between values predicted by a model or theory and the actual observed values was used to check the accuracy of experimental values. The RMSD values were very low for all the DESs as presented in table 5.9, which indicates that the predicted values are close to the observed values, suggesting a good fit and accuracy of the model.

6.8.2 Prediction of Refractive Indices by Lorentz-Lorenz (L-L) Equation

The Lorentz-Lorenz equation was also used to predict the ideal refractive index values. The equation used to predict the values is presented in Chapter 3 on equation (3.37). The experimental values were then correlated with the predicted values which helps to evaluate the performance of the DESs. The root mean square deviation (RMSD), a measure of the average differences between values predicted by a model or theory and the actual observed values were used to check the accuracy of experimental values. The RMSD values were very low for all the DESs as presented in Table 5.9, which indicates that the predicted values are close to the observed values. suggesting a good fit and accuracy of the model.

CHAPTER 7: CONCLUSION

This work has covered several objectives. including preparation of deep eutectic solvents, which were proven to have formed by the different characterization techniques including, FTIR and NMR. The prepared deep eutectic solvents were then used to examine the impact of temperature as well as separation potential on various volatile organic compounds using chromatography to determine the activity coefficients at infinite dilutions. The intermolecular interactions were determined from the partitioning of the activity coefficients and further determined the capacity and selectivity of the investigated deep eutectic solvents. The activity coefficients were determined using gas chromatography for different solutes at different temperatures in the prepared DESs:

- DES1 (1-butyl-2,3-dimethylimidazolium chloride + ethylene glycol) (1:3)
- DES2 (1-butyl-2,3-dimethylimidazolium chloride + diethylene glycol) (1:2)
- DES3 (1-butyl-2,3-dimethylimidazolium tetrafluoroborate + ethylene glycol) (1:3)
- DES4 (1-butyl-2,3-dimethylimidazolium tetrafluoroborate + diethylene Glycol) (1:3)

The effect of using the different HBD and HBA were also investigated which shows that there is an influence by the type of anion of the HBA and the length of the HBD also plays a role in the activity coefficients at infinite dilution as well as the thermal stability (presented by the TGA analysis) of these DESs. The different separation of azeotropic mixtures with DESs as the entrainer has also been investigated, showing much potential in different industrial separations.

The thermophysical property measurements were also investigated with the aid of densitometer and refractometer. The instruments were used to measure thermophysical properties which include density, speed of sound, and refractive index at different temperatures for the different DESs.

- DES5 (1-butyl-1-methylpyrrolidinium bromide + ethylene glycol)
- Des6 (1-butyl-3-methylimidazolium chloride + ethylene glycol)

New data for the densities, speed of sound, and refractive indices have been analysed as a function of temperature for [DES5 + acetic acid or ethanol and DES6 + acetic acid or ethanol] mixtures over a range of mole fractions (x_1=0 to x_1=1). Excess properties were determined using the measured properties such as excess molar volume, isentropic compressibilities, deviation in isentropic compressibility, and intermolecular free length. The negative values and combination of negative and positive were observed and explained in detail in terms of the interactions occurring in the binary mixtures. The measured densities and refractive indices were correlated using the Lorentz-Lorenz correlation, the values showed to be much closer to the measured values. The mean square deviations were measured to determine correlation between the two groups of values. From the calculated standard deviations, it was determined that there is a good correlation between experimental and calculated results.

The obtained results highlight the significant role of DESs in separation techniques based on the selectivity and capacities, the binary mixtures of the DESs and alcohols or acetic acid showed that there are different interactions occurring, these thermophysical properties play a vital role in understanding, designing, and optimizing processes involving binary mixtures.

REFERENCES

Abbott. A. P.. Barron. J. C.. Ryder. K. S. and Wilson. D. 2007. Eutectic-based ionic liquids with metal-containing anions and cations. *Chemistry–A European Journal*. 13 (22): 6495-6501.

Abbott. A. P.. Capper. G.. Davies. D. L.. Rasheed. R. K. and Tambyrajah. V. 2003. Novel solvent properties of choline chloride/urea mixtures. *Chemical communications*. (1): 70-71.

Abbott. A. P.. Harris. R. C.. Ryder. K. S.. D'Agostino. C.. Gladden. L. F. and Mantle. M. D. 2011. Glycerol eutectics as sustainable solvent systems. *Green Chemistry*. 13 (1): 82-90.

Abranches. D. O. and Coutinho. J. A. 2022. Type V deep eutectic solvents: Design and applications. *Current Opinion in Green and Sustainable Chemistry*. 35: 100612.

Abranches. D. O.. Martins. M. A.. Silva. L. P.. Schaeffer. N.. Pinho. S. P. and Coutinho. J. A. 2019. Phenolic hydrogen bond donors in the formation of non-ionic deep eutectic solvents: the quest for type V DES. *Chemical communications*. 55 (69): 10253-10256.

Álvarez. E.. Cancela. Á.. Maceiras. R.. Navaza. J. M. and Táboas. R. 2006. Density. viscosity. excess molar volume. and viscosity deviation of three amyl alcohols+ ethanol binary mixtures from 293.15 to 323.15 K. *Journal of Chemical & Engineering Data*. 51 (3): 940-945.

Arriaga. S. and Aizpuru. A. 2019. Innovative non-aqueous phases and partitioning bioreactor configurations. In: *Advances in Chemical Engineering*. Elsevier. 299-348.

Astumian. R. D. 2010. Thermodynamics and kinetics of molecular motors. *Biophysical journal*. 98 (11): 2401-2409.

Bejan. A. 2016. *Advanced engineering thermodynamics*. John Wiley & Sons.

Bhagour. S.. Solanki. S.. Hooda. N.. Sharma. D. and Sharma. V. 2013. Thermodynamic properties of binary mixtures of the ionic liquid [emim][BF4] with acetone and dimethylsulphoxide. *The Journal of Chemical Thermodynamics*. 60: 76-86.

Bi. Y.. Hu. Z.. Lin. X.. Ahmad. N.. Xu. J. and Xu. X. 2020. Efficient CO2 capture by a novel deep eutectic solvent through facile. one-pot synthesis with low energy consumption and feasible regeneration. *Science of The Total Environment*. 705: 135798.

Brennecke. J. F. and Maginn. E. J. 2001. Ionic liquids: innovative fluids for chemical processing. *American Institute of Chemical Engineers. AIChE Journal*. 47 (11): 2384.

Brouwer. T. and Schuur. B. 2021. Comparison of solvent-based affinity separation processes using C yrene and S ulfolane for aromatic/aliphatic separations. *Journal of Chemical Technology & Biotechnology*. 96 (9): 2630-2646.

Castro-Muñoz. R.. Msahel. A.. Galiano. F.. Serocki. M.. Ryl. J.. Hamouda. S. B.. Hafiane. A.. Boczkaj. G. and Figoli. A. 2022. Towards azeotropic MeOH-MTBE separation using pervaporation chitosan-based deep eutectic solvent membranes. *Separation and Purification Technology*. 281: 119979.

Chirea. M.. Freitas. A.. Vasile. B. S.. Ghitulica. C.. Pereira. C. M. and Silva. F. 2011. Gold nanowire networks: synthesis. characterization. and catalytic activity. *Langmuir*. 27 (7): 3906-3913.

Chueh. P. and Prausnitz. J. 1967. Vapor-liquid equilibria at high pressures: Calculation of partial molar volumes in nonpolar liquid mixtures. *AIChE Journal*. 13 (6): 1099-1107.

Craig. L. C.. Gregory. J. D. and Hausmann. W. 1950. Versatile laboratory concentration device. *Analytical Chemistry*. 22 (11): 1462-1462.

Cruickshank. A.. Gainey. B.. Hicks. C.. Letcher. T.. Moody. R. and Young. C. 1969. Gas-liquid chromatographic determination of cross-term second virial coefficients using glycerol. Benzene+ nitrogen and benzene+ carbon dioxide at 50 C. *Transactions of the Faraday Society*. 65: 1014-1031.

Cvjetko Bubalo. M.. Vidović. S.. Radojčić Redovniković. I. and Jokić. S. 2015. Green solvents for green technologies. *Journal of Chemical Technology & Biotechnology*. 90 (9): 1631-1639.

Dincer. I. 2000. Thermodynamics. exergy and environmental impact. *Energy sources*. 22 (8): 723-732.

Domańska. U. and Marciniak. A. 2008. Measurements of activity coefficients at infinite dilution of aromatic and aliphatic hydrocarbons. alcohols. and water in the new ionic liquid [EMIM][SCN] using GLC. *The Journal of Chemical Thermodynamics*. 40 (5): 860-866.

Domańska. U. and Paduszyński. K. 2010. Gas–liquid chromatography measurements of activity coefficients at infinite dilution of various organic solutes and water in tri-iso-butylmethylphosphonium tosylate ionic liquid. *The Journal of Chemical Thermodynamics*. 42 (6): 707-711.

Domańska. U.. Wlazło. M.. Karpińska. M. and Zawadzki. M. 2017. Separation of binary mixtures hexane/hex-1-ene. cyclohexane/cyclohexene and ethylbenzene/styrene

based on limiting activity coefficients. *The Journal of Chemical Thermodynamics*. 110: 227-236.

Duarte Ramos Matos. G.. Calabro. G. and Mobley. D. L. 2019. Infinite dilution activity coefficients as constraints for force field parametrization and method development. *Journal of chemical theory and computation*. 15 (5): 3066-3074.

Efimova. A.. Hubrig. G. and Schmidt. P. 2013. Thermal stability and crystallization behavior of imidazolium halide ionic liquids. *Thermochimica Acta*. 573: 162-169.

Everett. D. 1965. Effect of gas imperfection on GLC measurements: a refined method for determining activity coefficients and second virial coefficients. *Transactions of the Faraday Society*. 61: 1637-1645.

Fan. Y.. Luo. H.. Zhu. C.. Li. W.. Wu. D. and Wu. H. 2021. Hydrophobic natural alcohols based deep eutectic solvents: Effective solvents for the extraction of quinine. *Separation and Purification Technology*. 275: 119112.

Foco. G. M.. Bottini. S. B.. Quezada. N.. de la Fuente. J. C. and Peters. C. J. 2006. Activity coefficients at infinite dilution in 1-alkyl-3-methylimidazolium tetrafluoroborate ionic liquids. *Journal of Chemical & Engineering Data*. 51 (3): 1088-1091.

Fox. D.. Gilman. J. W.. De Long. H. and Trulove. P. C. 2005. TGA decomposition kinetics of 1-butyl-2. 3-dimethylimidazolium tetrafluoroborate and the thermal effects of contaminants. *The Journal of Chemical Thermodynamics*. 37 (9): 900-905.

Fredenslund. A.. Jones. R. L. and Prausnitz. J. M. 1975. Group-contribution estimation of activity coefficients in nonideal liquid mixtures. *AIChE Journal*. 21 (6): 1086-1099.

Gautreaux Jr. M. and Coates. J. 1955. Activity coefficients at infinite dilution. *AIChE Journal*. 1 (4): 496-500.

Ghaedi. H.. Akbari. S.. Zhou. H.. Wang. W. and Zhao. M. 2022. Excess Properties of and Simultaneous Effects of Important Parameters on CO2 Solubility in Binary Mixture of Water-Phosphonium Based-Deep Eutectic Solvents: Response Surface Methodology (RSM) and Taguchi Method. *Energy & Fuels*. 36 (4): 1960-1972.

González. B.. Domínguez. A. and Tojo. J. 2004. Dynamic viscosities. densities. and speed of sound and derived properties of the binary systems acetic acid with water. methanol. ethanol. ethyl acetate and methyl acetate at T=(293.15. 298.15. and 303.15) K at atmospheric pressure. *Journal of Chemical & Engineering Data*. 49 (6): 1590-1596.

Gupta. R. K.. Dunderdale. G. J.. England. M. W. and Hozumi. A. 2017. Oil/water separation techniques: a review of recent progresses and future directions. *Journal of Materials Chemistry A*. 5 (31): 16025-16058.

Hasan. M.. Hiray. A. P.. Kadam. U. B.. Shirude. D. F.. Kurhe. K. J. and Sawant. A. B. 2011. Densities. viscosities. speeds of sound. FT-IR and 1 H-NMR studies of binary mixtures of n-butyl acetate with ethanol. propan-1-ol. butan-1-ol and pentan-1-ol at 298.15. 303.15. 308.15 and 313.15 K. *Journal of solution chemistry*. 40: 415-429.

Hendriks. E.. Kontogeorgis. G. M.. Dohrn. R.. de Hemptinne. J.-C.. Economou. I. G.. Zilnik. L. F. and Vesovic. V. 2010. Industrial requirements for thermodynamics and transport properties. *Industrial & engineering chemistry research*. 49 (22): 11131-11141.

Hizaddin. H. F.. Sarwono. M.. Hashim. M. A.. Alnashef. I. M. and Hadj-Kali. M. K. 2015. Coupling the capabilities of different complexing agents into deep eutectic solvents to

enhance the separation of aromatics from aliphatics. *The Journal of Chemical Thermodynamics*. 84: 67-75.

Holbrey. J. D. and Seddon. K. 1999. Ionic liquids. *Clean products and processes*. 1 (4): 223-236.

Huang. J.. Guo. X.. Xu. T.. Fan. L.. Zhou. X. and Wu. S. 2019. Ionic deep eutectic solvents for the extraction and separation of natural products. *Journal of Chromatography A*. 1598: 1-19.

Hudson. G. and McCoubrey. J. 1960. Intermolecular forces between unlike molecules. A more complete form of the combining rules. *Transactions of the Faraday Society*. 56: 761-766.

Jessop. P. G. 2011. Searching for green solvents. *Green Chemistry*. 13 (6): 1391-1398.

Kabane. B.. de P Soares. R.. Deenadayalu. N. and Bahadur. I. 2023. Pre-screening of 1-ethyl-3-methylimidazolium tetrachloroaluminate and influence of diethylene glycol on the ionic liquid in separation of molecular solutes: Activity coefficients at infinite dilution and COSMO-SAC modelling. *Fluid Phase Equilibria*. 571: 113808.

Kabane. B. and Redhi. G. G. 2019. Application of trihexyltetradecylphosphonium dicyanamide ionic liquid for various types of separations problems: Activity coefficients at infinite dilution measurements utilizing GLC method. *Fluid Phase Equilibria*. 493: 181-187.

Kabane. B. and Redhi. G. G. 2020. Thermodynamic properties and activity coefficients at infinite dilution for different solutes in deep eutectic solvent: 1-butyl-3-methylimidazolium chloride+ glycerol. *Journal of Molecular Liquids*. 311: 113216.

Khattab. I. S.. Bandarkar. F.. Fakhree. M. A. A. and Jouyban. A. 2012. Density. viscosity. and surface tension of water+ ethanol mixtures from 293 to 323K. *Korean Journal of Chemical Engineering*. 29: 812-817.

Klincewicz. K. and Reid. R. 1984. Estimation of critical properties with group contribution methods. *AIChE Journal*. 30 (1): 137-142.

Knez. Ž.. Markočič. E.. Leitgeb. M.. Primožič. M.. Hrnčič. M. K. and Škerget. M. 2014. Industrial applications of supercritical fluids: A review. *Energy*. 77: 235-243.

Kojima. K.. Zhang. S. and Hiaki. T. 1997. Measuring methods of infinite dilution activity coefficients and a database for systems including water. *Fluid Phase Equilibria*. 131 (1-2): 145-179.

Krishnan. K. 1961. The Raman spectra of organic compounds: Part I. Methyl. ethyl. n-propyl and n-butyl alcohols. In: Proceedings of *Proceedings of the Indian Academy of Sciences-Section A*. Springer. 151-167.

Królikowski. M.. Kasprzyk-Niedzicka. M.. Krolikowska. M. and Gąsiorowska. B. 2022. Physicochemical characterization and activity coefficients at infinite dilution of molecular compound in poly (ethylene glycol) dimethyl ether and the eutectic mixture composed of poly (ethylene glycol) with cyclic carbonate. *The Journal of Chemical Thermodynamics*. 169: 106747.

Krummen. M. and Gmehling. J. 2004. Measurement of activity coefficients at infinite dilution in N-methyl-2-pyrrolidone and N-formylmorpholine and their mixtures with water using the dilutor technique. *Fluid Phase Equilibria*. 215 (2): 283-294.

Kumar. H. and Katal. A. 2018. Volumetric. acoustic and spectroscopic studies (FT-IR) of trisodium (TSC) and tripotassium citrate (TPC) in aqueous solution of ionic liquid 1-

butyl-3-methylimidazolium tetrafluoro borate [C4mim][BF4] at different temperatures. *The Journal of Chemical Thermodynamics*. 116: 85-96.

Lecomte. H. A. and Liggat. J. J. 2006. Degradation mechanism of diethylene glycol units in a terephthalate polymer. *Polymer degradation and stability*. 91 (4): 681-689.

Li. G.. Chen. J.. Song. B.. Wang. S.. Pan. R.. Pei. L.. Liu. S. and Yang. Q.-Y. 2021. Separation of toluene from benzene derivatives and extraction of toluene from water based on a flexible naphthalene diimide coordination network. *Separation and Purification Technology*. 256: 117781.

Li. X.. Han. J.. Liu. Y.. Dou. Z. and Zhang. T.-a. 2022. Summary of research progress on industrial flue gas desulfurization technology. *Separation and Purification Technology*. 281: 119849.

Li. X. and Row. K. H. 2016. Development of deep eutectic solvents applied in extraction and separation. *Journal of separation science*. 39 (18): 3505-3520.

Lide. D. R. 2004. *CRC handbook of chemistry and physics*. CRC press.

Lindenbaum. S. and Boyd. G. 1964. Osmotic and activity coefficients for the symmetrical tetraalkyl ammonium halides in aqueous solution at 25. *The Journal of Physical Chemistry*. 68 (4): 911-917.

Liu. J.-f.. Jiang. G.-b. and Jönsson. J. Å. 2005. Application of ionic liquids in analytical chemistry. *TrAC Trends in Analytical Chemistry*. 24 (1): 20-27.

Liu. X.. Xing. J.. Sun. M.. Su. Z.. Chen. Z.. Wang. Y. and Cui. P. 2022. Phase behavior and extraction mechanism of methanol-n-hexane separation using choline-based deep eutectic solvent. *Journal of Molecular Liquids*. 345: 118204.

Lomba. L.. Ribate. M. P.. Sangüesa. E.. Concha. J.. Garralaga. M. P.. Errazquin. D.. García. C. B. and Giner. B. 2021. Deep eutectic solvents: Are they safe? *Applied Sciences*. 11 (21): 10061.

Mallakpour. S. and Dinari. M. 2012. Ionic liquids as green solvents: progress and prospects. *Green solvents II: properties and applications of ionic liquids*: 1-32.

Manyoni. L. and Redhi. G. 2022a. 1.6-hexanediol based deep eutectic solvent and their excess data at infinite dilution. *Chemical Thermodynamics and Thermal Analysis*. 8: 100088.

Manyoni. L. and Redhi. G. G. 2022b. Measurements of infinite dilution activity coefficient for aromatic and aliphatic hydrocarbons in Deep Eutectic Solvent. 1-ethyl-1-methylpyrrolidinium bromide+ ethylene glycol at different temperatures and a stated molar ratio. *Chemical Thermodynamics and Thermal Analysis*. 7: 100057.

Martin. A. J. and Synge. R. L. 1941. A new form of chromatogram employing two liquid phases: A theory of chromatography. 2. Application to the micro-determination of the higher monoamino-acids in proteins. *Biochemical Journal*. 35 (12): 1358.

Martins. M. A.. Pinho. S. P. and Coutinho. J. A. 2019. Insights into the nature of eutectic and deep eutectic mixtures. *Journal of Solution Chemistry*. 48: 962-982.

McGlashan. M. and Potter. D. 1962. An apparatus for the measurement of the second virial coefficients of vapours; the second virial coefficients of some n-alkanes and of some mixtures of n-alkanes. *Proceedings of the Royal Society of London. Series A. Mathematical and Physical Sciences*. 267 (1331): 478-500.

Möllmann. C. and Gmehling. J. 1997. Measurement of activity coefficients at infinite dilution using gas− liquid chromatography. 5. Results for N-methylacetamide. N. N-

dimethylacetamide. N. N-dibutylformamide. and sulfolane as stationary phases. *Journal of Chemical & Engineering Data*. 42 (1): 35-40.

Muhammad. A. 2016. Thermal and kinetic analysis of pure and contaminated ionic liquid: 1-butyl-2.3-dimethylimidazolium chloride (BDMIMCl). *Polish Journal of Chemical Technology*. 18 (2): 122-125.

Nkosi. N.. Tumba. K. and Ramsuroop. S. 2018. Measurements of activity coefficient at infinite dilution for organic solutes in tetramethylammonium chloride+ ethylene glycol deep eutectic solvent using gas-liquid chromatography. *Fluid Phase Equilibria*. 462: 31-37.

Nkosi. N.. Tumba. K. and Ramsuroop. S. 2019. Activity coefficients at infinite dilution of various organic solutes in the deep eutectic solvent (tetramethylammonium chloride+ 1. 6 hexanediol in the 1: 1 molar ratio). *South African journal of chemical engineering*. 27 (1): 7-15.

Noble. R. D. and Agrawal. R. 2005. Separations research needs for the 21st century. *Industrial & engineering chemistry research*. 44 (9): 2887-2892.

Nowosielski. B.. Jamrógiewicz. M.. Łuczak. J. and Warmińska. D. 2022. Novel binary mixtures of alkanolamine based deep eutectic solvents with water—thermodynamic calculation and correlation of crucial physicochemical properties. *Molecules*. 27 (3): 788.

O'Connell. J. P. and Haile. J. M. 2005. *Thermodynamics: Fundamentals for applications*. Cambridge University Press.

Ortiz. A.. Ruiz. A.. Gorri. D. and Ortiz. I. 2008. Room temperature ionic liquid with silver salt as efficient reaction media for propylene/propane separation: Absorption equilibrium. *Separation and Purification Technology*. 63 (2): 311-318.

Pacheco-Fernández. I. and Pino. V. 2019. Green solvents in analytical chemistry. *Current Opinion in Green and Sustainable Chemistry*. 18: 42-50.

Pantoja-Espinoza. J. C.. Meléndez-Zaragoza. M. J.. Salinas-Gutiérrez. J. M.. López-Ortiz. A. and Collins-Martínez. V. H. 2021. Methanol and Triethanolamine Effect as Sacrifice Agents in the Photocatalytic Production of Hydrogen over Zinc Titanates.

Patel. Y. N. and Patel. M. P. 2012. Novel cationic poly [AAm/NVP/DAPB] hydrogels for removal of some textile anionic dyes from aqueous solution. *Journal of Macromolecular Science. Part A*. 49 (6): 490-501.

Pekel. A. G.. Kurtulbaş. E.. Toprakçı. İ. and Şahin. S. 2020. Menthol-based deep eutectic solvent for the separation of carbamazepine: reactive liquid-liquid extraction. *Biomass Conversion and Biorefinery*: 1-8.

Pereiro. A. and Rodriguez. A. 2007. Study on the phase behaviour and thermodynamic properties of ionic liquids containing imidazolium cation with ethanol at several temperatures. *The Journal of Chemical Thermodynamics*. 39 (6): 978-989.

Phan. S. and Luscombe. C. K. 2019. Recent advances in the green. sustainable synthesis of semiconducting polymers. *Trends in Chemistry*. 1 (7): 670-681.

Poling. B. E.. Prausnitz. J. M. and O'connell. J. P. 2001. *Properties of gases and liquids*. McGraw-Hill Education.

Ramsey. E.. Qiubai. S.. Zhang. Z.. Zhang. C. and Wei. G. 2009. Mini-Review: Green sustainable processes using supercritical fluid carbon dioxide. *Journal of Environmental Sciences*. 21 (6): 720-726.

Revelli. A.-L.. Mutelet. F.. Turmine. M.. Solimando. R. and Jaubert. J.-N. 2009. Activity coefficients at infinite dilution of organic compounds in 1-butyl-3-methylimidazolium tetrafluoroborate using inverse gas chromatography. *Journal of Chemical & Engineering Data*. 54 (1): 90-101.

Roy Choudhury. A. K. 2013. Green chemistry and the textile industry. *Textile Progress*. 45 (1): 3-143.

Salgado. J.. Parajó. J. J.. Fernández. J. and Villanueva. M. 2014. Long-term thermal stability of some 1-butyl-1-methylpyrrolidinium ionic liquids. *The Journal of Chemical Thermodynamics*. 74: 51-57.

Sánchez. P. B.. González. B.. Salgado. J.. Parajó. J. J. and Domínguez. Á. 2019. Physical properties of seven deep eutectic solvents based on L-proline or betaine. *The Journal of Chemical Thermodynamics*. 131: 517-523.

Sandler. S. 1996. Infinite dilution activity coefficients in chemical. environmental and biochemical engineering. *Fluid Phase Equilibria*. 116 (1-2): 343-353.

Schuur. B.. Brouwer. T.. Smink. D. and Sprakel. L. M. 2019. Green solvents for sustainable separation processes. *Current Opinion in Green and Sustainable Chemistry*. 18: 57-65.

Sharma. D.. Bhagour. S. and Sharma. V. 2012. Thermodynamic and topological studies of 1-ethyl-3-methylimidazolium tetrafluoroborate+ pyrrolidin-2-one and 1-methyl-pyrrolidin-2-one mixtures. *Journal of Chemical & Engineering Data*. 57 (12): 3488-3497.

Shekaari. H.. Zafarani-Moattar. M. T. and Mohammadi. B. 2017. Thermophysical characterization of aqueous deep eutectic solvent (choline chloride/urea) solutions in

full ranges of concentration at T=(293.15–323.15) K. *Journal of Molecular Liquids*. 243: 451-461.

Shekaari. H.. Zafarani-Moattar. M. T. and Mohammadi. B. 2020. Liquid-liquid equilibria and thermophysical properties of ternary mixtures {(benzene/thiophene)+ hexane+ deep eutectic solvents}. *Fluid Phase Equilibria*. 509: 112455.

Sheldon. R. A. 2005. Green solvents for sustainable organic synthesis: state of the art. *Green Chemistry*. 7 (5): 267-278.

Shuai. L. and Luterbacher. J. 2016. Organic solvent effects in biomass conversion reactions. *ChemSusChem*. 9 (2): 133-155.

Singh. S.. Bahadur. I.. Naidoo. P.. Redhi. G. and Ramjugernath. D. 2016. Application of 1-butyl-3-methylimidazolium bis (trifluoromethylsulfonyl) imide ionic liquid for the different types of separations problem: Activity coefficients at infinite dilution measurements using gas-liquid chromatography technique. *Journal of Molecular Liquids*. 220: 33-40.

Singh. S.. Bahadur. I.. Redhi. G. G.. Ebenso. E. E. and Ramjugernath. D. 2014. Density and speed of sound of 1-ethyl-3-methylimidazolium ethyl sulphate with acetic or propionic acid at different temperatures. *Journal of Molecular Liquids*. 199: 518-523.

Smith. R. M. 2006. *Superheated water: the ultimate green solvent for separation science*: Springer.

Soave. G. and Feliu. J. A. 2002. Saving energy in distillation towers by feed splitting. *Applied Thermal Engineering*. 22 (8): 889-896.

Tang. B. and Row. K. H. 2013. Recent developments in deep eutectic solvents in chemical sciences. *Monatshefte für Chemie-Chemical Monthly*. 144: 1427-1454.

Tsonopoulos. C. 1974. An empirical correlation of second virial coefficients. *AIChE Journal*. 20 (2): 263-272.

Tsonopoulos. C. and Dymond. J. H. 1997. Second virial coefficients of normal alkanes. linear 1-alkanols (and water). alkyl ethers. and their mixtures. *Fluid Phase Equilibria*. 133 (1-2): 11-34.

Tsonopoulos. C. and Heidman. J. 1990. From the virial to the cubic equation of state. *Fluid Phase Equilibria*. 57 (3): 261-276.

Wang. J.. Sun. W.. Li. C. and Wang. Z. 2008. Correlation of infinite dilution activity coefficient of solute in ionic liquid using UNIFAC model. *Fluid Phase Equilibria*. 264 (1-2): 235-241.

Wazeer. I.. Hizaddin. H. F.. El Blidi. L.. Ali. E.. Hashim. M. A. and Hadj-Kali. M. K. 2018. Liquid–liquid equilibria for binary azeotrope mixtures of benzene and alcohols using choline chloride-based deep eutectic solvents. *Journal of Chemical & Engineering Data*. 63 (3): 613-624.

Wen. Q.. Chen. J.-X.. Tang. Y.-L.. Wang. J. and Yang. Z. 2015. Assessing the toxicity and biodegradability of deep eutectic solvents. *Chemosphere*. 132: 63-69.

Zafarani-Moattar. M. T.. Shekaari. H. and Sadrmousavi-Dizaj. A. 2022. Some thermodynamic properties and computational study of DESs (choline chloride/ethylene glycol and choline chloride/malonic acid) in lithium nitrate+ propylene carbonate solutions at T= 298.15 K. *The Journal of Chemical Thermodynamics*. 165: 106642.